Julius-Maximilians-Universität Würzburg

Relevance of platelet count and ITAM-signalling pathway in murine models of haemostasis, thrombosis and thrombo-inflammation

Relevanz der Thrombozytenzahl und des ITAM-Signalwegs in Mausmodellen der Hämostase, Thrombose und Thromboinflammation

Doctoral thesis for a doctoral degree

at the Graduate School of Life Sciences

Section Biomedicine

submitted by

Martina Morowski

from Kassel

Würzburg, 2014

Submitted on:……..

Office stamp

Members of the *Promotionskomitee:*

Chairperson: Prof. Dr. Jörg Schultz

Primary Supervisor: Prof. Dr. Bernhard Nieswandt

Supervisor (Second): Prof. Dr. Thomas Dandekar

Supervisor (Third): Prof. Dr. Alma Zernecke-Madsen

Date of Public Defence:…….

Date of Receipt of Certificates:……..

Summary

Platelets are important players in haemostasis and their activation is essential to limit post-traumatic blood loss upon vessel injury. On the other hand, pathological platelet activation may lead to thrombosis resulting in myocardial infarction and stroke. Platelet activation and subsequent thrombus formation are, therefore, tightly regulated and require a well-defined interplay of platelet surface receptors, intracellular signalling molecules, cytoskeletal rearrangements and the activation of the coagulation cascade.

In vivo thrombosis and haemostasis models mimic thrombus formation at sites of vascular lesions and are frequently used to assess thrombotic and haemostatic functions of platelets. In this dissertation, different *in vivo* models were used in mice to address the question at what level a reduced platelet count (PC) compromises stable thrombus formation. To study this, mice were rendered thrombocytopenic by low-dose anti-GPIbα antibody treatment and subjected to a tail bleeding time assay as well as to four different *in vivo* thrombosis models. Haemostasis and occlusive thrombus formation in small vessels were only mildly affected even at severe reductions of the PC. In contrast, occlusive thrombus formation in larger arteries required higher PCs demonstrating that considerable differences in the sensitivity for PC reductions exist between these models.

In a second part of this study, mice were rendered thrombocytopenic by injection of high-dose anti-GPIbα antibody which led to the complete loss of all platelets from the circulation for several days. During recovery from thrombocytopenia, the newly generated platelet population was characterised and revealed a defect in immunoreceptor tyrosine-based activation motif (ITAM)-signalling. This defect translated into impaired arterial thrombus formation.

To further investigate ITAM-signalling *in vivo*, genetically modified mice were analysed which display a positive or negative regulation of platelet ITAM-signalling *in vitro*. Whereas mice lacking the adapter Grb2 in platelets showed a delayed thrombus formation *in vivo* after acetylsalicylic acid treatment, *Clp36*$^{\Delta LIM}$ bone marrow chimeric mice and SLAP/SLAP2-deficient mice displayed pro-thrombotic properties *in vivo*. Finally, mice lacking the adapter protein EFhd2 were analysed *in vitro* and *in vivo*. However, EFhd2-deficient platelets showed only a minor increase in the procoagulant activity compared to control.

Zusammenfassung

Thrombozyten sind wichtige Zellen für die Hämostase, die bei einer Verletzung der Gefäßwand aktiviert werden, um den Blutverlust zu begrenzen. Auf der anderen Seite kann die pathologische Aktvierung von Thrombozyten jedoch zu Thromboseereignissen und in Konsequenz zu Schlaganfall und Herzinfarkt führen. Die Aktivierung von Thrombozyten und die nachfolgende Thrombusbildung sind daher streng reguliert und setzen ein enges Zusammenspiel von Thrombozytenoberflächenrezeptoren, intrazellulären Signalmolekülen, Zytoskelettumstrukturierungen und die Aktivierung der Koagulationskaskade voraus.

In vivo Thrombose- und Hämostase-Modelle ahmen die Thrombusbildung in Gefäßen nach und werden häufig benutzt um die hämostatische und thrombotische Funktion von Thrombozyten zu untersuchen. In dieser Dissertation wurden verschiedene *in vivo* Modelle in Mäusen genutzt, um zu klären, ab welcher Thrombozytenzahl eine stabile Thrombusbildung beeinträchtigt ist. Für diese Untersuchung wurden Mäuse mit geringen Dosen anti-GPIbα Antikörper behandelt, die zu einer Reduktion der Thrombozytenzahl führen. Anschließend wurden die Mäuse in einem Blutungszeitmodel und vier verschiedenen thrombotischen Modellen untersucht. Hämostase oder okklusive Thrombusbildung in kleinen Gefäßen waren auch bei einer sehr starken Reduktion der Thrombozytenzahl kaum beeinträchtigt. Im Gegensatz dazu war für eine normale Thrombusbildung in größeren Gefäßen eine höhere Thrombozytenzahl nötig. Verschiedene *in vivo* Modelle zeigen daher eine unterschiedliche Sensitivität gegenüber einer Reduktion der Thrombozytenzahl.

Im zweiten Teil dieser Arbeit wurden Mäuse mit einer hohen Dosis anti-GPIbα Antikörper behandelt, die zu einem völligen, mehrtägigen Verlust aller Thrombozyten im Blutkreislauf führte. Während sich die Thrombozytenzahl erholte, wurden neu generierte Thrombozyten charakterisiert, die einen deutlichen Defekt im ITAM-Signalweg zeigten. Dieser Defekt führte zu einer verminderten arteriellen Thrombusbildung.

Um Auswirkungen eines Defektes im ITAM-Signalweg detaillierter *in vivo* zu untersuchen, wurden genetisch veränderte Mäuse, die *in vitro* eine reduzierte oder verstärkte ITAM-Signaltransduktion in Thrombozyten zeigen, untersucht. Während Mäuse, die in Thrombozyten kein Grb2 exprimieren nach Acetylsalicylsäurebehandlung *in vivo* eine verlangsamte Thrombusbildung zeigten, war die Thrombusbildung in *Clp36*$^{\Delta LIM}$ Knochenmarkchimären und SLAP/SLAP2-defizienten Mäusen beschleunigt. Darüber hinaus

wurden EFhd2-defiziente Mäuse *in vitro* und *in vivo* analysiert. EFhd2-defiziente Thrombozyten zeigten jedoch nur eine geringe Steigerung in der prokoagulatorischen Aktivität im Vergleich zu Kontrolltieren.

Abbreviations

$[Ca^{2+}]$	Calcium concentration
$[Ca^{2+}]_i$	Intracellular calcium concentration
°C	Degree Celsius
a.u.	Arbitrary unit
ACD	Acid citrate dextrose
ADP	Adenosine diphosphate
APS	Ammonium persulfate
ASA	Acetylsalicylic acid
ATP	Adenosine triphosphate
BM	Bone marrow
bp(s)	Base pair(s)
BSA	Bovine serum albumin
cAMP	Cyclic adenosine monophosphate
CLP	Cecal puncture and ligation
CRP	Collagen-related peptide
CVX	Convulxin
DAG	Diacylgylcerol
ddH_2O	Double-distilled water
DMSO	Dimethylsulfoxide
ECL	Enhanced chemiluminescence
EDTA	Ethylenediaminetetraacetic acid
EGTA	Ethylene glycol tetraacetic acid
FACS	Fluorescence-activated cell sorting
FITC	Fluorescein isothiocyanate
FL	Fluorescence
FSC	Forward scatter
GP	Glycoprotein
GPCR(s)	G protein-coupled receptor(s)
h(s)	Hour(s)
HCT	Haematocrit
HE	Haematoxylin-eosin
HEPES	N-2-hydroxyethylpiperazone-N'2-ethanesulfonic acid
HRP	Horse radish peroxidase
IFI	Integrated fluorescence intensity
Ig	Immunoglobulin
IP_3	Inositol-1,4,5-triphosphate
IP_3-R	Inositol-1,4,5-triphosphate receptor
ITAM	Immunoreceptor tyrosine-based activation motif
ITP	Immune thrombocytopenia
LAT	Linker for activation of T cells

mAb	Monoclonal antibody
MFI	Mean fluorescence intensity
min(s)	Minute(s)
MK(s)	Megakaryocyte(s)
MPV	Mean platelet volume
n.s.	Not significant
PAF	Platelet-activating factor
PAR	Protease-activated receptor
PBS	Phosphate buffered saline
PCR	Polymerase chain reaction
PE	Phycoerythrin
PFA	Paraformaldehyde
PGI_2	Prostacyclin
PLC	Phospholipase C
PMCA	Plasma membrane Ca^{2+} ATPase
ppp	Platelet-poor plasma
prp	Platelet-rich plasma
PVDF	Polyvinylidene fluoride
RC	Rhodocytin
rpm	Revolutions per minute
RT	Room temperature
SD	Standard deviation
SDS	Sodium dodecylsulfate
SECRA	Sarcoplasmic/ endoplasmic reticulum Ca^{2+} ATPase
SLP-76	Src homology 2 domain-containing leukocyte protein of 76 kDa
SOCE	Store-operated calcium entry
SSC	Side scatter
STIM	Stromal interaction molecule
TAE	TRIS acetate EDTA buffer
TBS	Tris-buffered saline
TE	TRIS EDTA buffer
TF	Tissue factor
tMCAO	Transient middle cerebral artery occlusion
TRIS	Tris(hydroxymethyl)-aminomethane
TTC	Triphenyltetrazolium chloride
TxA_2	Thromboxane A_2
U	Units
UV	Ultraviolet
vWF	Von Willebrand factor
wt	Wild-type

Table of contents

1 Introduction

Platelets are anucleated discoid cell fragments which are only found in mammalians and represent the second most abundant cell type in whole blood with approximately 250 platelets/nL in humans and 1000 platelets/nL in mice. In humans and mice, they represent the smallest cell type in the blood system with a diameter of 1-3 µm and 0.5-1 µm, respectively.[1] During their life time, platelets circulate in the blood stream in an inactive state for about 8-12 days in humans and 3-5 days in mice and "survey" the integrity of the vascular system. At the end of their life time, platelets are removed from the circulation by the reticuloendothelial system of liver and spleen.[2] Most platelets in the circulation never undergo activation, but upon endothelial damage they rapidly adhere to the exposed extracellular matrix (ECM) of the vessel wall and become activated. This initial platelet activation induces a complex series of signalling events which lead to the recruitment of more platelets from the circulation to form platelet aggregates, eventually resulting in the formation of a stable haemostatic plug that seals the site of injury. Platelet activation and subsequent platelet recruitment is, therefore, essential to limit posttraumatic blood loss, but is also a major pathomechanism causing thrombotic vessel occlusion resulting in ischaemic diseases such as myocardial infarction and stroke. The use of anti-thrombotic drugs which prevent uncontrolled excessive platelet activation is, therefore, important for the treatment or prophylaxis of ischaemic diseases. However, current anti-thrombotic drugs such as acetylsalicylic acid (ASA) or $P2Y_{12}$ receptor antagonists simultaneously increase the risk of bleeding. A detailed understanding of how platelet adhesion, activation and inhibition are regulated is, therefore, essential for the exploration of new therapeutic targets.

Besides their best-characterised function in haemostasis and thrombosis, platelets are also involved in other physiological and pathological processes. For instance, adhesive receptors of platelets prevent bleeding from newly formed vessels during angiogenesis.[3] Similarly, platelets contribute to embryonic development[4] and the separation of the blood and lymphatic vasculature.[5] Furthermore, platelets play an important role in the innate immune response[6], inflammation[7], sepsis[8], wound healing[9], tumour metastasis[10] and atherosclerosis.[11]

1.1 Origin of platelets

Platelets originate from the cytoplasm of sessile bone marrow megakaryocytes (MKs) during a complex but not fully understood process which can be divided into two phases: MK maturation and development and the generation of pro- and preplatelets. During the first phase which takes several days MKs become polyploid, massively enlarge their cytoplasm, accumulate platelet components such as granules and cytoskeletal proteins and develop a demarcation membrane system.[12] In the second phase, which is completed within hours, MKs constantly extend dynamic proplatelet-like protrusions into microvessels which through contact with the flowing blood are shed into the blood stream. The resulting barbell-shaped cell fragments are so-called proplatelets (Figure 1.1).

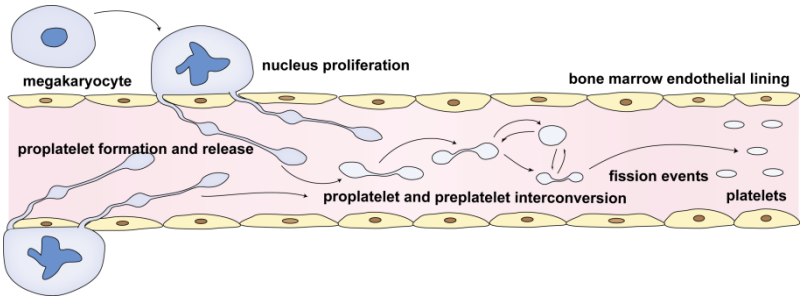

Figure 1.1: MK development in adult bone marrow. After MK maturation, proplatelet-like protrusions are extended into the vessel and eventually shed into the blood stream. Fission events of proplatelets lead to the formation of mature platelets in the circulation. (Figure adapted from: Machlus et al., *J Cell Biol*, 2013).[13]

The production of proplatelets has been imaged *in vivo* and a recent study reveals that the sphingosine 1-phosphate receptor (S1pr1) regulates the formation of MK protrusions and the release of proplatelets.[14,15] However, the understanding of how proplatelet formation in MKs is triggered and how proplatelets evade activation during migration through collagen-rich bone marrow vessel walls remains elusive.

Proplatelets mature while circulating in the blood stream but this process is poorly understood. Recently, the microtubule-dependent reversible conversion of proplatelets into discoid preplatelets has been discovered as an intermediate stage in proplatelet maturation but its impact remains unknown.[13] Finally, fission events of mature proplatelets result in the appearance of platelets in the circulation.[16]

1.2 Platelet activation and thrombus formation

From the beginning of initial platelet adherence upon endothelial damage to subsequent platelet accumulation and aggregation which finally results in the formation of a stable thrombus, platelet activation is a tightly regulated process which can be divided into three major steps: (I) platelet tethering, (II) platelet activation and secretion and (III) firm platelet adhesion and thrombus growth (Figure 1.2). Additionally, thrombus formation depends on the rheological properties in the vessel at the site of injury.

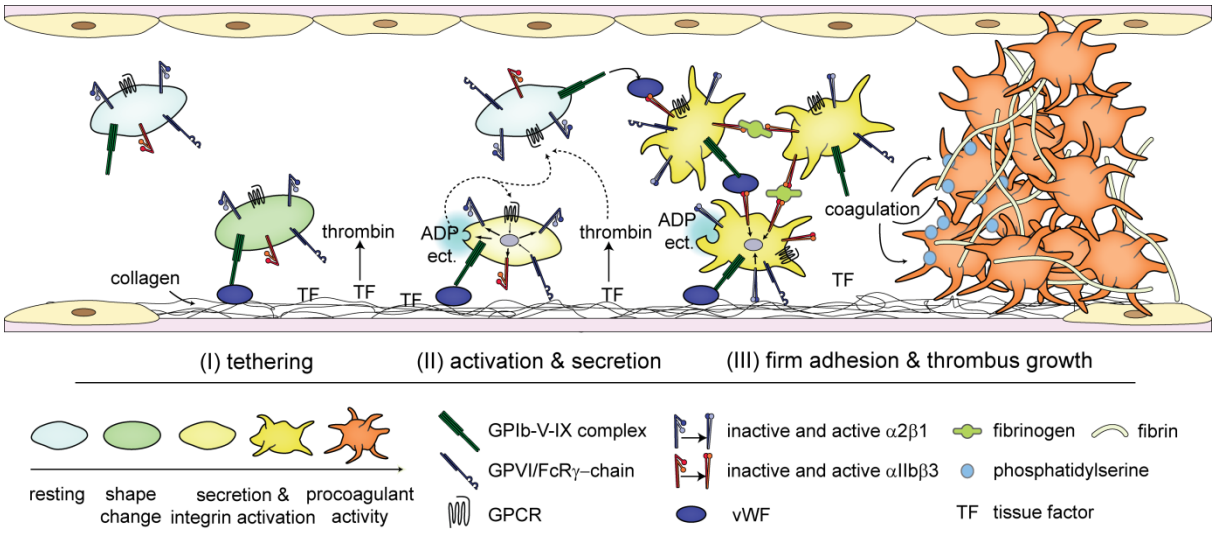

Figure 1.2: Model of initial platelet adhesion leading to stable thrombus formation at sites of vascular injury. Platelets are initially decelerated by interaction of the platelet glycoprotein (GP)Ib-V-IX complex with von Willebrand factor (vWF) bound to collagen which keeps the platelets in close contact to the vessel wall thereby enabling the contact of the platelet receptor GPVI to collagen. GPVI receptor binding triggers an intracellular signalling cascade which induces the release and generation of secondary mediators which activate G protein-coupled receptors (GPCR), platelet shape change and Ca^{2+}-mobilization. Together these events lead to the recruitment of further platelets from the circulation and reinforce platelet activation finally resulting in the functional up-regulation of integrin adhesion receptors. Activated integrins mediate stable platelet adhesion to the vessel wall and stable thrombus formation. (Figure adapted from: Varga-Szabo et al., *Arterioscler Thromb Vasc Biol*, 2008 and Versteeg et al., *Physiol Rev*, 2013).[17,18]

1.2.1 Rheological conditions in the vessel and platelet tethering via GPIb

Platelet tethering depends on the rheological conditions present in the blood vessel.[19] An important measure are shear rates which can be approximated if it is assumed that blood is an Newtonian fluid, the vessel is cylindrical, straight and has inelastic walls and finally the blood flow is steady and laminar.[20] Blood flow is fastest at the vessel center and zero at the vessel wall and shear rates are the resulting velocity gradient. The shear rate is inversely correlated to the vessel diameter and can range from <500 s^{-1} in venules, up to 10,000 s^{-1} in small arterioles and can even reach >20,000 s^{-1} in stenosed vessels.[21-23] An additional factor

for platelet adherence in stenosed vessels is the shear gradient which is the shear acceleration and deceleration at the site of vessel narrowing.[24] Depending on the prevailing shear rate, three different ways of platelet adhesion under flow can be distinguished.

At shear rates of >1000 s^{-1}, the first step of platelet tethering largely depends on the initial interaction of the glycoprotein (GP)Ib-V-IX complex with von Willebrand factor (vWF) immobilised on the exposed subendothelial ECM which contains a large number of macromolecules such as laminin, fibronectin and collagen.[17,25] At extremely high shear rates >10,000 s^{-1}, especially when shear gradients prevail, platelet aggregation through binding of immobilised and soluble vWF to GPIbα, the ligand binding subunit of the GPIb-V-IX complex, may be sufficient to induce thrombus formation, even in the absence of cellular activation.[26] In contrast, at low shear rates <500 s^{-1} found in veins and large arteries, this interaction may not be relevant to trigger thrombus formation (Figure 1.2).[27]

The binding of the GPIb-V-IX complex to vWF is characterised by a fast on and off rate and is thus insufficient to mediate stable platelet adhesion to the vessel wall. However, these multiple interactions result in a deceleration of the platelets and keep them in close proximity to the vessel wall. This so-called platelet 'rolling' is crucial to establish the binding of GPVI to collagen exposed on the subendothelial matrix (Figure 1.2).[17]

1.2.2 The GPVI/FcRγ-chain complex and ITAM-signalling

GPVI is a 62 kDa type I transmembrane receptor of the Ig superfamily that is exclusively expressed in platelets and MKs.[28-30] GPVI is the major activating collagen receptor on the platelet surface and due to its positively charged arginine residue in its transmembrane region non-covalently associated with the immunoreceptor tyrosine-based activation motif (ITAM)-bearing Fc-receptor (FcR)γ-chain (Figure 1.3).[31] In its cytoplasmic tail, GPVI contains a proline-rich motif that selectively binds to the Src homology 3 (SH3) domain of the Src family tyrosine kinases Fyn and Lyn.

An essential step of platelet activation upon injury is the binding of GPVI dimers to collagen.[32] This interaction is unable to mediate stable platelet adhesion to the vessel wall but allows Fyn and Lyn to induce the tyrosine phosphorylation of the FcRγ-chain on its ITAM (Figure 1.3). This phosphorylation enables the binding and activation and of the tyrosine kinase Syk which further phosphorylates downstream targets such as the transmembrane

linker for activation of T-cells (LAT) and the Src homology 2 domain-containing leukocyte protein of 76 kDa (SLP-76). Finally, these signalling events lead to the activation of phospholipase γ2 (PLCγ2), thereby effectively inducing platelet activation (Figure 1.4, violet).[33,34]

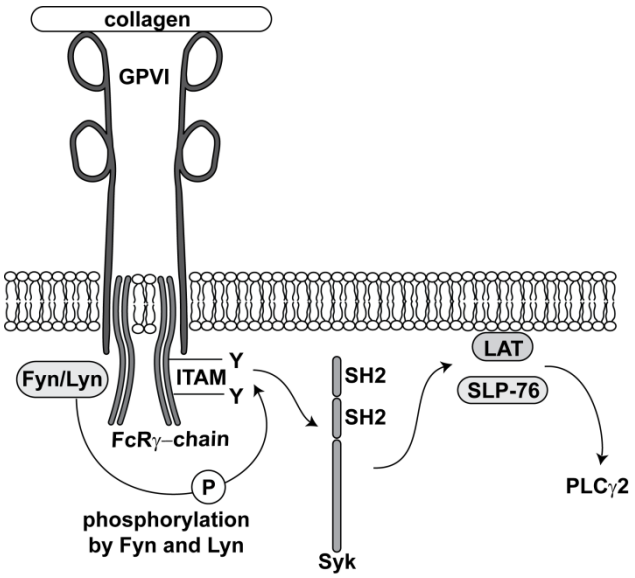

Figure 1.3: Structure of the GPVI-signalling complex. Upon binding of collagen to GPVI dimers, the ITAM of the FcRγ-chain becomes phosphorylated by the Src family tyrosine kinases Fyn and Lyn. ITAM phosphorylation induces the activation of the tyrosine kinase Syk finally leading to the activation of PLCγ2. (Figure adapted from: Li et al., *Arterioscler Thromb Vasc Biol*, 2010).[34]

Similar signalling patterns in platelets are induced by ligand binding of the hemITAM receptor C-type lectin receptor 2 (CLEC-2)[35] (Figure 1.4, violet), which, through phosphorylation of its hemITAM by both Src and Syk tyrosine kinases leads to the activation of PLCγ2.[36] In contrast, immunoreceptor tyrosine-based inhibition motif (ITIM)-bearing receptors such as PECAM-1,[37] G6b-B[38] and CEACAM1[39] have been shown to negatively regulate platelet activation via GPVI and partially via CLEC-2. Additionally, recent studies indicate an important regulatory role of protein-tyrosine phosphatases (PTPs) such as CD148, PTP-1B and Shp1 in these platelet activating pathways.[40] However, the underlying regulatory mechanisms during platelet activation via the GPVI-ITAM-signalling pathway are still not completely understood.

Upon activation, PLCγ2 cleaves the membrane phospholipid phosphatidylinositol 4,5-biphosphate (PIP_2) into the second messengers 1,2-diacylglycerol (DAG) which activates protein kinase C (PKC) and inositol 1,4,5-triphosphate (IP_3) which mobilizes Ca^{2+} from intracellular stores. Ca^{2+} store release into the cytoplasm is followed by Ca^{2+} entry through

the plasma membrane (PM), a process referred to as store-operated calcium entry (SOCE). Key players in this major way of Ca^{2+} entry in platelets are stromal interaction molecule 1 (STIM1), which is a Ca^{2+} sensor in the intracellular Ca^{2+} stores and the transmembrane channel protein Orai1 (Figure 1.4, green). SOCE and the subsequent increase of intracellular Ca^{2+} levels promote platelet activation through different mechanisms such as the secretion of secondary mediators stored in platelet α- and dense granules (Figure 1.4, gray) and the generation of thrombin by the blood coagulation cascade.[41]

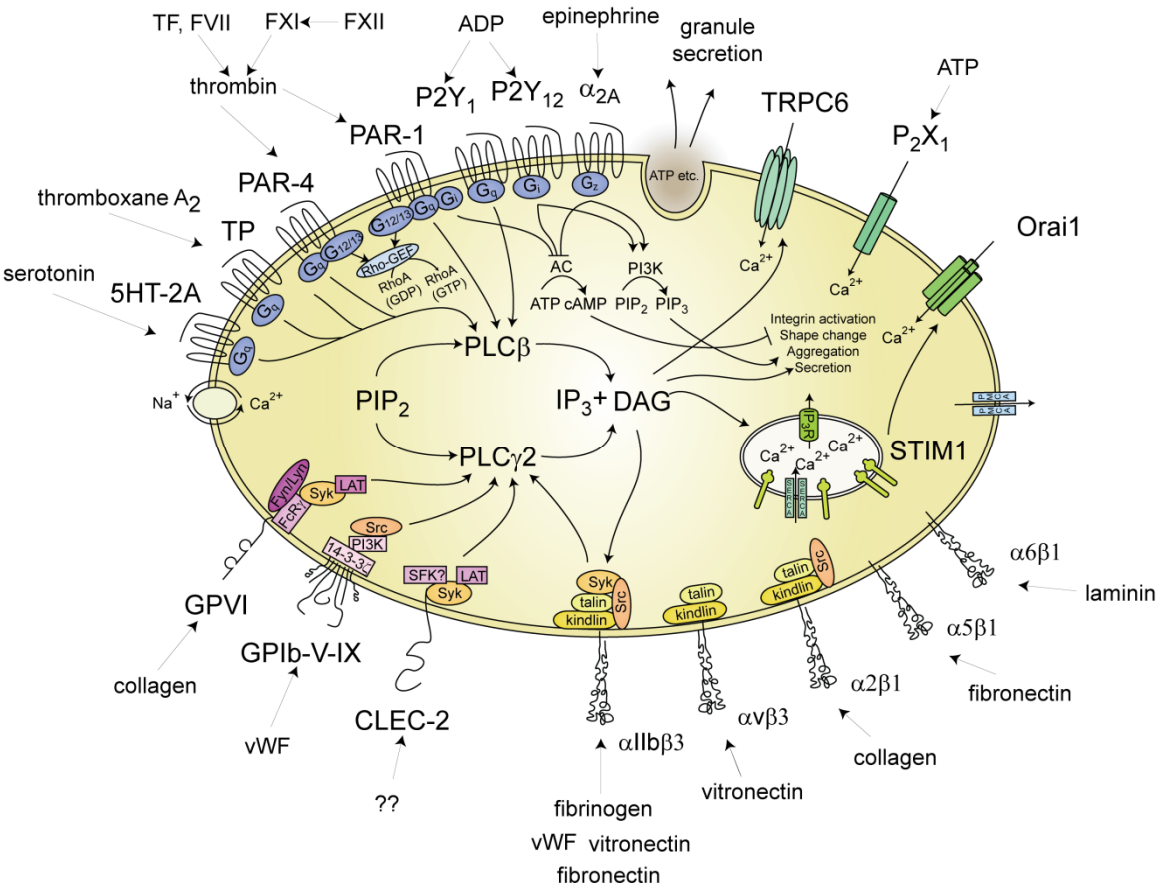

Figure 1.4: Main signalling pathways in platelets. Stimulation of the GPIb-V-IX complex and platelet adhesion via GPVI initiates platelet signalling via PLCγ2 (violet). PLCγ2 cleaves PIP_2 into the second messengers DAG, which activates PKC, and IP_3 which mobilizes Ca^{2+} from intracellular stores. Ca^{2+} store release into the cytoplasm is followed by Ca^{2+} entry through the PM (green) which leads to the secretion of platelet-derived secondary mediators such as ADP and thromboxane A_2 (TxA_2) and subsequently to the generation of thrombin. These mediators act through different GPCRs (blue). $G_{12/13}$ stimulation induces cytoskeletal rearrangements via Rho/Rho kinases. $G_{i/z}$ protein-coupled receptors inhibit the formation of cAMP by adenylyl cyclase (AC). G_q stimulation activates PLCβ. The activation of PLCβ further reinforces platelet activation. Together these events lead to the 'final common pathway' of platelet activation which is characterised by the functional up-regulation of transmembrane adhesion receptors of the integrin class (orange) which lead to firm platelet aggregation and adhesion. Abbreviations: PAR, protease-activated receptor; Rho-GEF, Rho-specific guanine nucleotide exchange factor (Figure adapted from: Varga-Szabo et al., *Arterioscler Thromb Vasc Biol*, 2008).[17]

1.2.3 Platelet activation through G protein-coupled receptors

The secretion of mediators from platelet granules and the generation of mediators such as thrombin and thromboxane A_2 (TxA_2) are major pathways to amplify platelet activation and the recruitment of more platelets from the circulation.

Pro-thrombotic proteins released from α-granules of platelets are mainly vWF, fibrinogen, thrombospondin, growth and coagulation factors. Small inorganic molecules such as adenosine diphosphate (ADP), adenosine triphosphate (ATP) and serotonin derive from dense granules of platelets (Figure 1.4, gray). TxA_2 is released from platelets after intracellular generation by hydrolysis of phospholipids.[42] In contrast to secreted secondary mediators, thrombin is generated by cleavage of prothrombin upon activation of the blood coagulation cascade which can be initiated by two distinct pathways. The extrinsic pathway depends on the exposure of tissue factor (TF) from the damaged vessel wall. The intrinsic pathway is initiated by negatively charged surfaces but its physiological relevance is not fully understood.[43] The generation of thrombin by the coagulation system is strongly enhanced by activated platelets which expose negatively charged phosphatidylserines (PSs) thereby providing a catalytic surface for the activation of coagulation factors (Figure 1.2).[44,45]

Among these mediators of platelet activation, ADP, thrombin and TxA_2 are the most important ones and act through G protein-coupled receptors (GPCRs) (Figure 1.4, blue). G_q protein-coupled receptors lead to the activation of PLCβ and induce similar signalling cascades as PLCγ2 activation. $G_{12/13}$ protein-coupled receptors activate Rho/Rho kinases resulting in the phosphorylation of the myosin light chain, thereby inducing platelet shape change. G_i protein-coupled receptors activate platelets by inhibition of the adenylyl cyclase.[34,44]

1.2.4 Firm platelet adhesion and thrombus growth

Combined ITAM and GPCR-signalling events lead to the final common pathway of platelet activation. Thereby, integrin adhesion receptors are functionally up-regulated by shifting from an inactive into an active state. This process is called inside-out signalling (Figure 1.4, orange).[34] Whereas integrins α2β1, α5β1 and α6β1 mediate the linking between vessel wall and platelets through binding to collagen, fibronectin and laminin, respectively, the major integrin αIIbβ3 links platelets via fibrinogen and vWF and mediates platelet adhesion to the

vessel wall by binding to vWF immobilised on exposed collagen.[17] Upon this ligand binding, integrins undergo a second conformational change which induces outside-in signalling. Outside-in signalling reinforces granule secretion, induces platelet spreading and leads to the retraction of the blood clot, a process that is supposed to pull wound edges into closer proximity thereby facilitating wound healing.[34,46]

1.3 Platelet count

The platelet count is defined as platelets per volume and the average platelet count depends on the mammalian species. Whereas the platelet count of healthy humans is on average 250 platelets/nL blood, the platelet count in rodents such as mice and rats is approximately 1000 platelets/nL blood.[1]

A platelet count higher than average is called thrombocytosis and a lower one is called thrombocytopenia. Generally, thrombocytosis can be divided into two underlying disorders. Primary thrombocytosis is a myelo-proliferative disorder and may for instance be caused by myelofibrosis.[47] Secondary thrombocytosis can result from an underlying cause such as cancer, splenectomy or iron deficiency. Due to the many contributing factors in these disorders the risk of thrombosis in correlation to an increased platelet count is unknown.[47] Since a major part of this dissertation deals with the reduction of the platelet count, the next chapter focuses on thrombocytopenia.

1.3.1 Thrombocytopenia

The platelet count of healthy humans is on average 250 platelets/nL blood and thrombocytopenia is diagnosed at platelet counts below 150 platelets/nL blood.[48] Thrombocytopenia occurs relatively frequent in humans and can be caused by different mechanisms in the context of a large variety of pathologies or medical treatments. Generally, thrombocytopenia can be divided into three different categories: primary immune thrombocytopenia (ITP), secondary ITP and non-immune thrombocytopenia.[49]

1.3.1.1 Primary immune thrombocytopenia

Primary ITP is an autoimmune disease in which auto-antibodies directed against platelet surface antigens trigger platelet destruction and/or suboptimal platelet production[49] and may cause moderate to severe bleeding symptoms.[50] The majority of platelet auto-

antibodies involved in primary ITP is directed against epitopes on αIIbβ3 or GPIb. These are the two most prominent membrane glycoproteins on the surface of platelets and anti-αIIbβ3 and anti-GPIb auto-antibodies account for 70-80% and 20-40% of ITP cases, respectively. A minority of patients display auto-antibodies against both and/or other glycoproteins present on the platelet surface such as GPV.[51-53] Similar to auto-antibody-mediated thrombocytopenia in humans, a reduction of the platelet count can also be observed in mice upon injection of rat monoclonal antibodies (mAbs) against αIIbβ3 and GPIb. Interestingly, the mechanism of platelet clearance by antibody-induced thrombocytopenia in mice very much depends on the antigenic specificity of the antibody.[54]

Thrombocytopenia mediated by anti-αIIbβ3 mAbs is a Fc-dependent process, because $F(ab)_2$ fragments of these mAbs fail to produce thrombocytopenia.[54] Concomitantly to the thrombocytopenic effect, injection of anti-αIIbβ3 mAbs also results in acute systemic reactions. This can be suppressed by administration of platelet-activating factor (PAF) inhibitor without affecting anti-αIIbβ3 mediated thrombocytopenia. The source of PAF in this pathology has not been identified. However, an interaction of the Fc portion of platelet-associated antibodies with Fc gamma receptor (FcγR)-bearing cells of the reticuloendothelial system may be relevant because these cells are able to release PAF upon phagocytosis of opsonized cells.[54] In contrast, anti-GPIb-mediated thrombocytopenia shows only minor systemic effects in mice and thrombocytopenia can also be achieved by administration of anti-GPIb $F(ab)_2$ fragments.[54] This indicates that anti-GPIb-mediated platelet clearance involves an Fc-independent mechanism in mice. In line with this observation that anti-GPIb-mediated thrombocytopenia is independent from FcγR-bearing cells, patients with auto-antibodies against GPIb often appear resistant to treatment with steroids. A further progress in the understanding of how anti-GPIb mediates thrombocytopenia in mice was achieved by a recent study by Van der Wal et al.[55] In this study, it was found that anti-GPIb antibodies induce platelet activation and desialylation, P-selectin and PS exposure and apoptosis of platelets. Desialylation thereby seems to be essential in anti-GPIb-mediated thrombocytopenia as platelet activation as well as a reduction of the platelet count is abrogated under prior treatment with a neuraminidase inhibitor. Desialyated platelets are apparently cleared from the circulation by the Ashwell-Morell receptor (AMR) because blocking the AMR rescued the platelet count. Notably, the clearance of long-term refrigerated platelets (>48 h, 4 °C) similarly causes the desialylation of glycans on the platelet

surface and if transfused, these platelets display only a short life time and are removed by the AMR within hours. Interestingly, the enhanced clearance of these platelets mainly depends on exposed β-galactose on GPIbα.[56]

1.3.1.2 Secondary immune thrombocytopenia

Secondary ITP develops in the context of other disorders and its etiology is diverse.[49] It can be triggered by autoimmune disorders such as lupus erythematosus or the antiphospholipid syndrome.[49] Peripheral platelet destruction in immune-mediated drug-induced thrombocytopenia is caused by medication and drug-dependent antibodies which bind to platelet surface glycoproteins only in the presence of the sensitizing drug.[57-60] Secondary ITP can also be observed after infections with the human immunodeficiency virus (HIV) or the hepatitis C virus amongst others. HIV-induced thrombocytopenia can be caused by anti-HIV antibodies cross-reacting with platelet glycoproteins leading to an enhanced clearance of platelets from the circulation. Additionally, the infection of MKs with HIV may reduce the platelet production.[61] The hepatitis C virus can bind to the platelet membrane and attract anti-hepatitis C virus antibodies thereby causing platelet destruction by the immune system. Furthermore, hepatitis C infections can extensively damage the liver thus leading to a reduced production of thrombopoietin which is a glycoprotein hormone regulating platelet production.[62] The exact mechanisms of secondary ITP after infections with HIV and hepatitis C virus are not yet fully understood.

1.3.1.3 Non-immune thrombocytopenia

Non-immune thrombocytopenias can be induced through the side effects of drugs which e.g. affect platelet production in the bone marrow through direct myelosuppression.[59] Furthermore, thrombocytopenia can be an accessory syndrome of hereditary diseases e.g. the gray platelet syndrome (GPS), Bernard-Soulier syndrome (BSS) or Wiskott-Aldrich syndrome (WAS) which are also often associated with morphological alterations of the platelets. GPS is a rare disease and is characterised by a variable thrombocytopenia and enlarged platelets which lack α-granules and their contents. GPS is caused by a mutation in the BEACH domain of neurobeachin-like 2 (NBEAL2)[63] and patients exhibit a heterogeneous bleeding phenotype.[64] BSS is characterised by enlarged platelets and the absence of the functional GPIb-V-IX receptor complex on the platelet surface which is necessary to initiate platelet adherence to the exposed subendothelial matrix. Patients suffering from BSS often

exhibit prolonged bleeding symptoms.[65] A rare platelet disorder causing thrombocytopenia is the WAS which is caused by the mutation of the *WAS* gene. This gene is mainly expressed in haematopoietic cells. The severity of this disease correlates with the specific gene mutation and ranges from mild to severe haematopoietic dysfunctions.[66,67]

1.3.2 Haemostasis and thrombosis during thrombocytopenia

In general, thrombocytopenia rarely leads to severe bleeding[68] and is characterised by mild or no impairment of health. Thus, medical treatment of thrombocytopenia with functional platelets is recommended only at relatively low platelet counts of less than 30 platelets/nL blood.[50,69-71] However, it is widely accepted that the decision to treat thrombocytopenia should not entirely be based on the platelet count (PC), but rather made in the context of clinical symptoms and disease progression.[50,72] Indeed, studies in humans have shown that the bleeding risk at reduced PCs is influenced by the individual's age,[73,74] the occurrence of trauma,[75] genetic susceptibility, environmental effects, medication or comorbidity.[76-79] Similarly, studies in mice have shown that low PCs alone do not cause spontaneous bleeding, but rather a combination of a low platelet count and additional factors, such as binding of antibodies to endothelial cells,[80] inflammation,[81] or the nature of the target antigen of anti-platelet antibodies[54] determine the occurrence of haemorrhage.

On the other hand, the link between PCs and the occurrence of acute ischaemic disease states, such as myocardial infarction or stroke, remains unclear. Two studies revealed an increased incidence of thromboembolic events in humans suffering from ITP and proposed different mechanisms that may explain the thrombotic tendency.[48,82] Among these mechanisms, the presence of thrombogenic microparticles after platelet destruction and the antiphospholipid syndrome are the most commonly suggested risk factors in ITP. Thus thromboembolic events in humans with ITP are not uncommon showing that a reduced platelet count, at least in this setting, does not prevent the occurrence of thrombotic events. Even less is known about the thrombotic risk during thrombocytopenia unrelated to immune components. Multiple variables such as medication and comorbidity make it difficult to determine the contribution of platelets in these settings.

1.3.3 'Young' and 'young stressed' platelets and their properties

Under physiological conditions, continuous platelet production goes along with the removal of old platelets from the circulation. The platelet population in the circulation consists, therefore, of platelet subpopulations of different age. These platelet subpopulations display differences in morphology as well as heterogeneity in platelet function.[83,84] Young platelets are known to be large and the platelet attains its final size over time while circulating in the blood stream. Additionally, young platelets have been associated with pro-thrombotic properties.[82,84] In an early study by Hirsh et al. it was shown that young platelets of rabbits adhere to collagen more readily than older platelets.[85] Accordingly, Peng et al. showed by *in vivo* biotin-labelling of dog platelets that aged platelets became less responsive to thrombin.[86] Both studies, which were performed under steady-state conditions of physiological platelet production and removal, clearly indicate that over time platelet functionality decreases and that young platelets display higher activity than old ones.

Different from young platelets, so-called 'young stressed' platelets are platelets which have been produced under non-physiological conditions or during the recovery from acute thrombocytopenia by a fast release of (pro-)platelets from bone marrow MKs. They display an increased size, different morphology[87] and are present within hours after induction of thrombocytopenia by administration of anti-platelet serum in rats and precede any changes in size, ploidy, and number of MKs.[88] Similar to young platelets, young stressed platelets display a greater functional response compared to old platelets in rats[89] and rabbits.[83] Taking into account that large young stressed platelets are more active than old ones, the presence of these young platelets in ITP patients may, together with other factors, explain the paradoxically shortened bleeding time of ITP patients.[68] This pro-thrombotic effect is also widely discussed as possible cause for the increase of thrombotic events observed in patients suffering from ITP. However, more studies are necessary to address this hypothesis. Furthermore, more detailed research is required to elucidate how newly formed platelets under these circumstances evade activation during migration through collagen-rich bone marrow vessel walls.

1.3.4 Treatment of thrombocytopenia

As mentioned above, there are different causes for thrombocytopenia. The standard therapy of thrombocytopenia, therefore, considers besides the platelet count also the platelet

function, underlying diseases and the risk of bleeding. Furthermore, findings of an increased pro-thrombotic tendency in young stressed platelets partly present during ITP have to be considered. Before the beginning of treatment an accurate diagnosis of the underlying cause is, therefore, absolutely essential.[49]

Whereas for secondary thrombocytopenias or hereditary diseases the general therapy primarily tries to solve or attenuate the underlying mechanism which leads to a reduced PC, standard therapy for primary ITP can be divided into first and second line therapy. First line therapy includes glucocorticoids and the administration of intravenous immunoglobulins (IVIG) which dampens the immune system and acts through inhibitory Fc receptors.[72] Second line treatment involves splenectomy, treatment with rituximab which is a chimeric monoclonal antibody, or the administration of thrombopoietin receptor agonists such as romiplostin or eltrombipag.[74] Considering that thrombocytopenia is in the most cases anti-αIIbβ3 antibody (Fc-dependent) or anti-GPIb antibody-mediated (Fc-independent), which differ in their mechanism of platelet clearance, current first line therapy of primary ITP may have to be reconsidered. Indeed, a first study shows that IVIG treatment ameliorates αIIbβ3 auto-antibody related primary ITP, whereas GPIb auto-antibody mediated primary ITP is less responsive to this treatment. Identification of whether thrombocytopenia is anti-αIIbβ3 antibody or anti-GPIb antibody mediated may, therefore, be important for therapy and explain why some primary ITP patients are refractory to the standard treatment with IVIG or glucocorticoids.[90,91]

However, if patients display a permanently and strongly reduced platelet count (below 10 platelets/nL blood), e.g. due to the treatment with chemotherapeutics, guidelines recommend platelet transfusion.[92]

1.4 Arterial thrombosis and haemostasis models in mice

Platelets are essential for physiological haemostasis and play a major role in the occurrence of thrombotic diseases. Considerable progress in the understanding of platelet physiology and platelet signalling has been made by the *in vitro* investigations of platelets. *In vitro* studies, however fail to mimic the myriad of haemodynamic and spatiotemporal cellular interactions which prevail in the physiological environment of platelets under which thrombus formation takes place.[93] In order to circumvent this major shortcoming, a lot of

effort has been made to develop animal models which allow the investigation of thrombotic diseases and haemostatic plug formation *in vivo*. The most widely used laboratory animals are mice because they are small, easy to handle, highly fertile and can be kept in large numbers. Additionally, many genetically modified mice are available which allow the investigation of the functional relevance of proteins for platelet physiology.

Among these *in vivo* models, the tail bleeding time assay is closest to haemostatic plug formation in humans. A small injury, in mice preferably the amputation of 1 mm tail tip, is made and the time until haemostatic plug formation is either determined by absorption of blood with filter paper or by immersing the tail in saline solution. A study on haemostatic function in humans by applying a small standardized incision demonstrates, that humans show no increased bleeding tendency until the platelet count falls below 100 platelets/nL blood.[68]

In recent years, many mouse models of thrombotic diseases have evolved, each with its specific requirements and disadvantages. There are models for venous or arterial thrombosis and the site of injury ranges from large vessels to very small arterioles and venules of the microcirculation. Additionally, certain models seem to trigger thrombus formation through a thrombin and TF-driven pathway, whereas others trigger thrombus formation to a large extent through an ITAM-dependent pathway.

One of the most common mouse models of arterial thrombosis is the $FeCl_3$-induced injury of mesenteric arterioles or the carotid artery resulting in the formation of platelet-rich thrombi[94] which appear histologically similar to thrombi found in humans.[95] Until recently, it was commonly agreed that application of $FeCl_3$ leads to the generation of reactive oxygen species which denude the endothelium allowing platelets to adhere to the exposed ECM.[94] However, two recent studies show that the endothelium remains intact. Barr et al. describe a red blood cell-mediated mechanism of platelet adherence to the intact endothelium.[96] In agreement with this, Eckly et al. show that $FeCl_3$-treatment causes severe damage in all layers of the vessel wall without rupturing the internal elastic lamina. Rather, $FeCl_3$ damages proteins and induces a very strong presence of TF which activates the blood coagulation cascade thereby resulting in the generation of thrombin.[97] Another possibility to induce an injury is the systemic injection of the photo-reactive substance Rose Bengal which decomposes under light (λ_{ex} = 540 nm) thereby releasing reactive oxygen species which trigger endothelial denudation.[98]

The laser injury model can be performed in the microvasculature and by modulation of the laser exposure time and intensity, allows the infliction of differentiated injuries ranging from superficial to severe grades. Hence, using this model it has been shown that different types of injuries may involve different signalling pathways leading to platelet adherence. A superficial injury involves platelet activation and adherence via a vWF and collagen-mediated pathway. At sites of severe injuries, thrombin contributes to platelet activation and adherence additionally to collagen and vWF.[99,100]

A more direct way to induce endothelial denudation is a mechanically-inflicted injury. Due to the fragility of smaller vessels, it is mainly applied to larger arteries such as the abdominal aorta, the carotid artery or femoral artery. The mechanical denudation in these models is performed either by a firm compression with a forceps,[101] ligation with a filament[101] or by introduction of a guide wire into the vessel and its withdrawal with a rotating motion.[102] All mechanical thrombosis models lead to the exposure of collagen and have been shown to be more dependent on ITAM-signalling.[102]

Platelets play an important role in inflammation. Thrombosis and inflammation are closely related in the settings of ischaemic stroke which is a leading cause of disabilities and death world-wide.[103] Cerebral ischaemia accounts for 80% of all strokes and leads to a reduced oxygen and glucose supply of the brain which may result in infarction and consequently in neurological deficits.[104] Thrombolysis and/or thrombectomy to achieve vessel recanalization are, therefore, very important in ischaemic stroke treatment. However, despite successful recanalization, patients may still develop a secondary infarct growth. The mechanism of this so-called reperfusion injury is poorly understood but recent research shows that interactions of platelet GPIb and GPVI with the vessel wall are pathogenic factors in infarct progression by mediating a subsequent inflammatory response. This “thrombo-inflammatory” function of platelets in ischaemic stroke can be analysed in mice by the transient middle cerebral artery occlusion (tMCAO) model.[105] In this model a filament is inserted into the right common artery and advanced inside the internal carotid artery in order to occlude the origin of the middle cerebral artery. The filament is usually withdrawn after one hour to allow reperfusion and the global neurologic status as well as the extent of infarction is assessed 24 and 25 h after tMCAO, respectively.[106]

Using mice to study thrombus formation *in vivo* is supported by the quality and quantity of available experimental thrombosis and haemostasis models. Additionally, many receptors

and signalling pathways in platelets as well as the platelet ultrastructure are strikingly similar in mice and humans.[2,93,107] Despite this, the presented models remain artificial for several reasons. In murine thrombosis models, experimental injuries are normally induced in healthy blood vessels whereas arterial thrombosis in humans typically occurs in diseased vessels. Furthermore, human platelets display twice the size of murine platelets but platelet counts in humans are on average only one quarter of those in mice. Additionally, the expression of several proteins is partly different in mice compared to humans (e.g. protease-activated receptors (PARs), FcγRIIa), indicating that these proteins may serve different functions in different species.[93,107] Extrapolation of data obtained in mice to humans must, therefore, be carefully evaluated.[93]

1.4.1 Arterial thrombosis models in genetically modified mice

Physiological platelet function requires the coordinated action of a variety of proteins such as adapter proteins, surface receptors, proteins that are essential for cytoskeletal rearrangement as well as proteins involved in vesicle trafficking and granule release. A major progress in the understanding of the role of these proteins in platelet physiology was possible due to the availability of genetically modified mice**.** These mice offer the opportunity to investigate the impact of specific proteins on platelet signalling as well as on thrombosis and haemostasis.

Many proteins, among them prominent adapter proteins such as LAT, SLP-76 and Gads,[108] are part of the LAT signalosome which is essential for GPVI-mediated platelet activation.[109] In the following chapters, several proteins are introduced which have been shown or were considered to modulate GPVI-signalling. In this thesis, the respective genetically modified mouse strains were analysed *in vivo*.

1.4.1.1 CLP36

C-terminal LIM domain protein of 36 kDa (CLP36) belongs to the PDZ/LIM domain protein family. All PDZ/LIM family members contain at least one PDZ domain and one LIM domain in their protein structure. Members of this family such as actinin-associated LIM protein (ALP), reversion-induced LIM protein (RIL), Mystique and Enigma act as scaffold proteins and assist in actin cytoskeletal rearrangements by binding to filamentous actin-associated proteins. CLP36 belongs to the ALP subfamiliy and contains one C-terminal LIM and one N-terminal

PDZ domain.[110] In human platelets, CLP36 is associated with the platelet plasma membrane Ca^{2+}-ATPase (PMCA) which is essential to keep the cytosolic Ca^{2+} concentration low in resting platelets.[111] Furthermore, CLP36 is associated with stress fibers and actin filaments in activated platelets and endothelial cells.[112] In the human placental choriocarcinoma BeWo cell line, knockdown of CLP36 results in a reduced development of stress fibers and focal adhesion.[113] Additionally, CLP36 is important for α-actinin-1 recruitment to F2408 fibroblast stress fibers and the regulation of stress fiber dynamics.[114] In a recent study by Dr. Shuchi Gupta et al. from our group, CLP36 was shown to be the only member of PDZ/LIM domain protein family expressed in murine platelets. Absence of CLP36 in platelets resulted in enhanced GPVI-signalling while GPCR-signalling remained unaffected. The actin cytoskeletal rearrangements upon activation were unaltered in platelets lacking CLP36. The same results were obtained in mice which express a truncated form of CLP36 lacking the LIM domain.[115]

1.4.1.2 Grb2

Growth factor receptor-bound protein 2 (Grb2) is a ubiquitously expressed adapter protein that contains one Src homology 2 (SH2) domain flanked by two SH3 domains and is essential for several signalling processes. Grb2 links the epidermal growth factor receptor tyrosine kinase to Ras signalling in mammalian cells.[116] Furthermore, Grb2 is essential for early embryonic development and T and B cell development in mice.[117-119] In human platelets, Grb2 undergoes tyrosine phosphorylation[109] and interacts with LAT[120] upon activation with CRP or convulxin (CVX), respectively. Indeed, in a recent study by Dr. Sebastian Dütting et al. from our group the functional relevance of Grb2 in GPVI and CLEC-2-mediated platelet signalling due to the stabilization of the LAT signalosome has been demonstrated in mice.[121]

1.4.1.3 SLAP and SLAP2

Src-like adapter proteins (SLAP and SLAP2) are expressed in different cells and have been intensively investigated in lymphocytes. The two protein family members contain an SH3 and an SH2 domain next to unique N- and C-terminal regions.[122] In T and B cells, SLAP proteins are involved in the negative regulation of T cell receptor and B cell receptor signalling complexes as well as ubiqitination and trafficking of components thereof.[122] In human platelets, SLAP2 has been shown to negatively regulate GPVI-mediated platelet signalling indicating that SLAP family members may also have a function in GPVI-signalling in murine platelets.[123]

1.4.1.4 EFhd2

EF-hand domain containing 2 (EFhd2, Swiprosin-1) belongs to the EF-hand superfamily[124] which through the helix-loop-helix structure of the characteristic EF-hand motif is able to bind Ca^{2+}, thereby regulating cellular processes.[125] EFhd2 was first identified by Vuadens et al. as a cytoskeletal adapter protein in human $CD8^+$ cells[126] and is expressed in various cell types, including platelets. Structural analysis revealed that EFhd2 is a 240 amino-acid protein of 27 kDa which contains four myristylation sites, a coiled-coil domain at the C-terminus, three predicted SH3 binding sites and two EF-hand domains.[127] Human and murine EFhd2 share high homology (91%) and are homologous to EFhd1.[127]

In B cells, EFhd2 is involved in apoptosis by amplifying the B cell receptor-induced Ca^{2+} influx through positive regulation of Syk tyrosine phosphorylation.[127,128] As described above, Syk is an essential kinase which regulates platelet activation via ITAM-signalling implying a possible interaction of Syk with EFhd2 in platelets that might be relevant for GPVI-signalling. Besides this, EFhd2 is associated with lipid rafts of the immature B cell line WEHI231.[129] Lipid rafts are supposed to be membrane micro-domains with a high content of cholesterol, glycolipids and sphingolipids and thought to be involved in membrane associated processes such as receptor signalling, vesicular trafficking and cytoskeletal rearrangements. Lipid rafts have also been associated with SOCE in human platelets.[130]

Cytoskeletal rearrangements are important during shape change and platelet aggregation. Several proteins assemble actin monomers (G-actin) to filamentous structures (F-actin) and thereby regulate platelet structure and various cellular processes. In the human mast cell line HMC-1, EFhd2 co-localises with F-actin and regulates actin remodelling.[131,132] In B16F10 melanoma cells, EFhd2 was shown to be an actin-binding protein modulating lamellipodial dynamics by facilitating the formation of clustered F-actin. Thereby, EFhd2 induced a structural re-organisation of actin filaments thus regulating the accessibility of F-actin to cofilin. Overexpression of EFhd2 in these melanoma cells increased lamellipodia formation, whereas knockdown of EFhd2 had an inhibitory effect.[133] Additionally to these cell types, EFhd2 is also expressed in spleen, lung, liver and especially the brain.[127,134]

Next to the possible function of EFhd2 in cytoskeletal rearrangement and lipid rafts which may be relevant for platelet signalling, EFhd2 also shows interesting expression profiles in platelets and MKs during sepsis or upon stimulation. In the cecal ligation and puncture (CLP)

model of inflammation, sepsis-induced changes in the MK-platelet transcriptional axis generated platelets that were strongly lymphotoxic via the cytotoxic serine protease granzyme B. Interestingly, analysis of mRNA expression profiles of platelets 24 and 48 h after CLP revealed that EFhd2 was up-regulated 82- and 200-fold, respectively.[135] A second study showed a 1.5 fold up-regulation of EFhd2 in the rat and human platelet proteome upon stimulation with thrombin.[136]

Taken together, EFhd2 has been demonstrated to contribute to a variety of cellular functions in different cell types. In platelets, the function of EFhd2 is completely unknown.

1.5 Aim of this study

Platelets are important players in haemostasis and thrombosis which upon vessel damage become rapidly activated, form aggregates and finally lead to the formation of a haemostatic plug or a pathological thrombus. The understanding of how platelet activation is regulated is, therefore, of medical interest and may serve as a basis for the identification of new targets to treat ischaemic diseases and the development of new anti-thrombotic drugs.

In humans, the platelet count is at approximately 250 platelets/nL blood, however in a large context of diseases the platelet count may vary. A reduced platelet count does not necessarily correlate with an increased bleeding tendency, but there is only limited data available about the risk to develop a thrombotic disease during thrombocytopenia. The aim of this thesis was (I) to identify the impact of thrombocytopenia on different arterial thrombosis models as well as in the tMCAO model of ischaemic stroke in mice. In a different approach (II), early platelets of mice which were produced during the recovery from acute thrombocytopenia by a fast release of (pro-)platelets from the bone marrow were functionally characterised *in vivo* and *in vitro*.

The (III) aim of this thesis was the *in vivo* analysis of different genetically modified mouse strains which have been shown or were supposed to display abnormal GPVI-ITAM-signalling, namely *Clp36*$^{\Delta LIM}$, *Grb2*$^{fl/fl,Pf\text{-}4\text{-}Cre+/-}$, SLAP/SLAP2- and EFhd2-deficient mice. EFhd2-deficient platelets were also analysed *in vitro*.

2 Materials and methods

2.1 Materials

Standard chemicals were purchased from Roth and Sigma-Aldrich.

2.1.1 Chemicals and reagents

Chemicals and other materials are listed in Table 2.1.

Table 2.1: List of all reagents used.

Chemical/reagent	Supplier
2-methyl-2-butanol	Sigma-Aldrich (St. Louis, USA)
4-12% NuPage Bis-Tris gradient gels	Life Technologies (Carlsbad, USA)
6 x SDS gel loading dye solution	Thermo Scientifics (Waltham, USA)
ADP	Sigma-Aldrich (St. Louis, USA)
Agarose	Roth (Karlsruhe, Germany)
Ammonium persulfate (APS)	Roth (Karlsruhe, Germany)
Aptipamezole	Pfizer (New York, USA)
Apyrase grade III	Sigma-Aldrich (St. Louis, USA)
Beta-mercaptoethanol	Roth (Karlsruhe, Germany)
Bovine serum albumin (BSA)	AppliChem (Darmstadt, Germany)
Complete Mini protease inhibitors (+EDTA)	Roche Diagnostics (Mannheim, Germany)
Convulxin (CVX)	Enzo Life Sciences (Farmingdale, USA)
dNTP mix	Thermo Scientifics (Waltham, USA)
DyLight-488	Life Technologies (Carlsbad, USA)
EDTA	AppliChem (Darmstadt, Germany)
Epinephrine	Sigma-Aldrich (St. Louis, USA)
Ethidium bromide	Roth (Karlsruhe, Germany)
Fat-free dry milk	AppliChem (Darmstadt, Germay)
Fentanyl	Janssen-Cilag GmbH (Neuss, Germany)
Fibrilar type I collagen (Horm)	Nycomed (Opfikon, Switzerland)
Flumazenil	Delta Select GmbH (Dreieich, Germany)
Fluorescein-isothiocyanate (FITC)	Life Technologies (Carlsbad, USA)
Forene (isoflurane)	Abott (Abott Park, USA)
GeneRuler 1kb DNA ladder	Thermo Scientifics (Waltham, USA)
Haematoxylin	Roth (Karlsruhe, Germany)
High molecular weight heparin	Ratiopharm (Ulm, Germany)
Horseradish peroxidase-conjugated streptavidin	Dianova (Hamburg, Germany)
Human fibrinogen	Sigma-Aldrich (St. Louis, USA)

Igepal CA-630	Sigma-Aldrich (St. Louis, USA)
Iron chloride hexahydrat ($FeCl_3$ x $6H_2O$)	Roth (Karlsruhe, Germany)
Medetomidine	Pfizer (New York, USA)
Midazolam	Roche Pharma AG (Grenzach-Wyhlen, Germany)
Midori Green advanced DNA stain	Genetics Nippon Europe (Düren, Germany)
Naloxon	Delta Select GmbH (Dreieich, Germany)
PageRuler prestained protein ladder	Thermo Scientifics (Waltham, USA)
Phenol/chlorofom/isoamylalkohol	Roth (Karlsruhe, Germany)
Platelet-activating factor inhibitor CV-6209 (PAF)	Santa Cruz Biotechnology, (Santa Cruz, USA)
Pluronic F-127	Life Technologies (Carlsbad, USA)
Prostacyclin (PGI_2)	Sigma-Aldrich (St. Louis, USA)
R-phycoerythrin	EUROPA (Cambridge, UK)
Sodium chloride solution 0.9% (w/v)	B.Braun Melsungen AG (Melsungen, Germany)
SpheroTM Accu count fluorescent particles 5.2µm	Spherotech (Lake Forest, USA)
Taq-polymerase	Thermo Scientifics (Waltham, USA)
Taq-polymerase buffer (10 x)	Thermo Scientifics (Waltham, USA)
Thrombin (20 U/mL)	Roche Diagnostics (Mannheim, Germany)
Thrombin (100 /mL)	Sigma-Aldrich (St. Louis, USA)
Triton X-100	AppliChem (Darmstadt, Germany)
U46619	Enzo Life Sciences (Farmingdale, USA)
Western Lightning Chemiluminescence	PerkinElmer (Waltham, USA)
Fura-2 acetoxymethyl ester (AM)	Life Technologies (Carlsbad, USA)
Triphenyltetrazolium chloride (TTC)	Sigma-Aldrich (St. Louis, USA)
Aquatex aqueous mounting medium	Merck Co KG (Darmstadt, Germany)

Rhodocytin (RC) was a generous gift from Dr. Johannes Ebele (University Hospital Frankfurt, Germany). Collagen-related peptide (CRP) was kindly provided by Dr. Steve P. Watson (University of Birmingham, UK). Medetomidine, midazolam and fentanyl were used according to the regulation of the district government of Lower Frankonia (Bezirksregierung Unterfranken).

2.2 Antibodies

2.2.1 Primary and secondary antibodies

All antibodies used are listed in Table 2.2.

Table 2.2: List of all primary and secondary antibodies used.

Antibody	Supplier
Polyclonal rabbit anti-mouse EFhd2 and EFhd1	Dr. Sebastian Brachs and Dr. Dirk Mielenz, University of Erlangen, Germany[129]
Rat anti-mouse IgG-HRP	DAKO (Hamburg, Germany)
Goat anti-rabbit IgG-HRP	Cell Signalling (Cambridge, UK)
Rabbit anti-mouse platelet serum	Accurate Chemical (Westbury, USA)
Polyclonal rat anti-mouse GPIbα	Emfret Analytics (Eibelstadt, Germany)
Irrelevant rat IgG	Emfret Analytics (Eibelstadt, Germany)
Anti-phosphotyrosine (4G10)	Merck Millipore (Billerica, USA)

2.2.2 Monoclonal antibodies

Monoclonal antibodies (mAbs), generated and modified in our laboratory, are listed in Table 2.3. These mAbs were available non-labelled, FITC-labelled or PE-labelled if required. Anti-GPIX mAb was also available labelled with DyLight-488.

Table 2.3: List of all mAbs used.

Antibody	Clone	Isotype	Antigen	Reference
p0p4	15E2	IgG2b	GPIbα	[54]
p0p6	56F8	IgG2b	GPIX	[54]
DOM2	89H11	IgG2a	GPV	[54]
ULF1	96H10	IgG2a	CD9	[54]
JAQ1	98A3	IgG2a	GPVI	[137]
JON6	14A3	IgG2b	αIIbβ3	unpublished
LEN1	12C6	IgG2b	α_2	unpublished
INU1	11E9	IgG1	CLEC-2	[138]
JON/A	4H5	IgG2b	αIIbβ3	[139]
WUG1.9	5C8	IgG1	P-selectin	unpublished
MWReg30	5D7	IgG1	αIIbβ3	[140]

2.2.3 Buffers

For the preparation of all buffers ddH_2O from a MilliQ Water Purification System (Millipore, Schwalbach, Germany) was used. If necessary the pH was adjusted with 1 M HCl or 1 M NaOH. All buffers used are listed in Table 2.4.

Table 2.4: List of all buffer used.

Buffer	Components
50 x TAE buffer, pH 8.0	0.2 M TRIS, 5.7% (v/v) acetic acid, 10% (v/v) 50 mM EDTA
Acid-citrate-dextrose buffer (ACD), pH 4.5	85 mM tri-sodium citrate dehydrate, 65 mM anhydrous citric acid, 110 mM anhydrous glucose
Citrate buffer, pH 7.0	0.129 M sodium citrate
FACS buffer	PBS, 0.1% (w/v) BSA, 0.02% (w/v) NaN_3
IP buffer, pH 8.0	15 mM TRIS, 155 mM NaCl, 1 mM EDTA, 0.005% (w/v) NaN_3
Laemmli buffer for SDS-PAGE, pH 8.3	40 mM TRIS, 0.95 M glycine, 0.5% (w/v) SDS
Lysis buffer (DNA isolation)	100 mM TRIS, 5 mM EDTA, 200 mM NaCl, 0.2% (w/v) SDS, add 100 µg/ml Proteinase K
Phosphate buffered saline (PBS), pH 7.14	127 mM NaCl, 2.7 mM KCl, 1.5 mM KH_2PO_4, 8 mM Na_2HPO_4
SDS sample buffer, 2x	10% (v/v) β-mercaptoethanol, 10% (v/v) TRIS Buffer, 20% (v/v) glycerol, 4% (w/v) SDS, 0.02% (w/v) bromophenol blue
Separating gel buffer, pH 8.8	1.5 M TRIS
Stacking gel buffer, pH 6.8	0.5 M TRIS
Stripping buffer, pH 2.0	62.5 mM TRIS, 2% (w/v) SDS, 100 mM β-mercaptoethanol
TE buffer, pH 8.0	10 mM TRIS, 1 mM EDTA
Tris-buffered saline (TBS), pH 7.3	137 mM NaCl, 20 mM TRIS
Tyrode's buffer, pH 7.4	137 mM NaCl, 2.7 mM KCl, 12 mM $NaHCO_3$, 0.43 mM NaH_2PO_4, 2 mM $CaCl_2$, 1 m $MMgCl_2$, 5 mM HEPES, 0.35% (w/v) BSA, 0.1% glucose
TRIS buffer, pH 6.8	13% (w/v) TRIS
Washing buffer (Western blot)	0.1% (w/v) Tween 20 in PBS
Transfer buffer (Western blot)	50 mM TRIS ultra, 40mM glycine, 20% (v/v) methanol
Heparin buffer	20 U/mL heparin in TBS

2.2.4 Mice

Mice were bred in our animal facility and maintained on a standard chow diet. Specific pathogen free C57BL/6J and NMRI mice were purchased from Janvier Labs, Saint Berthevin, France. 129/Sv mice were kindly provided by Johannes Grosse, MD, Takeda Cambridge Ltd, UK. EFhd2-deficient mice on a C57BL/6J background were kindly provided by Dr. Sebastian

Brachs and Dr. Dirk Milenz, University of Erlangen, Germany and analysed in collaboration with Dr. Sebastian Dütting in our laboratory. *Clp36*$^{\Delta LIM}$ mice on mixed background were generated by Dr. Attila Braun and Dr. Shuchi Gupta in our laboratory. These mice express a truncated form of CLP36 lacking the LIM domain. SLAP/SLAP2-deficient mice on a Balb/c background were kindly provided by Dr. Leonard Dragone, University of Colorado, USA and analysed *in vivo* in collaboration with Deya Cherpokova in our laboratory. Mice carrying two loxP sites flanking exon 2 of the *Grb2* gene were kindly provided from Dr. Daniel Radtke and Dr. Lars Nitschke, University of Erlangen, Germany. *Grb2*$^{fl/fl,PF4\text{-}cre+/-}$ mice on a C57BL/6J background were generated in our laboratory by Dr. Sebastian Dütting and Timo Vögtle by crossing of these mice with mice carrying a Cre recombinase under the control of the MKs/platelet-specific platelet factor 4 promoter. *Grb2*$^{fl/fl,PF4\text{-}cre+/-}$ mice lack Grb2 only in platelets and MKs. Mice were sacrificed by cervical dislocation in strict accordance with the guidelines of the Federation of the European Laboratory Animal Science Association (FELSA). Animal studies were approved by the district government of Lower Franconia (Bezirksregierung Unterfranken). Mice were between 6 and 12 weeks of age, if not indicated differently.

2.3 Methods

2.3.1 Genotyping of mice

2.3.1.1 Isolation of murine genomic DNA

To isolate murine genomic DNA an approximately 5 mm^2 piece of the mouse ear or the mouse tail tip (1 mm) was cut off and dissolved in 500 µL lysis buffer containing proteinase K (100 µg/mL) under shaking conditions (1000 rpm) at 56 °C overnight. Then, 500 µL of a phenol/chloroform/isoamylalkohol mixture was added to the sample tubes. After vigorous vortexing, the samples were centrifuged at 10,000 rpm for 10 min at room temperature (RT) to obtain phase separation. The supernatant of the sample was then transferred into a tube containing 700 µL isopropanol. The sample was vortexed again and centrifuged at 14,000 rpm for 10 min at 4 °C. The precipitated DNA at the bottom of the tube was then washed twice with 70% ethanol at 14,000 rpm for 10 min and dried at 37 °C. Finally, the DNA pellet was resuspended in 50 µL TE buffer by shaking at 400 rpm at 37 °C for 30 min. 1 µL of this solution was used for polymerase chain reaction (PCR).

2.3.1.2 Detection of the Efhd2 allele by PCR

Two PCRs are needed to detect the wild-type allele and/or the knock-out allele of *Efhd2*$^{+/+}$, *Efhd2*$^{-/-}$ and *Efhd2*$^{+/-}$ mice. The band size of the amplified DNA sequence of the wild-type- and the knock-out allele was 641 bp and 277 bp, respectively. For genotyping of the EFhd2 mouse strain, the composition of the sample (Table 2.5) with the respective primers (Table 2.7 and Table 2.8) was subjected to the PCR program shown in Table 2.6.

Table 2.5: Composition of the sample for PCR amplification.

Buffer	Quantity
Taq buffer (10x)	5 µL
25 mM $MgCl_2$	5 µL
10 mM dNTPs	1 µL
Primer A	1 µg
Primer B	1 µg
DNA	1 µL
DMSO	1.5 µL
Taq polymerase	0.5 µL
H_2O	Add up to 50 µL

Table 2.6: PCR program to detect wild-type and knock-out allele.

Step	T/°C	Time
1	95 °C	2 min
2	95 °C	30 s
3	58 °C	30 s
4, cycle back 29x to step 2	72 °C	30 s
5	72 °C	5 min
6	22 °C	hold

Table 2.7: Primers for the detection of the wild-type allele.

Primer	Primer sequence
3´SBpV-fwd	5´ GGT CAA GTT TAG TCC TCG G 3´
3´SBpV-rev	5´ TTC ATC AGT CAA ATG GCT G 3´

Table 2.8: Primers for the detection of the knock-out allele.

Primer	Primer sequence
βgal1-fwd	5´ AAC TGG CAG ATG CAC G 3´
βgal1-rev	5´ GCG CGT AAA AAT GCG 3´

2.3.1.3 Agarose gel electrophoresis

For genotyping, the products after PCR amplification were separated by agarose gel electrophoresis. For this, agarose was dissolved in TAE buffer (1.5% (w/v)) by heating in a microwave. After heating, 5 µL ethidium bromide (2 mg/mL) or 5 µL Midori green were added. The liquid was then poured into a gel tray with combs. After the gel became solid, it was placed in an electrophoresis chamber with TAE buffer. The PCR products were then diluted with 5 µL 6x loading buffer and loaded into the slots of the gel. One slot was used to determine the size of the PCR products and loaded with GeneRuler 1 kb DNA ladder. The electrophoresis chamber was run at 120 V. To visualise the band size the gel was placed under UV light.

2.3.2 *In vitro* analysis of platelet function

2.3.2.1 Preparation of washed platelets and platelet-rich plasma

Mice were anesthetised by isoflurane inhalation and bled from the retro-orbital plexus into a tube containing 300 µL 20 U/mL heparin in TBS or ACD buffer. From this sample platelet-rich plasma was obtained by two centrifugation steps. After the first centrifugation step at 1,800 rpm for 5 min at RT (Eppendorf 5415C), the supernatant and buffy coat were transferred into a new tube and a second centrifugation at 800 rpm (6 min, RT) was performed to obtain platelet-rich plasma (prp). The prp was then centrifuged at 2,800 rpm for 5 min in the presence of 0.1 µg/mL prostacyclin (PGI_2) and 0.02 U/mL apyrase and the resulting pellet was resuspended in 1 mL Tyrode's buffer without Ca^{2+} and incubated again with PGI_2 and apyrase for 10 min at 37 °C. During the incubation interval the platelet count was determined with a Sysmex cell counter KX 21N (Sysmex Deutschland GmbH, Germany). Finally, a second washing step was performed at 2,800 rpm for 5 min and the resulting pellet was resuspended in Tyrode's buffer without Ca^{2+} in the presence of PGI_2 and apyrase and left to incubate for 30 min at 37 °C prior to the experiment.

2.3.2.2 Calculation of the platelet count

2.3.2.2.1 Sysmex cell counter

To calculate the platelet count, mice were anaesthetised using isoflurane anaesthesia and 50 µL blood was drawn from the retro-orbital plexus with heparinised microcapillaries. The

blood sample was transferred into a tube containing 300 µL 20 U/mL heparin and further diluted to 1:20 with Tyrode's buffer. The platelet count of this sample was analysed in a Sysmex cell counter KX 21N (Sysmex Deutschland GmbH, Germany).

2.3.2.2.2 Flow cytometric analysis of the platelet count

Another method used to determine the platelet count, especially for thrombocytopenic mice, was flow cytometry (FACS). The blood sample (50 µL) was further diluted with Tyrode's buffer to a final dilution of 1:20. 50 µL of the diluted sample were incubated with PE-labelled anti-integrin αIIbβ3 (14A3) antibody and FITC-labelled anti-GPV antibody (89H11) at saturating concentrations for 15 min at RT. This double antibody staining was used to identify the platelet population in whole blood. After addition of 500 µL PBS, a defined number of fluorescent beads (AccuCount fluorescent particles, 5.2 µm) were added and the sample was analysed on a FACSCalibur (Becton Dickinson, USA) (Figure 2.1).

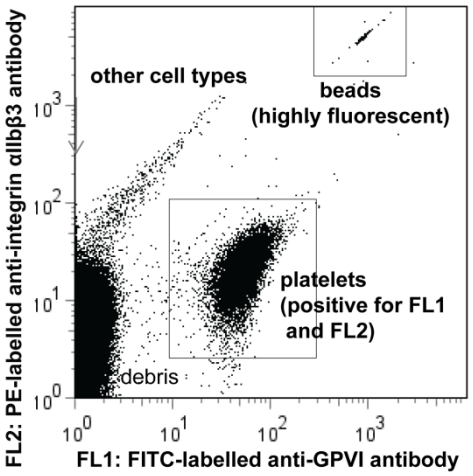

Figure 2.1: Flow cytometric calculation of the platelet count with beads. Platelets of a 50 µL blood sample were stained with FITC-labelled anti-GPV antibody (89H11) and PE-labelled anti-integrin αIIbβ3 (14A3) antibody. Platelets can be identified in whole blood as the cell population which is positive for FL (fluorescence) 1 and FL2. A defined number of highly fluorescent particles was detected in the upper right corner and used to calculate the platelet count.

The FACS settings to determine the platelet count were according to Table 2.9, Table 2.10 and Table 2.11. The platelet count was calculated as following:

$$\frac{A}{B} \times \frac{C}{D} = Number\ of\ cells\ per\ \mu L$$

A = number of events for the test sample; B = number of events for the fluorescent particles; C = number of fluorescent particles per 50 µL; D = volume of test sample initially used in µL.

Table 2.9. Detector/Amps FACS settings for the calculation of the platelet count.

Parameter	Detector	Voltage
P1	FSC	E01
P2	SSC	299
P3	Fl1	630
P4	Fl2	518
P5	Fl3	150

Table 2.10: Threshold FACS settings for the calculation of the platelet count.

Value	Parameter
253	FSC-H
52	SSC-H
52	Fl1-H
52	Fl2-H
52	Fl3-H

Table 2.11: Compensation FACS setting for the calculation of the platelet count.

Value	Parameter
Fl1	2.4% of Fl2
Fl2	7.0% of Fl1
Fl2	0% of Fl3
Fl3	0% of Fl2
Fl1	2.4% of Fl2

2.3.2.3 Western blotting

2.3.2.3.1 Western blotting of platelet lysates

Platelet-rich plasma was prepared as described under 2.3.2.1 and washed twice in PBS/5 mM EDTA and centrifuged at 2,800 rpm for 5 min. The final pellet was then lysed in IP buffer containing protease inhibitors and 1% NP-40. The resulting platelet lysate corresponded to 2 x 10^6 platelets/µL.

To separate the proteins, 12% or 15% SDS-PAGE with a 4% stacking part assembled in a chamber filled with Laemmli buffer were used. Before loading the gel, the protein lysates were mixed with 4x SDS sample buffer and boiled at 95 °C for 5 min. During the stacking the gel ran at 14 mA, then the current was increased to 25 mA.

For semi-dry immunoblotting, the gel and 16 sheets of blotting paper (Whatman, USA) were soaked in transfer buffer, the polyvinylidene difluoride (PVDF) membrane was first worked in methanol and then in transfer buffer. The blotting stack was assembled as follows: eight

sheets of blotting paper, the PVDF membrane, the gel and eight more sheets of blotting paper. The blotting was performed for 30-60 min at 50 mA. After blotting the PVDF membrane was blocked overnight at 4 °C or for 2 h at RT under shaking conditions with either 5% BSA or 5% fat-free milk dissolved in TBS. The membranes were then incubated with the respective primary antibody in 5% BSA or 5% fat-free milk dissolved in TBS overnight at 4 °C under shaking conditions. After three washing steps for 10 min with washing buffer the HRP-coupled secondary antibody dissolved in washing buffer was applied to the membrane for 1 h at RT. After this step the membrane was again washed three times with washing buffer for 10 min. Finally, the proteins were visualised using enhanced chemiluminescence (ECL).

2.3.2.3.2 Western blotting for tyrosine phosphorylation assay

To investigate different phosphorylation patterns of platelets upon stimulation, washed platelets (0.7 x 10^6 platelets/µL) were stimulated with 0.01 U/mL thrombin, 5 µg/mL CRP or 0.1 µg/mL CVX at constant stirring conditions (1,000 rpm) at 37 °C. To stop the reaction, ice-cold lysis buffer was added to the platelet suspension. The platelet lysates were then separated under reducing conditions by SDS-PAGE on NuPAGE 4-12% Bis-Tris gradient gels and transferred onto a PVDF membrane as described above. The membrane was blocked for 1 h at RT with 5% BSA in TBS-T and then incubated overnight at 4 °C with the primary α-phosphotyrosine antibody 4G10. The membrane was then washed four times for 15 min in washing buffer and eventually incubated with the secondary rabbit anti-mouse immunoglobulin-HRP. After washing, proteins were visualised by application of ECL to the membranes. Tyrosine phosphorylation assays were carried out in collaboration with Dr. Shuchi Gupta in our laboratory.

2.3.2.4 Flow cytometric analysis of platelets

To determine glycoprotein expression levels in platelets, samples of diluted blood were incubated with FITC-labelled monoclonal antibodies for 15 min at RT and analysed on a FACSCalibur.

For platelet activation, 50 µL of the diluted blood samples were washed twice in Tyrode's buffer without Ca^{2+} and then diluted in Tyrode's buffer containing 2 mM $CaCl_2$. Samples were activated with different agonists, stained with FITC-coupled anti-P-selectin antibody and PE-coupled JON/A antibody at saturating concentrations for 15 min at 37 °C. To stop the

reaction 500 µL PBS were added to the samples. For the analysis of platelet activation the following FACS settings were used (Table 2.12, Table 2.13 and Table 2.14).

Table 2.12: Detector and Amps FACS settings used for determination of the glycoprotein expression levels and platelet activation.

Parameter	Detector	Voltage
P1	FSC	E01
P2	SSC	380
P3	Fl1	650
P4	Fl2	580
P5	Fl3	150

Table 2.13: Threshold FACS settings used for determination of the glycoprotein expression levels and platelet activation.

Value	Parameter
253	FSC-H
52	SSC-H
52	Fl1-H
52	Fl2-H
52	Fl3-H

Table 2.14: Compensation FACS settings used for determination of the glycoprotein expression levels and platelet activation.

Detector	Setting
Fl1	2.4% of Fl2
Fl2	7.0% of Fl1
Fl2	0% of Fl3
Fl3	0% of Fl2

2.3.2.5 Aggregation

To study the aggregation of platelets in response to different agonists, 50 µL washed platelets or prp from heparinised blood adjusted to a concentration of 0.5 x 10^6 platelets/µL was diluted with 110 µL Tyrode's buffer containing 2 mM Ca^{2+}. To this platelet suspension agonists (concentrated 100 x) were added and light transmission was recorded over a 10 min observation period on an Apact 4 channel optical aggregation system (APACT, Hamburg, Germany) under stirring conditions at 37 °C. In order to calibrate the level of aggregation, the platelet suspension was set as 0% aggregation, whereas Tyrode's buffer (for washed platelets) or plasma (for prp) was set as 100% aggregation. The aggregation of washed

platelets was performed in the presence of 100 µg/mL fibrinogen. For thrombin induced aggregation, Tyrode's buffer containing 2 mM Ca^{2+} without fibrinogen was used.

2.3.2.6 Platelet adhesion under flow conditions

Coverslips (24 x 60 mm) were coated with 200 µg/mL fibrillar type I collagen solution overnight at 37 °C. One hour prior to the experiment, the coverslips were blocked with 1% BSA in H_2O. Mice were bled (700 µL) from the retro-orbital plexus using isoflurane anaesthesia and the blood was collected into a tube containing 300 µL 20 U/mL heparin buffer. Platelets were then labelled with 5 µL of a 1:10 dilution of a Dylight-488 conjugated anti-GPIX antibody (56F8) for 5 min at 37 °C. Finally, the blood was filled into a syringe and the perfusion studies were performed in a transparent flow chamber. The flow chamber covered with the coated coverslips form a chamber with 50 µm depth. Perfusion of the blood through this chamber was performed using a pulse-free pump using shear rates resembling those in arteries. Depending on the shear rates of 1000 s^{-1}, 1700 s^{-1} or 7700 s^{-1}, each perfusion takes 5, 4 or 2 min, respectively. Thereafter, the chamber was washed 1-4 min with Tyrode's buffer at the same shear rate to remove unbound platelets. At least five different phase contrast and fluorescent images were recorded from five different visual fields. Image analysis was performed with MetaMorph software (Visitron, Germany). Thrombus formation was analysed as the mean percentage of the total area covered by platelets/thrombi in phase contrast images. Mean integrated fluorescence intensity per mm^2 gave an indication about thrombus size and volume.

2.3.2.7 Phosphatidylserine exposure

Washed platelets were adjusted to 5 x 10^7 platelets/mL in Tyrode's buffer containing 2 mM Ca^{2+}. 50 µL of this platelet suspension were activated with different agonists and then incubated with 10 µL Annexin-A5 DyLight-488 for 15 min at RT. The samples were then analysed with a FACSCalibur with the settings described in Table 2.12, Table 2.13 and Table 2.14.

2.3.2.8 Clot retraction

To study clot retraction, platelets were adjusted to a concentration of 3 x 10^8 platelets/mL in platelet poor plasma (ppp). In order to contrast the clot, 1 µL of red blood cells, which were left over from the platelet preparation, were added to 250 µL of this platelet suspension.

Additionally, the platelet suspension was adjusted to a concentration of 20 mM $CaCl_2$ prior to the experiment. To induce clotting, 4 U/mL thrombin were added to the platelet suspension and clotting was recorded at 37 °C without stirring for 4 h by taking images at different time points.

2.3.2.9 Platelet spreading assay

Coverslips (24 x 60 mm) were covered with 100 µL of a 100 µg/mL fibrinogen solution and left overnight in a humid chamber at 4 °C. One hour prior to the experiment, the cover slides were blocked with 1% (w/v) BSA in PBS, pH 7.14. Washed platelets were prepared and adjusted to a concentration of 1.5 x 10^8 platelets/mL. After stimulation with thrombin (0.01 U/mL) the platelet suspension was immediately placed on the coated coverslips. At indicated time points the platelets were fixed with 4% PFA in Tyrode's buffer and counted with an inverted microscope (Zeiss HBO 100, 100 x objective, Zeiss, Germany) using Metavue software. Four different stages of platelet spreading spreading were evaluated: stage 1 - roundish; stage 2 - filopodia only; stage 3 - filopodia and lamellipodia; stage 4 - fully spread.

2.3.2.10 Intracellular Ca^{2+} measurements

Washed platelets in Tyrode´s buffer without Ca^{2+} were loaded with fura-2 AM (5 µM) in the presence of pluronic F-127 (0.2 µg/mL) for 20 min at 37 °C. To remove extracellular dye, platelets were centrifuged for 5 min at 2,800 rpm and resuspended in Tyrode's buffer containing 1 mM Ca^{2+}. Platelets were then activated under stirring conditions with the respective agonist and fluorescence was measured with an LS 55 fluorimeter (PerkinElmer, USA). The excitation wavelength was alternated between 340 and 380 nm and the emission was measured at 509 nm. Each measurement was calibrated adding 1% Triton X 100 to determine the maximal Ca^{2+} concentration, followed by adding EGTA to determine the baseline.

2.3.3 *In vivo* models in mice

2.3.3.1 Anaesthesia

For all experiments mice were anaesthetised intra-peritoneally with a combination of medetomidine/fentanyl/midazolam (50/500/5 mg/g bodyweight) or inhalation of isoflurane.

2.3.3.2 In vivo *platelet depletion in mice*

There are different methods to reduce the platelet count and in this dissertation three different antibody-mediated approaches were used.

For platelet depletion in chapter 3.1, mice received different amounts of polyclonal rat anti-mouse GPIbα antibody in PBS intravenously 12 hours prior to the experiment. Control mice received the same volume of vehicle control (PBS) or irrelevant rat IgG. Alternatively, the platelet count was reduced by intravenous injection of different amounts of rabbit anti-mouse platelet serum in PBS. The platelet count for each mouse was determined prior to the experiment.

For platelet depletion in chapter 3.2 the mice received 100 µg polyclonal rat anti-mouse GPIbα or 100 µg monoclonal rat anti-mouse αIIbβ3 in combination with PAF inhibitor CV-6209 (3mg/kg bodyweight). Control mice received the same volume of vehicle control (PBS) or irrelevant rat IgG.

2.3.3.3 Determination of platelet life span

Mice were injected intravenously with 5 µg of the DyLight-488 conjugated anti-GPIX antibody (56F8). The percentage of GPIX-positive cells was determined by flow cytometry 1 h (day 0) after injection and was followed until day 5.

2.3.3.4 Mechanical injury of the abdominal aorta

The abdominal cavity of anaesthetised mice was opened to expose the abdominal aorta. An ultrasonic flowprobe (0.5PSB699; Transonic Systems, USA) was placed around the abdominal aorta, and thrombus formation was induced by a single firm compression with a forceps upstream of the flowprobe. Blood flow was monitored for 30 minutes (Figure 2.2 A).

2.3.3.5 Carotid artery injury model

The right carotid artery was exposed through a vertical midline incision in the neck. An ultrasonic flowprobe was placed around the vessel and thrombosis was induced by topical application of a 0.5 mm by 1 mm filter paper saturated with the indicated concentration of $FeCl_3$ for a certain time interval. Blood flow was monitored with an ultrasonic flowprobe (0.5PSB699, Transonic System, USA) for 30 min or until full occlusion (> 5 minutes) of the vessel occurred (Figure 2.2 B).

2.3.3.6 $FeCl_3$-induced injury of mesenteric arterioles

Mice were anesthetised and intravenously injected with 1 µL of DyLight-488-conjugated anti-GPIX antibody (56F8) (1.5 µg/mL) to label platelets *in vivo.* The mesentery was then gently exteriorised through a midline abdominal incision. Mesenterial arterioles with a diameter of 35-60 µm were visualised with an inverted Axiovert 200 (Zeiss, Germany) at 10x magnifications. The microscope was equipped with a 100 W mercury arc lamp to measure fluorescence and a CoolSNAP-EZ camera (Visitron, Germany). The injury was induced by topical application of a 3 mm^2 filter paper which was saturated with 20 % $FeCl_3$. Two time points were recorded: time to appearance (adhesion) of first thrombi and time to vessel occlusion. The observation period after injury was 40 min or until complete occlusion of the vessel occurred (no blood flow for >1 min). MetaMorph software (Visitron, Germany) was used to record and analyse the digital images. Mice were between 4 and 5 weeks of age (15-18 g) (Figure 2.2 C).

2.3.3.7 Tail bleeding time assay in saline solution

Mice were anesthetised, 1 mm of the tail tip was amputated with a scalpel and the tail was immersed in 0.9% (w/v) saline solution at 37 °C. The time to complete arrest of bleeding (no blood flow for 1 min) was determined. Experiments were stopped after 20 min (Figure 2.2 D, left panel).

2.3.3.8 Tail bleeding time assay with filter paper

Mice were anesthetised and 1 mm of the tail tip was amputated with a scalpel. Tail bleeding was checked at 20 s intervals by gently absorbing blood with filter paper without touching the wound site. Bleeding was determined to have ceased, if no blood was observed on the paper. Experiments were stopped after 20 min (Figure 2.2 D, right panel).

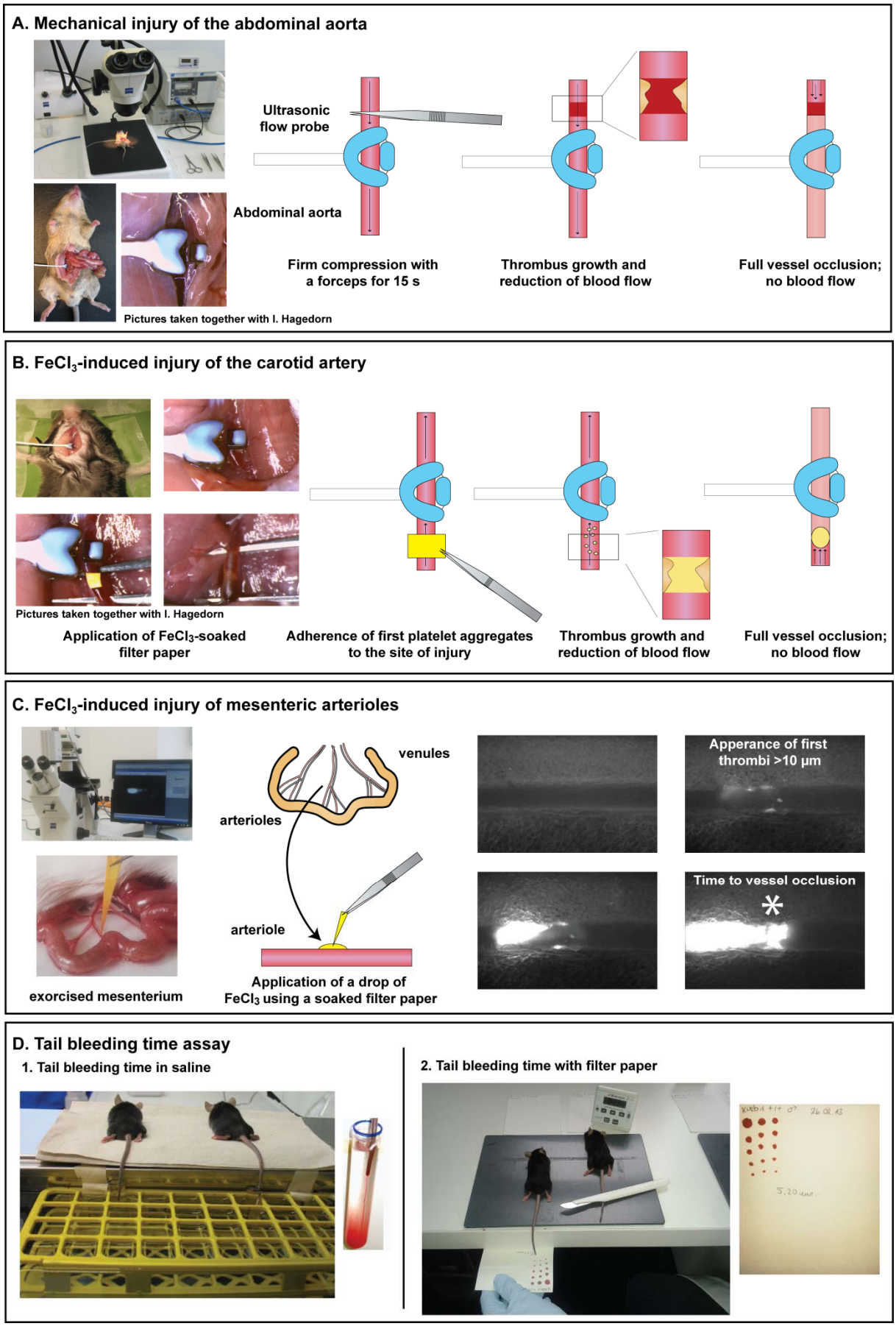

Figure 2.2: Detailed description and operation schemata for applied murine *in vivo* models.

2.3.3.9 Transient middle cerebral artery occlusion model

Mice were anaesthetised by inhalation of isoflurane and transient middle cerebral artery occlusion (tMCAO) was performed using the intraluminal filament (6021PK10; Doccol Corporation USA) technique. For this a thread was advanced through the carotid artery into the middle cerebral artery to reduce the cerebral blood flow. This thread was removed after one hour to allow reperfusion. The extent of infarction was assessed 25 h after reperfusion on 2,3,5-triphenyltetrazolium chloride (TTC)-stained brain sections. The global neurologic status 24 h after tMCAO was scored by two independent blinded investigators using the Bederson test. [141] Motoric function and coordination were graded 24 h after tMCAO using the grip test. These experiments were carried out in collaboration with Dr. Peter Kraft in the group of Prof. Guido Stoll, Department of Neurology, University of Würzburg, Germany.

2.3.4 Electron microscopy

2.3.4.1 Transmission electron microscopy

To prepare platelets for transmission electron microscopy (TEM), a suspension of washed platelets (5×10^8 platelets/mL) in Tyrode's buffer was fixed by adding cacodylate buffer containing 5% glutaraldehyde for 10 min at 37 °C followed by an incubation step of 1 h at RT. The samples were then further diluted 1:10 in cacodylate buffer, washed three times (5 min, 1,000 g) in the same buffer, resuspended in cacodylate buffer containing 2% low melting agarose (45 °C) and finally centrifuged for 5 min at 14,000 g (37 °C). 100 µL of the sample were then incubated on ice for 10 min until hardening, cut into 1 mm^2 pieces and stored in cacodylate buffer. The sample was further fixed by incubation with cacodylate buffer containing 1% OsO4 for 45 min. After washing twice with ddH_2O, incubation for 1 h at 4 °C in 2% uranylacetate in ddH_2O and three further washing steps with ddH_2O, the samples were dehydrated in 70% (4 x 5 min), 96% (3 x 15 min) and 100% (2 x 15 min) ethanol. Further processing of the sample was done by incubation in 100% propylene oxide (2 x 10 min) and 1 h in a 1:1 mixture of propylene oxide and epon under rotating conditions. Two further incubations in epon at RT were performed before the samples were embedded in gelatine capsules and left 48 h for drying at 60% relative humidity. A Leica Ultracut microtom UCT (Leica Microsystems, Germany) was used to cut 50 nm sections from these samples which were contrasted and analysed on an EM900 electron microscope (Zeiss, Germany). The

sample preparation and electron microscopic analysis were performed in collaboration with Jonas Müller in our laboratory.

2.3.5 Histology

2.3.5.1 Preparation of paraffin sections

The spleen or femur was removed from the animal and immediately fixed in PBS plus 4% PFA overnight at 4 °C. The femur was additionally decalcified in 10% EDTA. Afterwards, organs were dehydrated and embedded in paraffin. To prepare 3 µm paraffin sections the organs were cut using a Microm Cool Cut HM 355(Microm GmbH, Germany).

2.3.5.2 Haematoxylin and eosin staining

The sections were deparaffinised by two washing steps in xylene (5 min). Rehydration was performed by incubation with a 100, 90, 80 and 70% ethanol series for 2 min and a final washing step with ddH_2O. The sections were then stained with haematoxylin for 25 s and kept under running tab water for 5 min before staining with eosin for 2 min. After washing with ddH_2O, dehydration was performed with the reverse ethanol series. Finally, the sections were incubated with two steps of xylene for 5 min each and left to dry for 30 min. Aquatex aqueous mounting medium was then applied to the sections to seal the section with an object plate. The sections were analysed using a Leica DHI 4000B inverse microscope equipped with a Leica digital camera (Leica Microsystems, Germany).

2.3.6 Statistics

For statistical analysis between two groups of mice we applied the student's t-test. For statistical analysis between more than two experimental groups the one-way analysis of variance (ANOVA) [142] with Tukey as post-hoc test was applied. All statistical evaluation was done with OriginPro 8.6 (Origin Lab, USA). For test of independence the two-tailed Fisher`s test[143] for control versus the respective group was used. P <0.05 compared to control was considered statistically significant (p <0.05 = ∗; <0.01 = ∗∗; <0.001 = ∗∗∗).

3 Results

3.1 Analysis of the haemostatic and thrombotic function of platelets in thrombocytopenic mice

3.1.1 Injection of anti-GPIbα antibody induces thrombocytopenia dose-dependently

To study the impact of the platelet count on haemostasis and (experimental) thrombosis in mice, thrombocytopenia was induced by injection of polyclonal anti-GPIbα antibody which depletes circulating platelets independently of immune effector mechanisms.[54,144] In a first set of experiments, the antibody doses required to achieve defined PCs 12 hours after injection were determined. Injection of vehicle (PBS) or rat IgG (100 µg/mouse) had no detectable effect on the PC in control mice which averaged at approximately 1,100 platelets/nL blood and was similar to that previously reported by others.[1,145] The injection of increasing amounts (1-5 µg) of the anti-GPIbα antibody reduced the PC dose-dependently. Whereas the injection of 1.0 µg antibody reduced the platelet count to 635 ± 210 platelets/nL blood, a more severe thrombocytopenia to 592 ± 268; 391 ± 144; 307 ± 77; 147 ± 42 and 121 ± 52 platelets/nL blood was induced by 1.5; 2.0; 3.0; 4.0 and 5.0 µg antibody, respectively. To induce virtually complete platelet depletion (<15 platelets/nL blood), mice received 100 µg of the anti-GPIbα antibody (Figure 3.1).

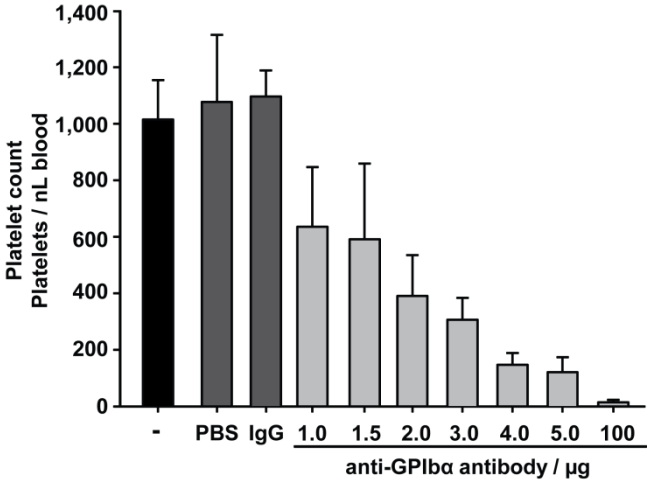

Figure 3.1: Injection of anti-GPIbα antibody induced thrombocytopenia dose-dependently. Mice were injected with PBS, IgG negative control or increasing amounts of anti-GPIbα antibody (1.0; 1.5; 2.0; 3.0; 4.0, 5.0 or 100 µg). The platelet counts were determined 12 hours after injection. Untreated mice (-) are shown as a control. The values represent the platelet count ± standard deviation (SD) for at least five mice per group.

Importantly, no signs of spontaneous bleeding in such severely thrombocytopenic mice were observed during visual inspection of the skin and inner organs. However, upon vessel injury during blood sampling or surgery, animals depleted to less than <15 platelets/nL blood had difficulties to seal the wound and showed increased and prolonged bleeding at the site of injury (data not shown).

3.1.2 Anti-GPIbα antibody treatment does not affect the remaining platelet population

To study possible effects of the anti-GPIbα antibody treatment on the circulating platelet population, mice received 2.0 µg antibody and platelets were analysed 12 hours after injection by flow cytometry. At this time point the PC was reduced to about 30% (334 ± 86 platelets/nL blood, control was 1,100 ± 99 platelets/nL blood) and compared to controls a significant increase of the mean fluorescence intensity (MFI) of major glycoproteins was detectable (Figure 3.2 A) and appeared visually as a shoulder in the respective histograms (Figure 3.2 C). By detailed analysis, this increase was attributed to the appearance of a small population of newly generated platelets displaying an increased size in flow cytometry and increased surface expression levels of prominent platelet glycoprotein receptors (Figure 3.2 D, left panel). If the newly appeared shoulder was excluded from analysis by its forward scatter/side scatter (FSC/SSC) characteristics, the size and surface glycoprotein expression levels in the main platelet population were found unaltered compared to vehicle-treated mice (Figure 3.2 D, right panel). Interestingly, we did not detect any changes in platelet size in anti-GPIbα antibody-treated mice in a Sysmex cell counter (Figure 3.2 B), indicating that alterations in platelet size were only minor and, therefore, only detectable by more sophisticated methods based on light scattering.

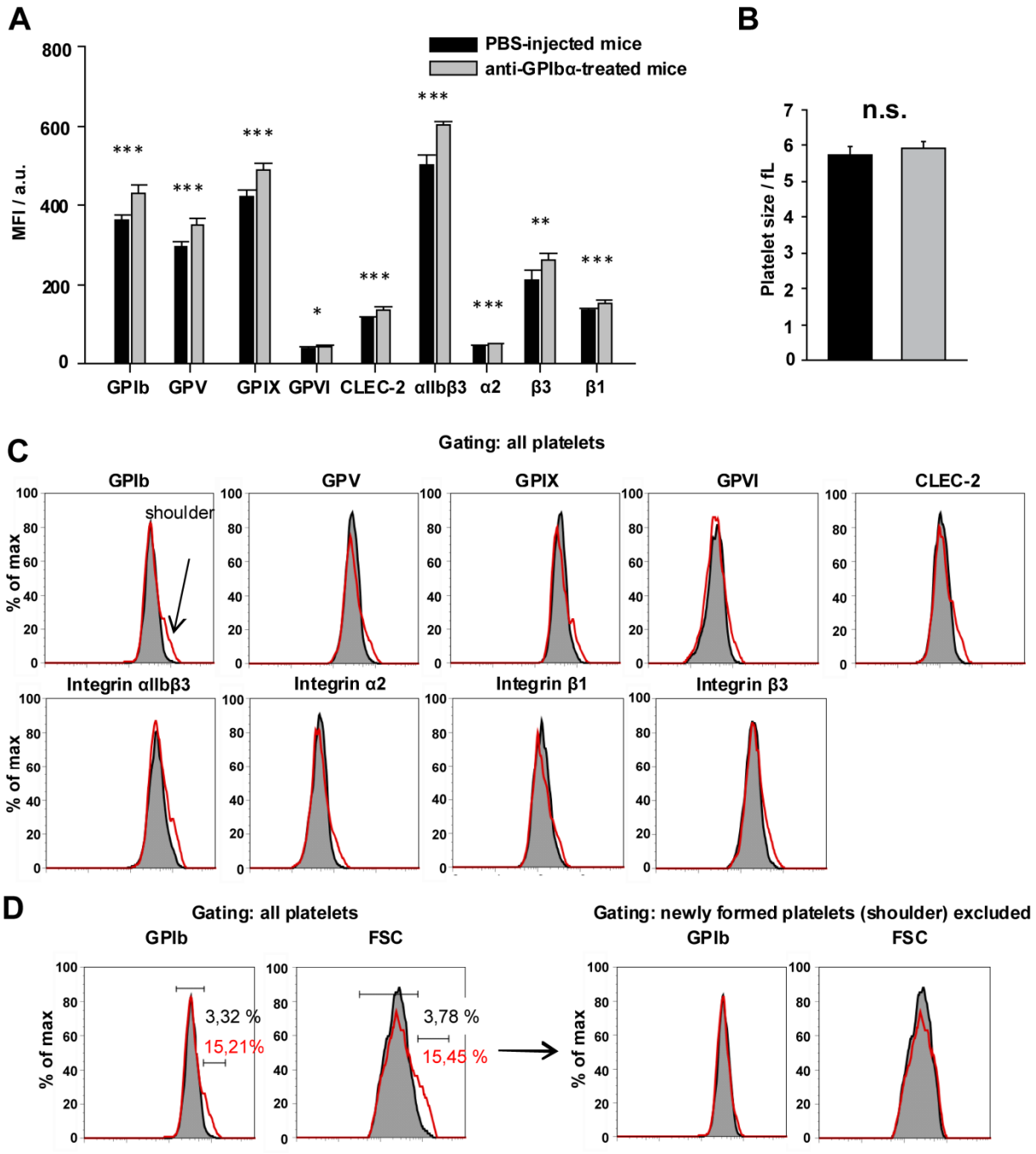

Figure 3.2: Platelet glycoprotein expression levels 12 hours after anti-GPIbα treatment revealed the appearance of a new platelet population. Mice were injected with 2.0 µg of polyclonal anti-GPIbα antibody resulting in a reduction of platelet counts to about 30% of control after 12 h (time point of analysis). (A) Significant increase in platelet glycoprotein expression levels in anti-GPIbα-treated mice compared to control shown as bar graphs. (B) Platelet size of control and anti-GPIbα-treated mice 12 h after injection assessed by a Sysmex cell counter. (C) Expression levels of glycoproteins in platelets of control (shaded area) and anti-GPIbα-treated mice (red line) assessed by flow cytometry. The histograms reveal a new population of platelets (shoulder) in the samples of anti-GPIbα-treated mice. (D) If this population is excluded from analysis based on its FSC/SSC characteristics (left panel), no differences in glycoprotein expression patterns between platelets from control and anti-GPIbα-treated mice were observed as exemplified here for GPIb (right panel) (n.s. = not significant, **p* <0.05, ***p* <0.01, ****p* <0.001).

The newly generated platelet fraction accounted for approximately 12% (15% - 3% = 12%) of the platelet population and young large platelets have been associated with pro-thrombotic properties and altered function.[82,84] To evaluate this possibility and to test whether anti-GPIbα antibody treatment itself alters platelet function, the reactivity of the overall platelet population in partially depleted mice was tested. The overall platelet population showed normal integrin αIIbβ3 activation and P-selectin exposure in response to different agonists (ADP, thrombin, convulxin (CVX)) (Figure 3.3). These results confirmed that anti-GPIbα treatment under the applied conditions efficiently reduced the PC in mice without affecting the function of the remaining overall platelet population.

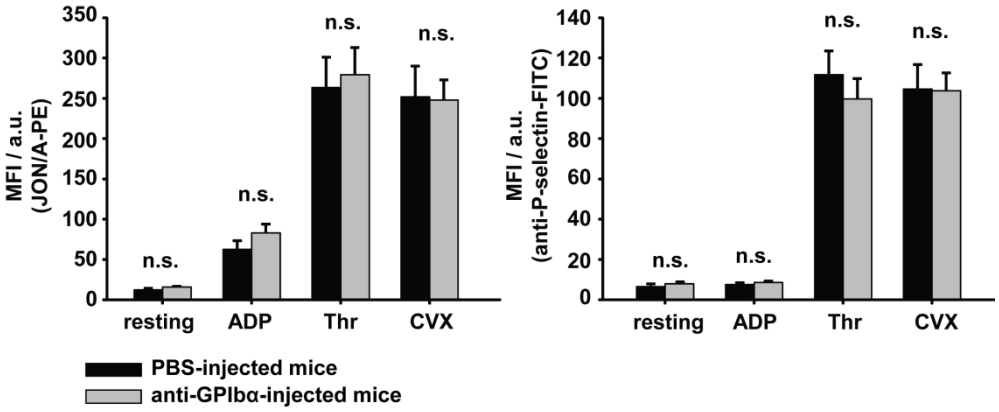

Figure 3.3: Flow cytometric analysis revealed that the activation of circulating platelets after induction of thrombocytopenia by anti-GPIbα was comparable to platelets of vehicle-treated mice. Bar graphs are representative for 8 animals from two independent experiments. Flow cytometric analysis of integrin αIIbβ3 activation (left panel) and degranulation-dependent P-selectin exposure (right panel) in response to ADP (10 µM), thrombin (Thr, 0.01 U/mL), and convulxin (CVX, 1 µg/mL). Results are means ± SD of 4-5 mice per group (n.s. = not significant).

3.1.3 Only very low platelet counts are required to maintain normal haemostasis in mice

To test the significance of the PC for normal haemostasis, mice were subjected to a tail bleeding time assay 12 hours after induction of thrombocytopenia (Figure 3.4). To do so, 1 mm of the tail tip was cut off and bleeding into 37 °C pre-warmed saline was monitored over a 20 min time period. In the control group, 48 out of 49 (48/49) mice arrested bleeding within the observation period with a mean occlusion time of 80 ± 35 s. At PCs ranging from 699-400 platelets/nL blood 25 out of 26 animals stopped bleeding within 412 s (mean was 128 ± 98 s), and similar results were also obtained in groups of mice with platelet counts of 399-300 platelets/nL blood (15/18; mean 138 ± 85 s) and 299-200 platelets/nL blood (10/13; mean 182 ± 82 s). Remarkably, also in the groups of mice with PCs ranging from 199-100

platelets/nL blood and 99-25 platelets/nL blood mice arrested bleeding, although the mean bleeding times were significantly prolonged compared to the control (mean tail bleeding times 175 ± 152 s (15/15, p =0.02) and 240 ± 235 s (9/13, p <0.001), respectively). In sharp contrast, when platelet counts were lowered to less than 25 platelets/nL blood (i.e. <2.5% of control) arrest of bleeding was abolished in all mice.

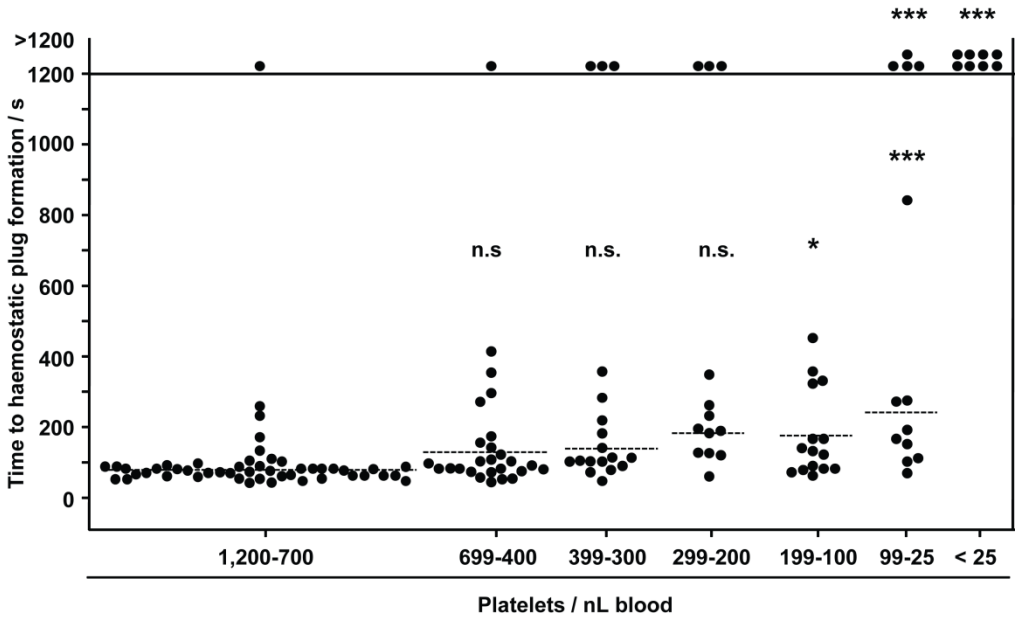

Figure 3.4: Robust haemostatic function in thrombocytopenic mice. Tail bleeding time of anti-GPIbα-depleted C57BL/6J mice was monitored over a 20 min time period. The horizontal dotted line indicates the mean value to haemostatic plug formation. Each symbol represents one mouse (n.s. = not significant, *p <0.05, ***p <0.001).

To rule out the possibility that the results were genetic background-specific or the treatment with anti-GPIbα may have influenced the platelets, these experiments were repeated in 129/Sv mice and performed in C57BL/6J mice which were treated with rabbit anti-mouse platelet serum to reduce the platelet count.

In the mouse strain 129/Sv, vehicle-treated animals had a bleeding time of 70 ± 31 s. This control group was compared to two groups of 129/Sv mice treated with anti-GPIbα. The bleeding time in the mouse group of 99-25 platelets/nL blood was significantly prolonged to 215 ± 64 s (p <0.001) and only two out of eight mice were not able to arrest bleeding (Figure 3.5). In the mouse group of <25 platelets/nL blood arrest of bleeding was abolished. In comparison to data obtained with anti-GPIbα-treated C57BL/6J mice, it can be excluded that mouse strain specific effects accounted for the unexpectedly low platelet count required to maintain normal haemostasis.

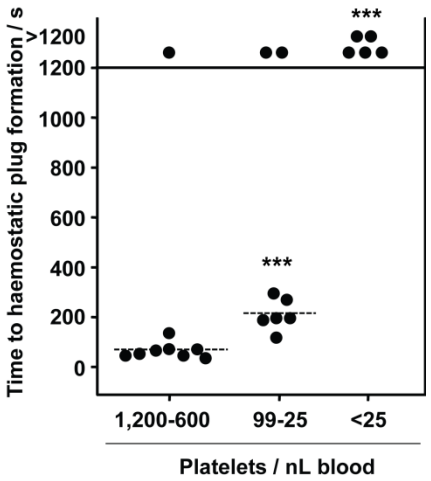

Figure 3.5: Robust haemostatic function in anti-GPIbα-depleted 129/Sv mice. Tail bleeding time of anti-GPIbα-depleted 129/Sv was monitored over a 20 min time period. The horizontal dotted line indicates the mean value to occlusive plug formation. Each symbol represents one mouse (n.s. = not significant, ****p* <0.001).

Secondly, it was analysed if unrecognised side effects of the platelet-depleting anti-GPIbα antibody contributed to the robust haemostatic function. For this, bleeding times were analysed in C57BL/6J mice in which thrombocytopenia was induced by a rabbit anti-mouse platelet serum. To establish the dose response curve mice were treated with either PBS (platelet count average was 1,037 ± 314 platelets/nL blood) as vehicle control, or 3, 6, 10, 20 or 30 µL of rabbit anti-mouse platelet serum. Comparably to anti-GPIbα-mediated platelet depletion, platelet counts of 370 ± 313; 123 ± 87; 92 ± 60; 28 ± 10 and 10 ± 1 platelets/nL blood were detected. However, as indicated by the standard deviation, the rabbit anti-mouse platelet serum-mediated platelet depletion was less reliable compared to anti-GPIbα-mediated platelet depletion (Figure 3.6 A). Additionally, this treatment did not only reduce the PC, but partially compromised the reactivity of the remaining platelet population to different agonists (Figure 3.6 C). Despite this unspecific side effect, bleeding time results were very similar to those of anti-GPIbα-treated C57BL/6J mice. For the group with 1,200-700 platelets/nL blood the average bleeding time was 79 ± 66 s, whereas for the platelet-depleted group with 99-21 platelets/nL blood the time to arrest bleeding was 342 ± 273 s and occlusive plug formation was abolished in mice with a platelet count of <21 platelets/nL blood (Figure 3.6 B).

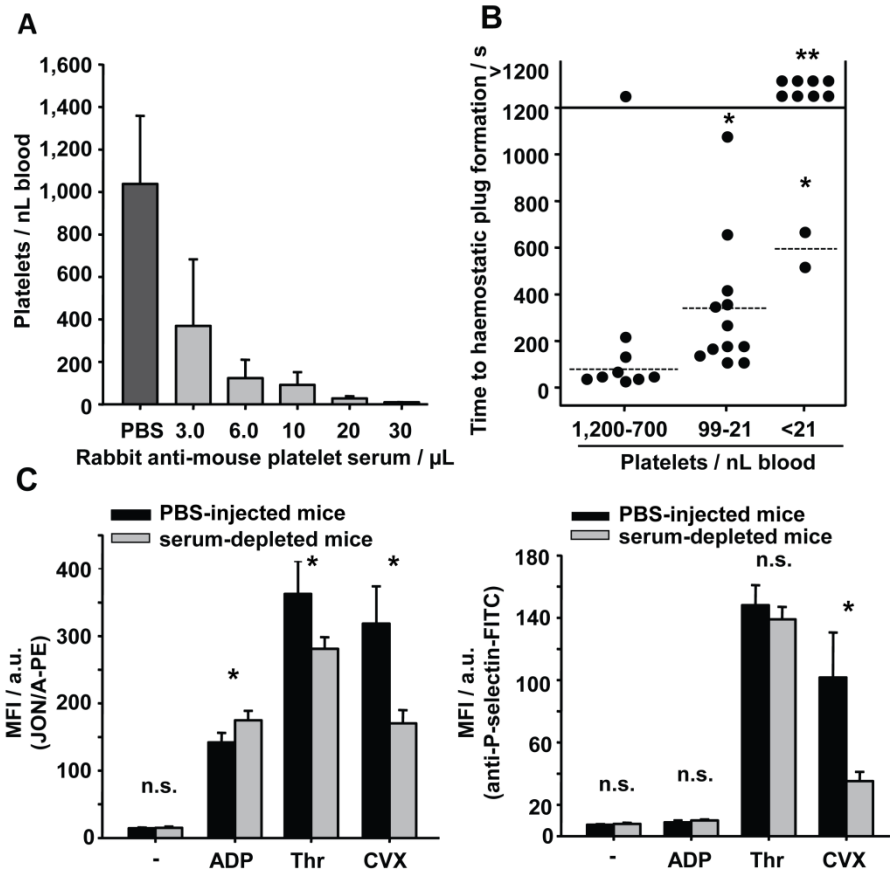

Figure 3.6: Flow cytometric platelet analysis and test of haemostatic function in rabbit anti-mouse platelet serum-treated C57BL/6J mice. (A) Injection of rabbit anti-mouse platelet serum in C57Bl/6J mice induced thrombocytopenia dose-dependently. Mice were injected with PBS or 3.0, 6.0, 10.0, 20.0 or 30.0 µL rabbit anti-mouse platelet serum and platelet counts were determined after 12 hours. (B) Tail bleeding time in rabbit anti-mouse platelet serum-depleted C57BL/6J mice was monitored over a 20 min time period. The horizontal dotted line shows the mean value to occlusive plug formation. Each symbol represents one mouse. (C) Flow cytometric analysis of the activation of circulating platelets after induction of thrombocytopenia by injection of 3 µL rabbit anti-mouse platelet serum. Bar graphs are representative for 8 animals from two independent experiments. Flow cytometric analysis of integrin αIIbβ3 activation (left panel) and degranulation-dependent P-selectin exposure (right panel) in response to ADP (10 µM), thrombin (Thr, 0.01 U/mL) and convulxin (CVX, 1 µg/mL). Results are means ± SD of 4-5 mice per group. Untreated platelets (-) are shown as a control. n.s. = not significant, **p* <0.05, ***p* <0.01.

Taken together, comparable results considering haemostatic function during thrombocytopenia were obtained in either anti-GPIbα-depleted or rabbit anti-mouse platelet serum-depleted C57Bl/6J mice and this was also reproduced in anti-GPIbα-depleted 129/Sv mice. These experiments showed that the method of platelet depletion and the genetic background of the mice did not account for the unexpectedly robust haemostatic function observed even under strongly reduced platelet counts. This suggests that haemostatic defects in thrombocytopenic mice may only occur if the low platelet counts are associated with altered platelet function, vascular defects or other pathogenic factors.

3.1.4 Only platelet count reductions >70% significantly affect occlusive thrombus formation in the aorta

To test the significance of PCs for occlusive arterial thrombus formation, groups of mice with defined degrees of thrombocytopenia were subjected to three well-established thrombosis models. In the first model, the abdominal aorta was mechanically injured and occlusive thrombus formation rapidly occurs through collagen-dependent mechanisms.[102,146] The aorta represents the largest artery in mice, with relatively low shear rates but high blood throughput. As shown in Figure 3.7 A, 24 out of 25 control mice formed occlusive thrombi within 438 s (mean occlusion time 247 ± 96 s). Very similar results were obtained in mice with platelet counts ranging from 699-400 platelets/nL blood although the time to occlusion was slightly increased (699-500 platelets/nL blood: mean time to occlusion 361 ± 188 s, 11 occluding vessels out of 13 (11/13), 499-400 platelets/nL blood: mean time to occlusion 374 ± 325 s, occlusive thrombus formation in all mice). In contrast, when platelet counts were lowered to 399-300 platelets/nL blood 12 out of 15 mice formed occlusive thrombi and this was significantly delayed compared to the controls (511 ± 335 s, p = 0.04). At PCs between 299-200 platelets/nL blood occlusive thrombus formation became severely impaired and two different outcomes were observed; either occlusive thrombus formation took place (461 ± 313 s, (4 out of 9 mice)) or occlusive thrombus formation was abolished (5 out of 9 mice, p = 0.002). At PCs below 200 platelets/nL blood, occlusion was only seen in 1 out of 9 mice and this occurred at a late time point (1,502 s).

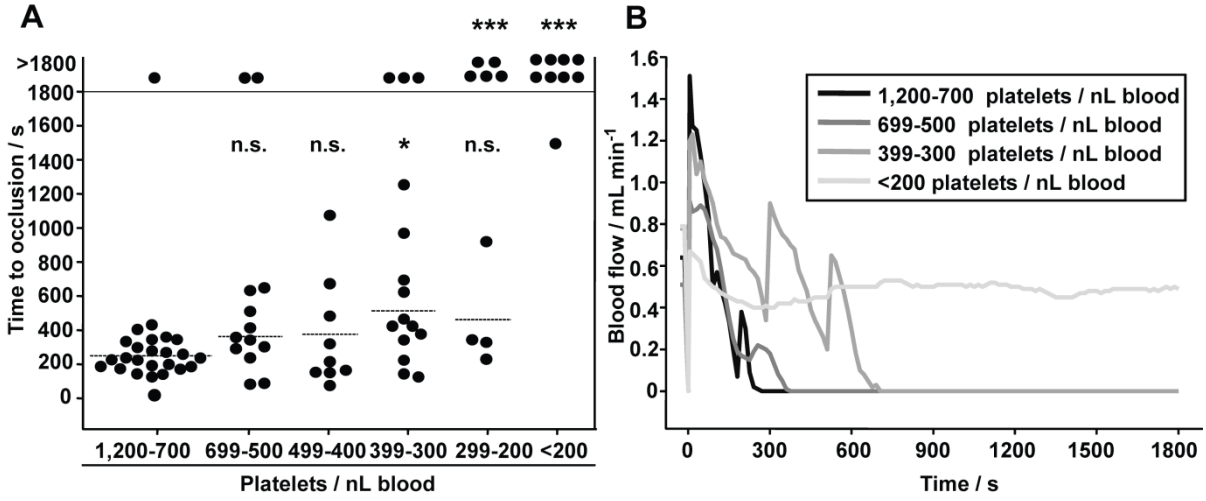

Figure 3.7: Mechanical injury of the abdominal aorta in thrombocytopenic mice. (A) The abdominal aorta was mechanically injured using a forceps (compression for 15 s) and then the blood flow was monitored by an ultrasonic flow probe for 30 min. The horizontal dotted line indicates the mean time to vessel occlusion. Each symbol represents one animal (n.s. = not significant, *p <0.05, ***p <0.001). (B) Representative blood flow measurements are shown.

Representative blood flow measurements are shown in Figure 3.7 B. The medium grey line (group 399-300 platelets/nL blood) indicates that the embolization of large thrombus fragments partly contributed to the delayed occlusion times. These results revealed that experimental occlusive thrombus formation in a mechanically injured large vessel of a mouse can efficiently occur at PCs of about 30% of control, whereas it is increasingly impaired upon further reduction of platelet numbers.

3.1.5 Occlusive thrombus formation in the $FeCl_3$-injured carotid artery is less affected by reduced platelet counts compared with the aorta injury model

To further assess the impact of the PC on arterial thrombosis, groups of mice with defined degrees of thrombocytopenia were subjected to a second widely used model. In this model the carotid artery is chemically injured by the topical application of $FeCl_3$ and thrombus formation occurs through collagen and thrombin-driven mechanisms (Figure 3.8).[146] The carotid artery represents a medium sized vessel where moderate shear rates prevail.

In the control group (1,200-700 platelets/nL blood) 18 out of 19 mice formed occlusive thrombi with a mean time to occlusion of 345 ± 58 s and very similar results were obtained in mice with PCs of 699-400 platelets/nL blood (395 ± 154 s) and 399-300 platelets/nL blood (378 ± 105 s). At platelet counts of 299-200 platelets/nL blood, a significant increase in the mean occlusion time compared to control was observed (477 ± 122 s, $p = 0.03$) and 2 out of 14 vessels did not occlude at all within the observation period. A further delay and impairment of occlusive thrombus formation was detected in mice with platelet counts of 199-100 platelet/nL blood with only 4 out of 7 vessels occluding within 653 s (mean time to occlusion 514 ± 121 s ($p = 0.06$)). This was clearly different from the aorta injury model were occlusive thrombus formation was already abrogated at PCs below 200 platelets/nL blood. At PCs below 100 platelets/nL blood 6 out of 7 vessels failed to occlude ($p = 0.0002$) and one vessel occluded very late (928 s) (Figure 3.8 A). In Figure 3.8 B representative blood flow measurements of mice with reduced platelet counts and the respective control are shown. These results revealed that occlusive thrombus formation in the chemically injured carotid artery is only severely impaired when platelet counts drop below 100 platelets/nL blood (i.e. approximately 10% of control).

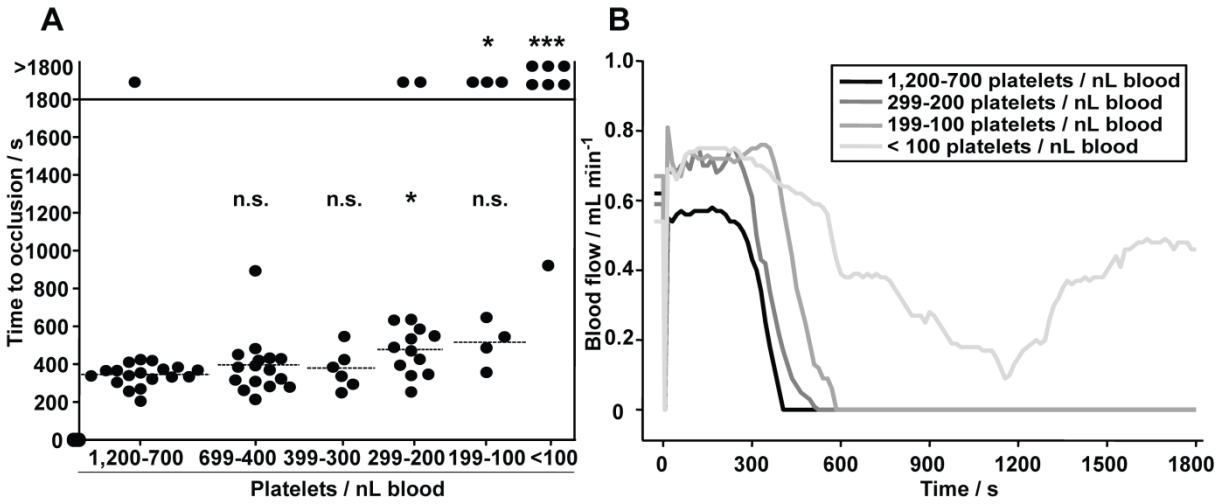

Figure 3.8: $FeCl_3$-induced injury of the carotid artery in thrombocytopenic mice. (A) Carotid arteries were topically injured with filter paper saturated with 10% $FeCl_3$ for 90 s and then the time to occlusion was determined with an ultrasonic flow probe. The horizontal dotted line indicates the mean time to occlusion. Each symbol represents one mouse (n.s. = not significant, **p* <0.05, ****p* <0.001). (B) Representative blood flow measurements are shown.

3.1.6 Platelet counts of 2.5% of control are sufficient to efficiently occlude $FeCl_3$-injured mesenteric arterioles

The data described above suggested that the vascular bed and/or the type of vessel injury influenced the threshold PC required to achieve vessel occlusion. To study this in more detail, groups of mice with defined PCs were tested in a third well-established thrombosis model, in which a $FeCl_3$-injury is induced in mesenteric arterioles, representing small vessels where high shear rates prevail. For these experiments, control and platelet-depleted mice were divided into six groups displaying different numbers of platelets in the circulation: 1,200-700 (control); 699-500; 499-300; 299-100; 99-25 and less than 25 platelets/nL blood. The injury was induced by topical application of 20% $FeCl_3$ and thrombus formation of fluorescently labelled platelets was monitored by intravital fluorescence microscopy. In all mice studied, the time to the formation of first thrombi with a diameter >10 µm (Figure 3.9 A) and the time to full vessel occlusion (no blood flow for more than 1 minute, Figure 3.9 B) were determined. Remarkably, the time to first thrombus formation was not significantly altered in mice with PCs down to 25 platelets/nL blood (Figure 3.9 A). However, at lower PCs two different observations were made; either the appearance of thrombi >10 µm was delayed or completely abolished (Figure 3.9 A, 4 out of 8 vessels). Furthermore, down to a platelet count of 100 platelets/nL blood also the time to vessel occlusion was not significantly altered compared to control (Figure 3.9 B).

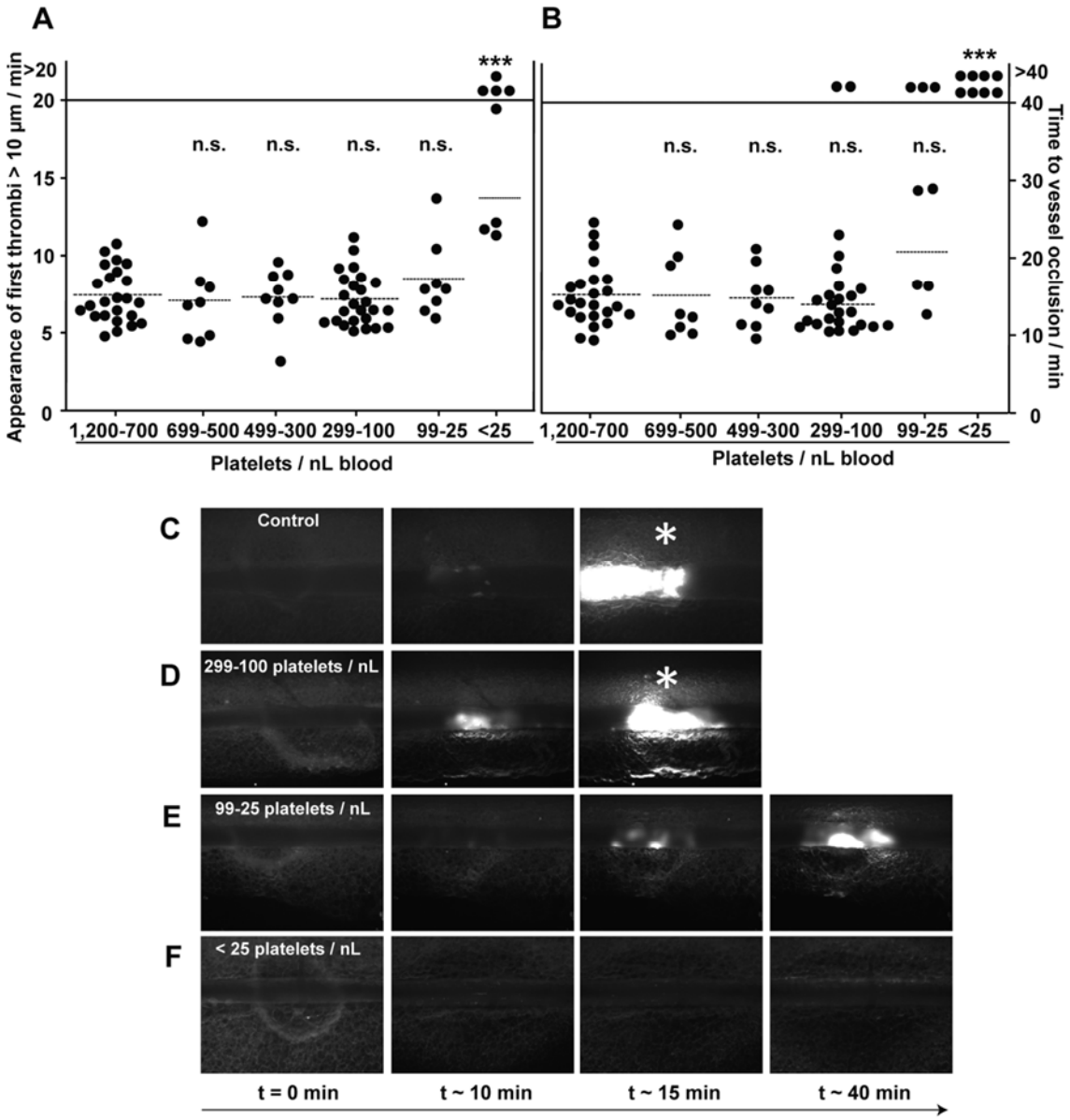

Figure 3.9: $FeCl_3$-induced injury of mesenteric arterioles in thrombocytopenic mice. Mesenteric arterioles were injured by topical application of 20% $FeCl_3$. Adhesion and thrombus formation of fluorescently labelled platelets were monitored by *in vivo* microscopy. Statistical evaluations of time to appearance of first thrombi >10 µm (A) and time to vessel occlusion (B) are shown. The horizontal dotted line indicates the mean value to vessel occlusion. Each symbol represents one arteriole (n.s. = not significant, ****p* <0.001). (C-F) Representative images of thrombus formation in different platelet count groups. Whereas appearance of first thrombi >10 µm in the mouse group of 299-100 platelets/nL blood was comparable to control, thrombus formation might be impaired at platelet counts between 99-25 platelets/nL blood. At platelet counts lower than 25 platelets/nL blood, platelet aggregation and thrombus formation was severely impaired. Asterisk indicates stable occlusion of the vessel.

When less than 100 platelets/nL blood were in the circulation, three different outcomes were observed: either occlusive thrombus formation was comparable to control, delayed or abolished (Figure 3.9 B). At a PC below 25 platelets/nL blood occlusive thrombus formation was abolished in all vessels (p = 0.0001). Representative images of thrombus formation of four groups are shown in Figure 3.9 C-F. In control mice and platelet count group 299-

100 platelets/nL blood time to appearance of first thrombi >10 µm and occlusive thrombus formation took place with comparable speed (Figure 3.9 C and D). In contrast, appearance of first thrombi and time to vessel occlusion might be delayed in mice with a platelet count of 99-25 platelet/nL blood (Figure 3.9 E). Occlusive thrombus formation was completely abolished in mice with a platelet count lower than 25 platelets/nL blood (Figure 3.9 F).

To rule out the possibility that that unrecognised side effects of the platelet-depleting anti-GPIbα antibody and/or the murine strain background of C57BL/6J mice contributed to the effect that thrombotic function is maintained at even very low platelet counts, experiments similar to the control experiments performed for the tail bleeding time assay were carried out.

In a set of experiments, 129/Sv mice which had been platelet-depleted 12 hours prior to the experiment with anti-GPIbα antibody were subjected to the $FeCl_3$-injury of mesenteric arterioles model. Similarly to C57BL/6J mice treated with anti-GPIbα antibody, a defect in thrombus formation became visible when the platelet count fell below 25 platelets/nL blood. In the groups 299-100 and 99-25 platelets/nL blood time to appearance of first thrombi >10 µm (7.57 ± 1.9 and 10.40 ± 4.33 min, respectively) was not significantly different from control (6.98 ± 1.7 min). In the mouse group of less than 25 platelets/nL blood, time to appearance of first thrombi >10µm took more than 20 min (Figure 3.10 A, left panel). Similar results were obtained for the time to vessel occlusion: In control mice, the average time to reach occlusive thrombus formation was 15.8 ± 4.2 min and was 20.5 ± 8.8, 24.6 ± 11.3 and more than 40 min (p <0.01) for the groups 299-100; 99-25 and less than 25 platelets/nL blood, respectively (Figure 3.10 A, right panel).

In a second experiment, C57BL/6J mice were platelet depleted with rabbit anti-mouse platelet serum. For the group 1,200-700 platelets/nL blood the average time to thrombus formation and time to occlusion was 6.8 ± 1.5 min and 14.5 ± 3.3 min, respectively. Similar results were obtained in mice with 299-100 platelets/nL blood (6.1 ± 1.4/18.1 ± 8.4 min, respectively). For the group of 99-25 platelets/nL blood, the observed times points were 8.5 ± 4.0 and 19.7 ± 8.8 min, respectively. However, in this group 50% of the vessels failed to occlude. In the group of less than 25 platelets/nL blood thrombus formation and vessel occlusion was completely abolished (both p <0.001) (Figure 3.10 B). Taken together, comparable results considering thrombotic function were obtained in either anti-GPIbα-depleted or rabbit anti-mouse platelet serum-depleted C57BL/6J mice. Furthermore,

experiments with anti-GPIbα depleted 129/Sv mice showed that mouse strain specific effects did not account for the unexpectedly low platelet count required to maintain normal thrombosis in small vessels.

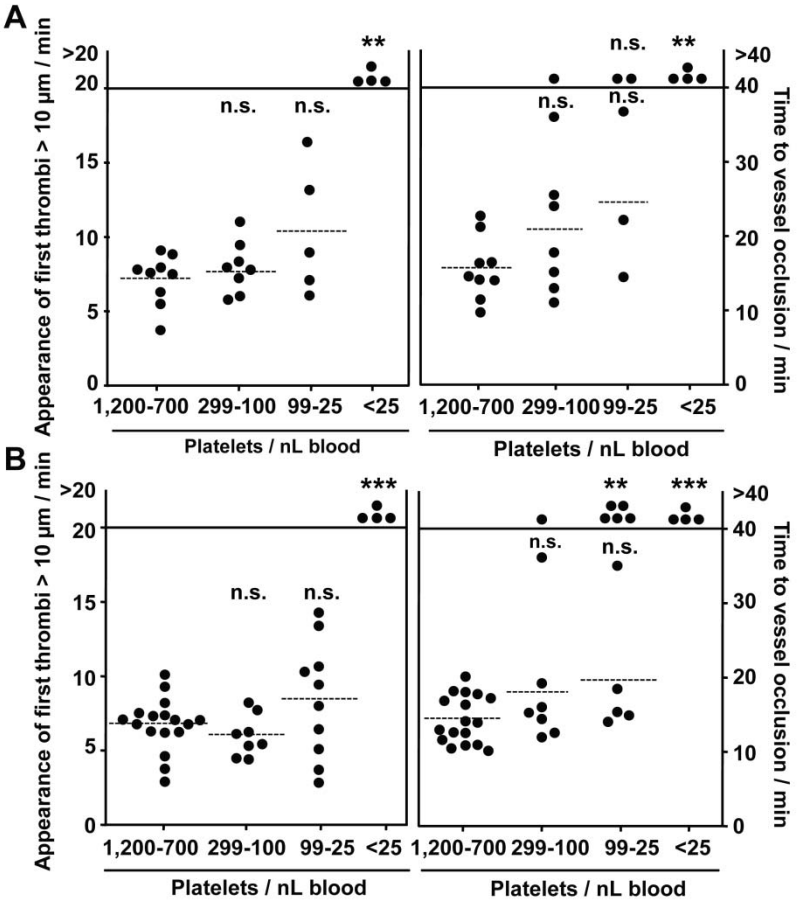

Figure 3.10: $FeCl_3$-induced injury in mesenteric arterioles in anti-GPIbα-depleted 129/Sv mice and rabbit anti-mouse platelet serum-depleted C57BL/6J mice. Mesenteric arterioles were injured by topical application of 20% $FeCl_3$. Adhesion and thrombus formation of fluorescently labelled platelets were monitored by *in vivo* microscopy. (A) Time to appearance of first thrombi >10 µm (left panel) and time to vessel occlusion (right panel) in anti-GPIbα-treated 129/Sv mice. (B) Time to appearance of first thrombi >10 µm (left panel) and time to vessel occlusion (right panel) in rabbit anti-mouse platelet serum-depleted C57BL/6J mice. The dotted horizontal line indicates the mean value to vessel occlusion. Each dot represents one arteriole (n.s. = not significant, ** p <0.01, *** p <0.001).

3.1.7 Only approximately 10% of the normal platelet count is sufficient to induce full brain infarction following tMCAO

Ischaemic stroke is caused by thromboembolic occlusion of a cerebral artery leading to focal ischaemia and infarction of the affected brain territory. Recently, it has been shown that the blocking of distinct platelet surface receptors essential for platelet adhesion and activation protects mice from ischaemic stroke after transient middle cerebral artery occlusion.[106,147,148]

To test the significance of the PC for infarct growth following focal cerebral ischaemia, groups of mice with defined PCs were subjected to tMCAO (60 min) and neurological deficits and the infarct size were assessed after 24 and 25 hours, respectively. tMCAO and the image acquisition as well as the neurological tests were carried out in collaboration with Dr. Peter Kraft, Department of Neurology, University of Würzburg, Germany.

Four groups of mice were analysed with platelet counts of 1,300-700 (control), 699-400, 399-110 and less than 110 platelets/nL blood. Remarkably, a reduction of PCs down to 110 platelets/nL blood had no significant effect on infarct size at 25 hours after tMCAO (Figure 3.11 A and B).

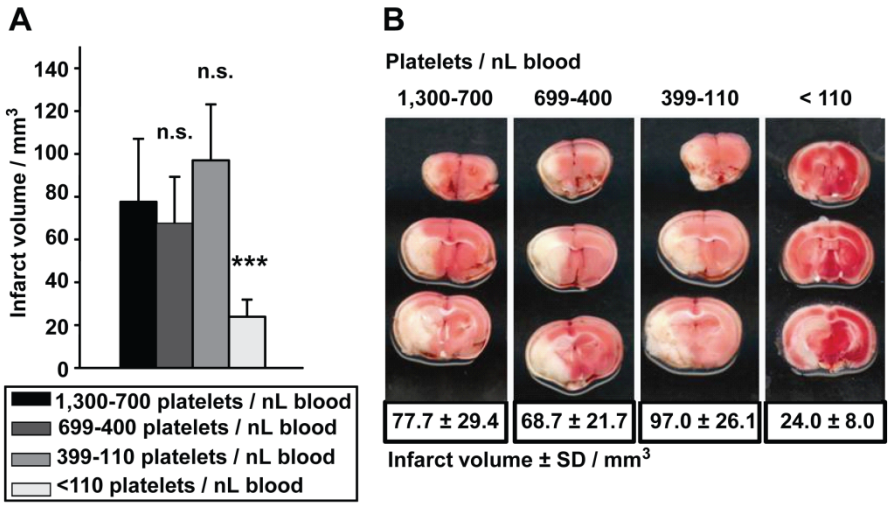

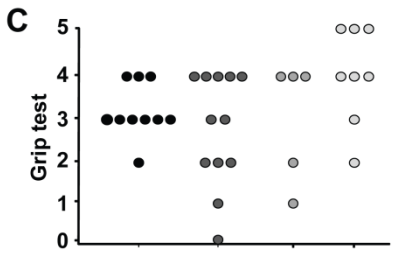

Group (platelets / nL)	Grip test ± SD
1,300 - 700	3.2 ± 0.6
699 - 400	2.8 ± 1.4
399 - 110	3.0 ± 1.4
< 110	4.0 ± 1.1

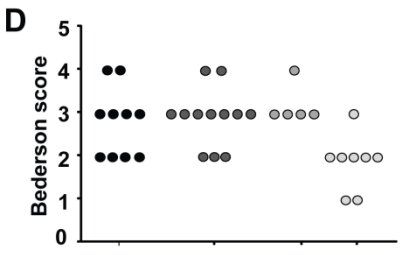

Group (platelets / nL)	Bederson score ± SD
1,300 -700	2.8 ± 0.8
699 - 400	2.8 ± 0.7
399 - 110	3.2 ± 0.5
< 110	1.8 ± 0.6

Figure 3.11: tMCAO in thrombocytopenic mice. (A) Brain infarct volumes in control and platelet-depleted mice 25 hours after a 60 min tMCAO are represented as mean ± SD (n.s. = not significant, ***p <0.001). (B) Representative images of corresponding coronal brain sections from control and platelet-depleted mice stained with 2,3,5-triphenyltetrazolium chloride 25 hours after tMCAO. Grip test (C) and Bederson score (D) were determined 24 hours after tMCAO.

Neurological deficits determined by the grip test (Figure 3.11 C), assessing coordination and motor function, and the Bederson score, assessing global neurological function, were also unchanged at platelet counts >110 platelets/nL blood (Figure 3.11 D).[141] The platelet dependency of this pathology became apparent when platelet counts were reduced to less than 110 platelets/nL blood. In these mice the infarct size at 25 hours was significantly reduced (p = 0.0003) to one third compared to control (Figure 3.11 A and B) and this was associated with improved neurological function (Figure 3.11 C and D). Interestingly, no major intracranial bleeding was observed in any of these mice, suggesting that even very low platelet numbers are sufficient to prevent haemorrhage in the ischaemic brain. These data revealed that approximately 10% of the normal platelet count is sufficient to mediate full brain infarction following focal cerebral ischaemia.

3.2 *In vitro* and *in vivo* platelet function during recovery from thrombocytopenia

Injection of low doses of anti-GPIbα antibody reduced the platelet count to a certain number. This mild thrombocytopenia led to the production of new platelets by MKs within hours, resulting in two different platelet populations present in the circulation (Figure 3.2). These newly produced platelets displayed an increased size and surface glycoprotein expression levels but selective characterisation was not possible as they formed only a minor subpopulation of all circulating platelets.

A different approach which led to the complete loss of all platelets from the circulation for several days was done by injection of high-dose anti-GPIbα depletion antibody (100 µg). On day five after injection the platelet count had recovered to about 50% of the normal platelet count and circulating platelets displayed a homogenous population of new platelets. These newly generated platelets were characterised considering platelet morphology, platelet glycoprotein expression and platelet activation. Additionally, the thrombotic function of these platelets was assessed *in vivo*.

3.2.1 Determination of the platelet count and size after high-dose anti-GPIbα antibody treatment

Mice were injected with high-dose anti-GPIbα depletion antibody (day 0) which led to a complete loss of all platelets from the circulation. To assess the recovery from this high-dose

anti-GPIbα-mediated thrombocytopenia, the platelet count and size was subsequently analysed by a Sysmex cell counter for a time period of seven days (Figure 3.12). The injection of the mice and the measurements were done in collaboration with Deya Cherpokova.

The injection of the anti-GPIbα depletion antibody (day 0) induced a strong thrombocytopenia and no platelets were in the circulation for approximately two days. On day three after injection, the platelet count started to recover and low numbers of platelets were detectable in the circulation, but these were not sufficient to assess the platelet size. On day five after injection small amounts of anti-GPIbα antibody on the surface of platelets were still detectable in blood samples by flow cytometry (data not shown). However, the platelet count had recovered to about 50-60% of normal (Figure 3.12 A). These platelets were larger compared to platelets from PBS-injected mice as shown by analysis with a Sysmex cell counter (Figure 3.12 B). Similar results were obtained by electron microscopic analysis of these platelets on day five (in collaboration with Dr. Shuchi Gupta in our laboratory) (Figure 3.12 E).

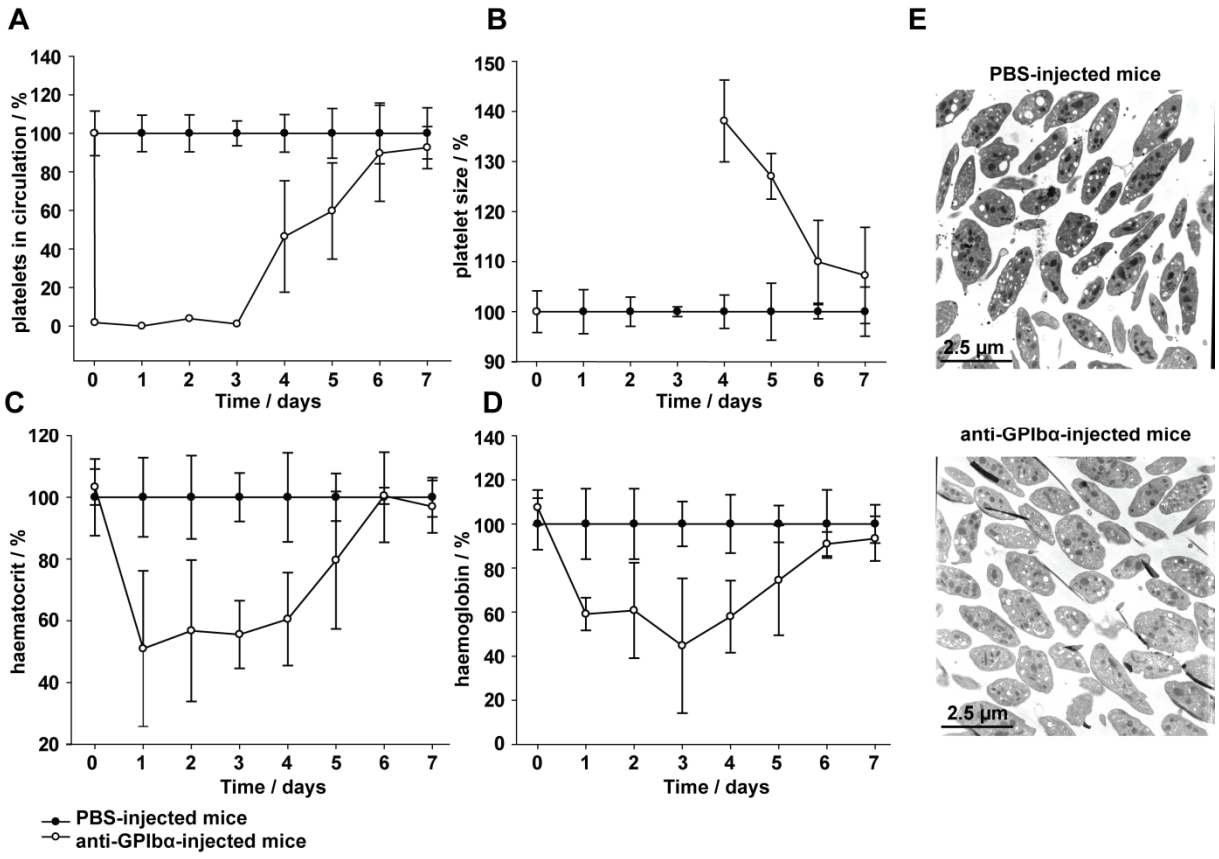

Figure 3.12: Platelet count, size, haemoglobin and haematocrit values for anti-GPIbα antibody injected mice relative to PBS-injected mice. (A) Anti-GPIbα-treated mice showed a profound thrombocytopenia for several days. (B) Newly generated platelets after anti-GPIbα antibody treatment showed an increased size. (C and D) Haematocrit and haemoglobin values were decreased in anti-GPIbα-treated mice. (E) Electron micrographs of platelets from PBS- and anti-GPIbα-treated mice (in collaboration with Dr. Shuchi Gupta).

On day six, the platelet count and size of anti-GPIbα-treated mice was comparable to control. To test whether high-dose anti-GPIbα antibody treatment lead to additional effects besides the removal of platelets from the circulation, several other blood parameters were assessed. Indeed, from day one until day four after injection the haemoglobin value and the haematocrit were significantly decreased compared to the PBS-injected controls. Possible causes for this may include subcutaneous bleeding which was observed in some of the anti-GPIbα-treated mice. These blood parameters reached normal values on day six (Figure 3.12 C and D).

3.2.2 Platelet glycoprotein expression levels are normal in high-dose anti-GPIbα antibody-treated mice

The glycoprotein expression levels of high-dose anti-GPIbα-treated mice were analysed during the recovery from thrombocytopenia on day five compared to PBS-treated mice. Day five was the earliest time point at which a reliable analysis of platelets (platelet count of 50% of control) was possible (Figure 3.12).

Despite the increased size of the platelets of mice which had been treated with 100 µg of anti-GPIbα antibody, the glycoprotein expression levels were normal on day five compared to control (Figure 3.13). This was unexpected in comparison to the newly produced platelets after low-dose anti-GPIbα treatment. Those were slightly increased in size and showed increased expression levels of prominent platelet surface receptors (Figure 3.2). To further test this observation and to rule out any anti-GPIbα-mediated effects, thrombocytopenia was induced by injection of 100 µg of platelet-depleting anti-αIIbβ3 antibody. This platelet-depleting antibody induces systemic side effects,[140] especially when high doses are administered. To counteract this, the antibody was injected in combination with a platelet-activating factor (PAF) inhibitor which inhibits PAF-induced systemic side effects such as hypotension and lethality. Similar to the treatment with the anti-GPIbα antibody, also the injection of 100 µg of anti-αIIbβ3 antibody induced a strong thrombocytopenia and the platelet count recovered to about 50% on day five (data not shown). At this time point the platelet size was increased but glycoprotein expression levels were comparable to PBS-treated mice, confirming the data obtained with high-dose anti-GPIbα treatment (data not shown and Figure 3.13). Taken together, these experiments showed that thrombocytopenia induced by a very high-dose of platelet-depleting antibody led to a several days lasting

thrombocytopenia and that newly generated platelets were massively enlarged. Furthermore, these platelets showed similar glycoprotein expression levels compared to PBS-treated mice.

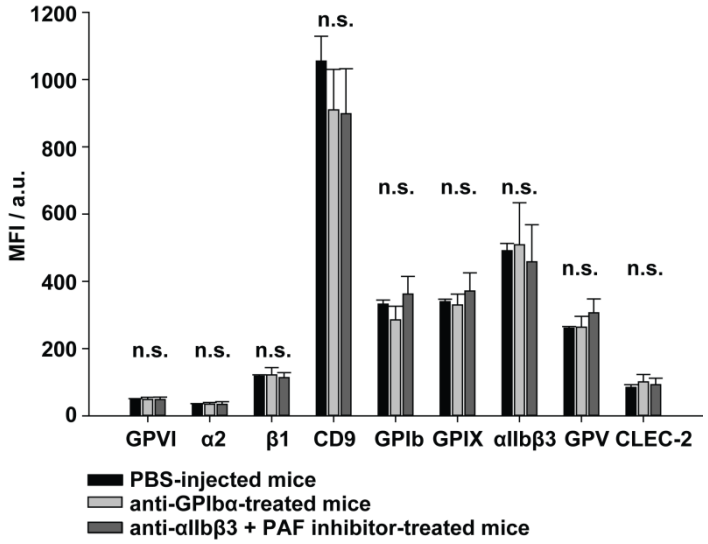

Figure 3.13: Glycoprotein expression levels of platelets of platelet-depleted mice on day five during recovery from thrombocytopenia. Glycoprotein expression levels of platelets of anti-GPIbα and anti-αIIbβ3 + PAF inhibitor-treated mice were comparable to PBS-injected mice on day five, n.s. = not significant.

3.2.3 Increased number of MKs in bone marrow but not in spleen

As shown in Figure 3.2, reduced numbers of platelets in the circulation rapidly induced the generation of new platelets by MKs within hours and this occurs before any changes in the number of MKs.[88] To test whether sustained thrombocytopenia was accompanied by an increased number of MKs in bone marrow or spleen, paraffin sections of the respective organs were analysed on day five. Indeed, the number of MKs was profoundly increased in the bone marrow of high-dose anti-GPIbα-treated mice compared to PBS-injected mice and was 11.3 ± 5.5 and 7.7 ± 2.3 per visual field (300 x 225 µm), respectively (Figure 3.14 A). Representative images are shown in Figure 3.14 B. The number of MKs in the spleen of high-dose anti-GPIbα-treated mice was unchanged (Figure 3.14 C). Representative images are shown in Figure 3.14 D. However, the spleen was massively enlarged compared to PBS-injected mice (Figure 3.14 E).

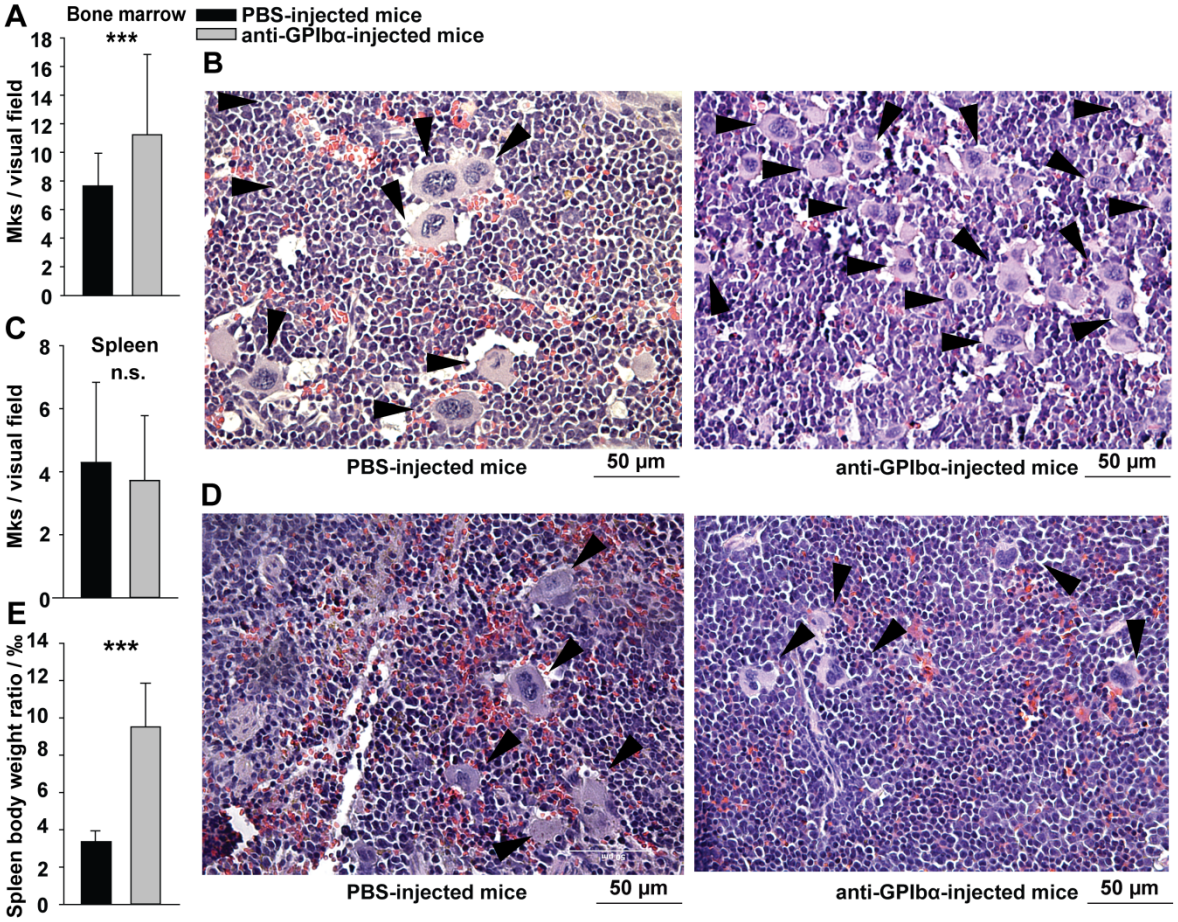

Figure 3.14: MKs of anti-GPIbα-injected mice on day five. (A) Determination of the MK number per visual field (300 x 225 µm) in the bone marrow. (B) Representative images of haematoxylin and eosin-stained bone marrow sections. (C) Determination of the MK number in spleen. (D) Representative images of haematoxylin and eosin-stained spleen sections. (E) Spleen to body weight ratio (n.s. = not significant, ***p <0.001).

3.2.4 Platelets of high-dose anti-GPIbα-treated mice display a specific ITAM-signalling defect

To analyse the functionality of platelets during recovery from thrombocytopenia, platelets from high-dose anti-GPIbα-treated mice were analysed on day five by flow cytometry upon stimulation with different agonists. To do so, platelets were incubated with a PE-conjugated JON/A antibody, which preferentially binds to the active form of αIIbβ3 integrin,[139] and a FITC-conjugated anti-P-selectin antibody. Whereas αIIbβ3 is a major integrin on the platelet surface which shifts from an inactive to an active state upon stimulation with agonists,[149] P-selectin is stored in α-granules of platelets and becomes exposed on the platelet surface only upon platelet activation. P-selectin is, therefore, a measure for platelet degranulation.[150] Due to the high dilution of the platelets in buffer, this assay specifically measures the primary platelet signalling response, because the release of secondary

mediators through platelet degranulation is negligible. Similar to the evaluation of the glycoprotein expression levels, platelets of anti-αIIbβ3 antibody and PAF inhibitor-treated mice were analysed concomitantly on day five, to rule out possible anti-GPIbα-mediated effects.

In this assay, platelets from anti-GPIbα-treated mice showed a significant increase of αIIbβ3 integrin activation at resting conditions compared to PBS-treated mice indicating that these platelets may be pre-activated (Figure 3.15). To test this in further detail, platelets were stimulated with epinephrine. Whereas epinephrine itself is only a very weak platelet agonist,[151] it can potentiate sub-threshold platelet activation.[152] However, stimulation of platelets with epinephrine revealed only minor differences between the tested platelet groups (Figure 3.15) indicating that these cells were not pre-activated.

In a second approach, platelets were stimulated with ADP, U46619 or thrombin. These agonists induce activation of platelets through GPCRs. For these agonists, no significant differences in activation between platelets of anti-GPIbα-treated and PBS-treated mice were detected (Figure 3.15).

To test whether platelets from anti-GPIbα-treated mice show differences in (hem)ITAM-signalling, they were stimulated with collagen-related peptide (CRP), CVX and RC. Interestingly, platelets of anti-GPIbα-treated mice showed a significantly decreased integrin activation and degranulation upon stimulation with CRP at high and intermediate agonist concentrations. At low agonist concentration, the decreased activation was not significant. In line with this, also platelet activation upon stimulation with CVX was reduced, indicating that ITAM-signalling in these platelets is compromised (Figure 3.15). Different from that, platelet activation with RC, which stimulates cells through a hemITAM-signalling pathway, was not altered for αIIbβ3-integrin activation and P-selectin exposure demonstrating an ITAM-specific defect in these newly generated platelets.

Alternatively, thrombocytopenia was also induced by injection of anti-αIIbβ3 and PAF inhibitor in mice and platelets were analysed on day five. Similar to the treatment with anti-GPIbα, also these platelets showed unaltered activation upon stimulation with GPCR agonists but a decreased activation response upon stimulation with CRP. Upon stimulation with CVX, the platelet activation in these thrombocytopenic mice was not significantly reduced. Taken together, two different thrombocytopenia-inducing antibodies resulted in an

ITAM-signalling defect in platelets on day 5 after injection, thus largely excluding antibody-specific effects.

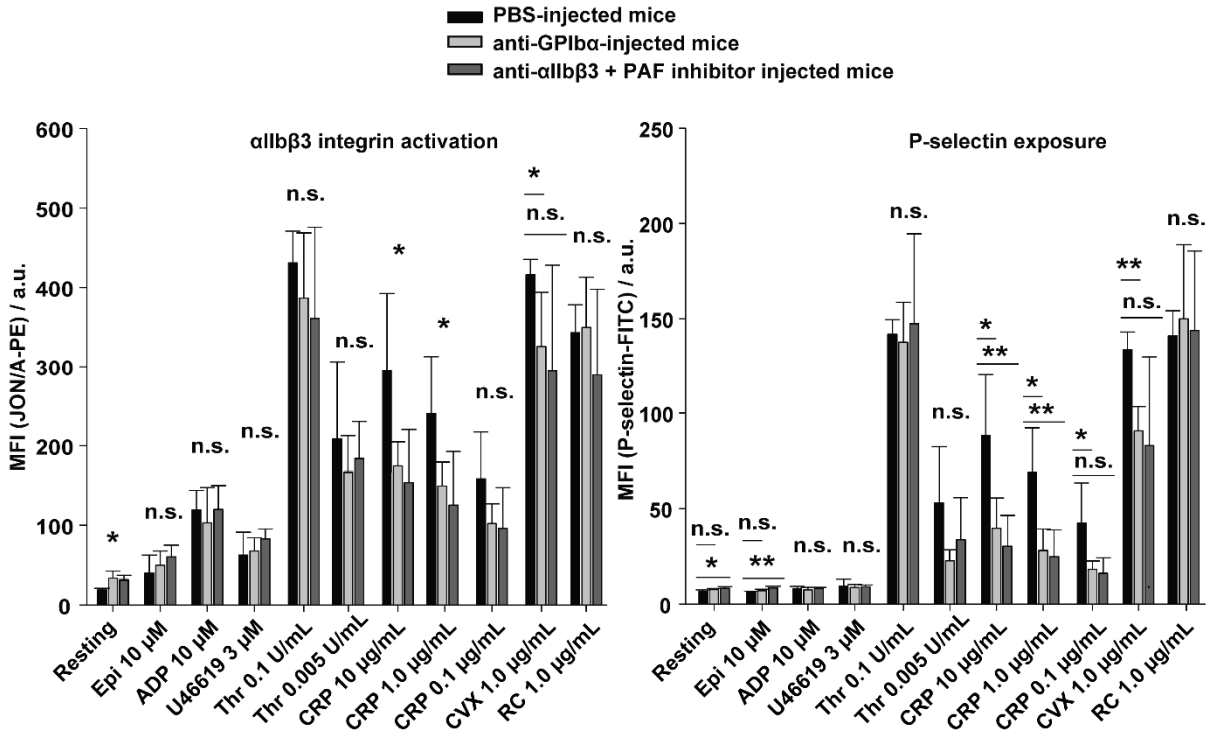

Figure 3.15: Platelet activation upon stimulation with different agonists of anti-GPIbα and anti-αIIbβ3 + PAF inhibitor-treated mice on day five. Platelet ITAM-signalling of anti-GPIbα and anti-αIIbβ3 + PAF inhibitor-treated mice on day five was reduced compared to control. GPCR-signalling of platelets of anti-GPIbα and anti-αIIbβ3 + PAF inhibitor-treated mice on day five was normal. Abbreviations: CRP = collagen-releated peptide, RC = rhodocytin, CVX = convulxin, Epi = epinephrine, n.s. = not significant, **p* <0.05; ***p* <0.01.

3.2.5 High dose anti-GPIbα-treated mice show a defective thrombus formation *in vivo*

To test whether this defect in platelet ITAM-signalling *in vitro* is translated into a defect in thrombus formation *in vivo,* high-dose anti-GPIbα-treated mice were subjected to the mechanical injury of the abdominal aorta model on day five.

In this model, occlusive thrombus formation was observed in 13 out of 15 control mice. In contrast, thrombus formation in anti-GPIbα-treated mice was significantly impaired and vessels in 11 out of 17 animals did not occlude (*p* <0.01). In the 6 occluding vessels of the anti-GPIbα-treated mice the time to occlusive thrombus formation was unaltered compared to control (high-dose anti-GPIbα-treated mice 381 ± 82 s, control 297 ± 139 s).

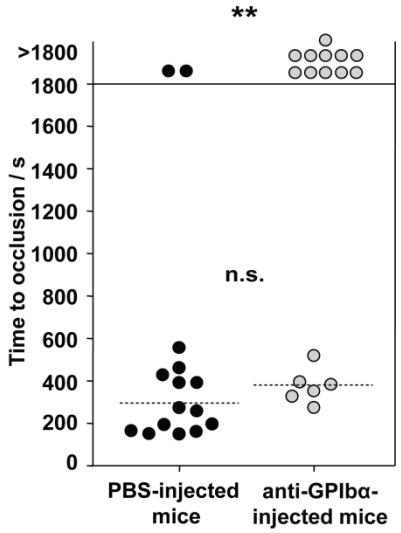

Figure 3.16. High-dose anti-GPIbα-injected mice display a defective thrombus formation in the mechanical injury of the abdominal aorta model on day five. The abdominal aorta was mechanically injured using a forceps (compression for 15 s) and then the blood flow was monitored by an ultrasonic flow probe for 30 min. The horizontal dotted line indicates the mean time to vessel occlusion. Each symbol represents one animal (n.s. = not significant, ***p* <0.01).

3.3 *In vivo* studies in genetically modified mice with modulated GPVI-signalling

During recovery from high-dose anti-GPIbα-mediated thrombocytopenia, platelets showed an ITAM-signalling defect in flow cytometry experiments upon stimulation with CRP and CVX *in vitro* (Figure 3.15). This defect also translated into a defective *in vivo* thrombus formation in these mice compared to control. To further investigate ITAM-signalling *in vivo*, three different mouse strains deficient for adapter proteins involved in platelet ITAM-signalling were analysed. Whereas *in vitro* studies of Grb2-deficient platelets show a profound defect in ITAM-signalling,[121] platelets of SLAP/SLAP2-double deficient mice (Deya Cherpokova, personal communication) and *Clp36*$^{\Delta LIM}$ mice,[115] display a profound hyperactivity upon activation with ITAM-signalling inducing agonists.

Breeding of *Grb2*$^{fl/fl,PF\text{-}4\text{-}Cre+/-}$ mice was done by Dr. Sebastian Dütting and Timo Vögtle in our laboratory. *Clp36*$^{\Delta LIM}$ bone marrow chimeric mice were generated by Dr. Attila Braun and Dr. Shuchi Gupta in our laboratory. Breeding of SLAP/SLAP2-deficient mice and platelet transfusions were performed in collaboration with Deya Cherpokova in our laboratory.

3.3.1 *Grb2*$^{-/-}$ mice display impaired thrombus formation after ASA treatment

As Grb2-deficient mice are embryonically lethal,[117] for all *in vivo* experiments *Grb2*$^{fl/fl,PF\text{-}4\text{-}Cre+/-}$ mice (further on referred to as *Grb2*$^{-/-}$ mice) and the respective littermates were used (*Grb2*$^{fl/fl,PF\text{-}4\text{-}Cre\text{-}/-}$, further referred to as *Grb2*$^{+/+}$). *Grb2*$^{-/-}$ mice lack Grb2 only in platelets and MKs.

The activation and aggregation of platelets from *Grb2*$^{-/-}$ mice as well as their intracellular Ca^{2+} mobilisation is compromised *in vitro* upon stimulation with (hem)ITAM-signalling inducing agonists. This defect also results in a reduced surface coverage after perfusion of whole blood over collagen and a decreased procoagulant activity upon stimulation with CRP and RC. Clot retraction and platelet spreading is normal.[121]

Unexpectedly, using standard *in vivo* settings, *Grb2*$^{-/-}$ mice did not differ from *Grb2*$^{+/+}$ in the mechanical injury of the abdominal aorta, which is a largely collagen-driven model due to exposed collagen after compression with a forceps.[102] In this model, the mean time to occlusion was 303 ± 101 s in *Grb2*$^{+/+}$ and 350 ± 98 s for *Grb2*$^{-/-}$ mice (Figure 3.17 A). To further investigate this, the $FeCl_3$-induced injury of mesenteric arterioles was performed in these mice with a standard concentration of 20% $FeCl_3$. Similarly to the results obtained in the mechanical injury of the abdominal aorta, no difference between *Grb2*$^{+/+}$ and *Grb2*$^{-/-}$ mice was observed. The time to appearance of first thrombi >10 µm was 7.06 ± 2.39 min and 7.84 ± 0.33 min and the mean time to vessel occlusion was 16.14 ± 5.71 min and 12.56 ± 1.94 min in *Grb2*$^{+/+}$ and *Grb2*$^{-/-}$ mice, respectively (Figure 3.17 B).

Besides the importance of ITAM-signalling, other factors contribute to thrombus formation *in vivo* such as the release of TxA_2 from activated platelets. In line with this, ASA treatment of mice with GPVI defect leads to a much severe bleeding phenotype compared to single GPVI defect only.[153] Thus, in a second set of experiments, taking into account that TxA_2-mediated thrombus formation may be relevant for our observation, *Grb2*$^{+/+}$ and *Grb2*$^{-/-}$ mice were subjected to the *in vivo* models after treatment with ASA (1 µg ASA/kg body weight). Indeed, this treatment led to a significantly reduced thrombus stability in *Grb2*$^{-/-}$ mice compared to *Grb2*$^{+/+}$ mice. In the mechanical injury model of the abdominal aorta the mean time to occlusion after ASA treatment in *Grb2*$^{+/+}$ mice was 295 ± 84 s whereas in *Grb2*$^{-/-}$ mice it was 419 ± 99 s (Figure 3.17 C, p <0.01). Additionally, 7 out of 17 *Grb2*$^{-/-}$ mice did not form occlusive thrombi after mechanical injury whereas only 1 out of 14 *Grb2*$^{+/+}$ did not occlude

(p <0.05). Similarly, in the $FeCl_3$-induced injury model of mesenteric arterioles the mean time to occlusion was 17.89 ± 4.13 min and 25.72 ± 5.20 min in *Grb2*$^{+/+}$ and *Grb2*$^{-/-}$ mice, respectively (Figure 3.17 D, p <0.01). In this model no difference was seen in the time to first thrombus appearance.

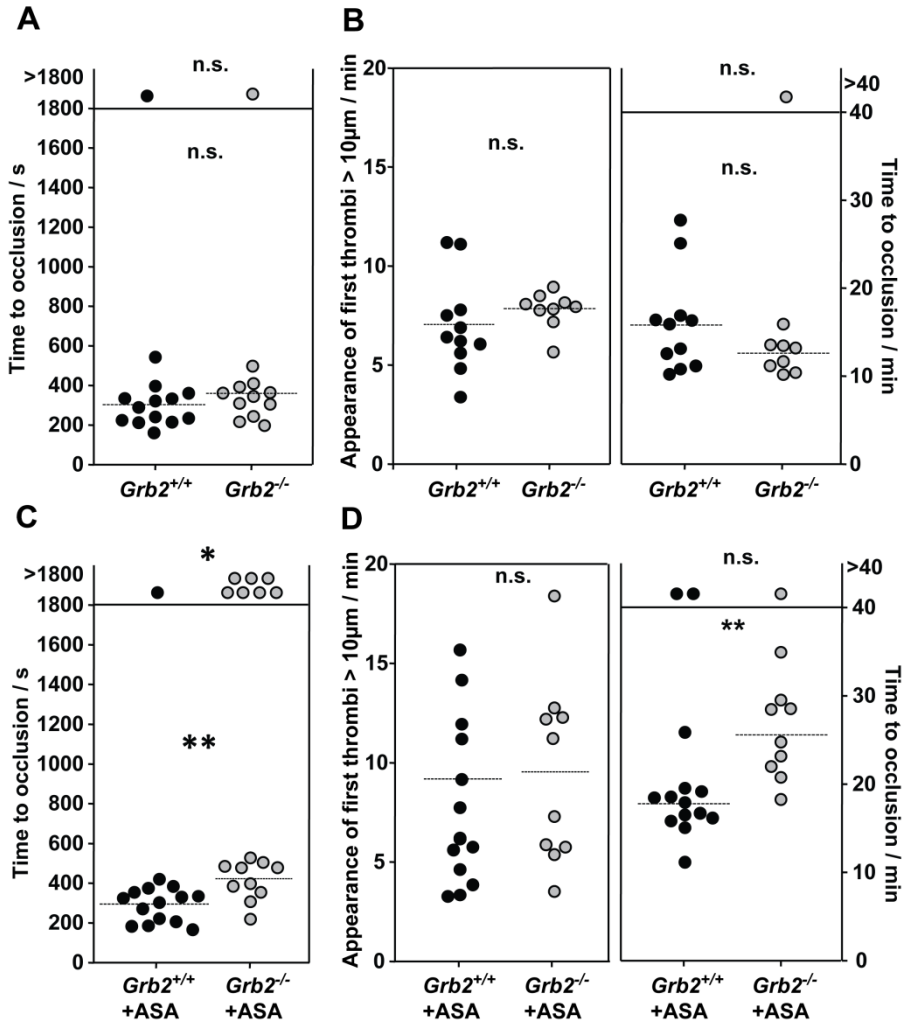

Figure 3.17: *Grb2*$^{-/-}$ mice treated with ASA showed prolonged time to occlusion in arterial thrombosis models compared to ASA-treated *Grb2*$^{+/+}$ mice. (A) Aorta injury model in *Grb2*$^{-/-}$ and *Grb2*$^{+/+}$ mice. (B) $FeCl_3$-induced injury model of mesenteric arterioles in *Grb2*$^{-/-}$ and *Grb2*$^{+/+}$ mice. (C) *Grb2*$^{-/-}$ and *Grb2*$^{+/+}$ mice treated with 1 µg ASA/kg body weight in the mechanical injury of the abdominal aorta model. (D) *Grb2*$^{-/-}$ and *Grb2*$^{+/+}$ mice after ASA treatment in the $FeCl_3$-induced injury model of mesenteric arterioles. The horizontal dotted line indicates the mean value (n.s. = not significant, *p <0.05; **p <0.01, ASA = acetylsalicylic acid). Each dot represents one injured aorta (A and C)/ arteriole (B and D).

3.3.2 *Clp36*$^{\Delta LIM}$ and SLAP/SLAP2-double-deficient mice display a pro-thrombotic phenotype *in vivo*

Grb2$^{-/-}$ mice displayed delayed thrombus formation *in vivo* after ASA treatment and showed compromised ITAM-dependent platelet activation *in vitro*. In contrast, *Clp36*$^{\Delta LIM115}$ and

SLAP/SLAP2-double deficient mice (Deya Cherpokova, personal communication) negatively regulate ITAM-signalling *in vitro.* To investigate whether this *in vitro* defect translates into enhanced thrombus formation *in vivo,* both mouse strains were analysed in different arterial thrombosis models.

Clp36$^{\Delta LIM}$ mice express a truncated form of CLP36 lacking the LIM domain.[115] As CLP36 is a protein that besides in platelets is also expressed in endothelial cells, lethally irradiated wild-type mice were transplanted with *Clp36$^{\Delta LIM}$* bone marrow and *vice versa* to rule out any endothelial contribution. In wild-type mice transplanted with *Clp36$^{\Delta LIM}$* bone marrow, the mean time to occlusion was 132 ± 56 s, whereas *Clp36$^{\Delta LIM}$* mice transplanted with wild-type bone marrows displayed a mean time to occlusion of 350 ± 132 s (p <0.001). This shows that *Clp36$^{\Delta LIM}$* platelets cause a pro-thrombotic phenotype. Non-irradiated wild-type mice in a control experiment showed a normal mean time to occlusion of 260 ± 60 s (Figure 3.18 A).

Similar to *Clp36$^{\Delta LIM}$* mice, also SLAP/SLAP2 double-deficient mice display enhanced ITAM-mediated platelet activity *in vitro*. However, as SLAP/SLAP2-deficient mice are on Balb/c background and, therefore, relatively small, these mice were subjected to a less invasive *in vivo* model of $FeCl_3$-induced injury of the carotid artery. Taking into account that thrombus formation may be enhanced in this mouse strain, a much lower concentration of 2.5% $FeCl_3$ than previously used was applied to perform this model. As described by Pamuklar et al.[154] under these settings, wild-type mice should not be able to form an occlusive thrombus after the chemically-induced injury and the blood flow is maintained. In contrast, more reactive platelets should still be able to form an occlusive thrombus. In this modified model, vessels in 9 out of 15 wild-type mice did not occlude, whereas 14 out of 15 of the SLAP/SLAP2-double deficient mice were able to form an occlusive thrombus (p <0.001). Additionally, the mean time to vessel occlusion in wild-type mice was 606 ± 145 s and is prolonged compared to SLAP/SLAP2-double deficient mice (mean time to occlusion: 482 ± 149 s, n.s., Figure 3.18 B).

Immune cells such as T cells are a pathogenic factor in thrombo-inflammatory diseases.[155] As SLAP and SLAP2 are also expressed in T cells,[122] the same assay was performed in platelet-depleted wild-type mice either transfused with *Slap/Slap2$^{+/+}$* or *Slap/Slap2$^{-/-}$* platelets. Similar to results obtained in the original mice, wild-type mice transfused with SLAP/SLAP2-double deficient platelets showed enhanced thrombus formation (11 out of 12 vessel occluded) and most of the wild-type mice transfused with wild-type platelets did not form an

occlusive thrombus (7 out of 10 vessels, p <0.05, Figure 3.18 C). The mean time to occlusion for wild-type mice transfused with wild-type platelets was 885 ± 201 s. For wild-type mice transfused with SLAP/SLAP2-double deficient platelets the mean time to occlusion was 803 ± 281 s (n.s., Figure 3.18 C).

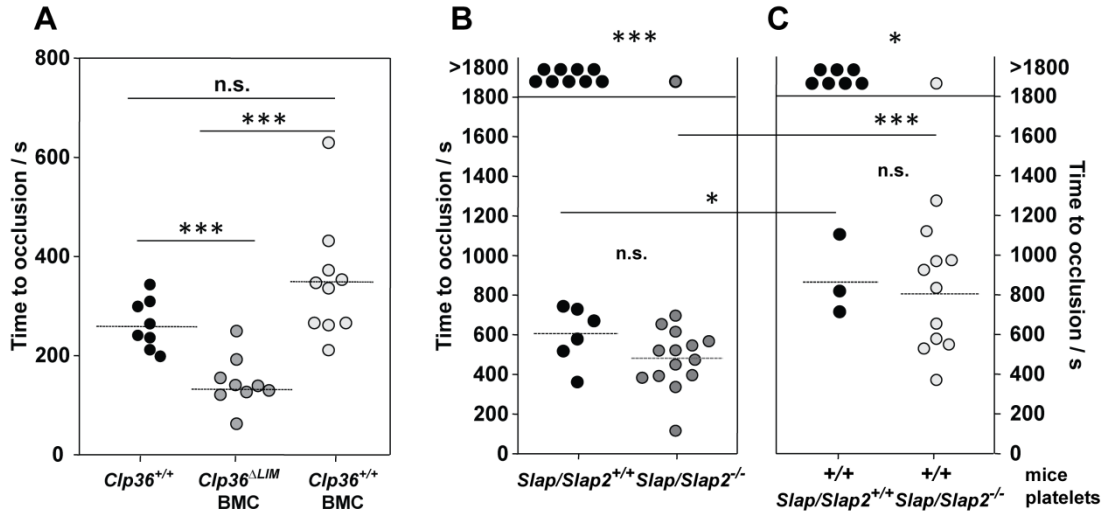

Figure 3.18: *Clp36$^{\Delta LIM}$* bone marrow chimeric (BMC) mice and SLAP/SLAP2-double deficient mice display a pro-thrombotic phenotype. (A) *Clp36$^{\Delta LIM}$* bone marrow chimeric mice show an increased ability to form occlusive thrombi in the mechanical injury of the abdominal aorta model. (B) SLAP/SLAP2-double deficient mice display a pro-thrombotic phenotype in the $FeCl_3$-induced injury of the carotid artery model. This phenotype was also observed in platelet-depleted wild-type mice either transfused with wild-type or SLAP/SLAP2-double deficient platelets. Normal mice compared to platelet-transfused mice (platelet count about 50%) showed a delayed time to occlusion after $FeCl_3$-induced injury in the carotid artery model. The horizontal dotted line indicates the mean value (n.s. = not significant, *p <0.05, ***p <0.001).

Interesting to note here is that the depleted and then transfused mice displayed about 50% of the normal platelet count. In these mice, the time to occlusion was significantly delayed compared to normal mice (normal wild-type: 606 ± 145 s and wild-type transfused with wild-type platelets 885 ± 201 s, p = 0.02; normal SLAP/SLAP2-deficient mice 482 ± 149 s and wild-type transfused with SLAP/SLAP2-deficient platelets 803 ± 281 s, p = 0.001, Figure 3.18 B and C). In chapter 3.1.5 it was shown that occlusive thrombus formation in the $FeCl_3$-induced injury model of carotid arteries ($FeCl_3$ concentration 10%) is only delayed at platelet counts lower than 30% (Figure 3.8). These different platelet count thresholds to maintain robust thrombotic function (platelet count >30% for injuries with 10% $FeCl_3$ solution and platelet count >50% for injuries with 2.5% $FeCl_3$ solution) may depend on the severity of the induced injury.

3.4 *In vivo* and *in vitro* analyses of EFhd2-deficient mice

Similar to Grb2, CLP36 and SLAP/SLAP2, EFhd2 has been proposed to modulate ITAM-signalling due to its association with Syk.[127] Furthermore, EFhd2 has been implicated in Ca^{2+} signalling and actin-dependent cytoskeletal rearrangements in different cell types.[129] To investigate the function of EFhd2 in platelets, EFhd2-deficient mice were analysed *in vivo* and *in vitro*.

3.4.1 EFhd2 is dispensable for platelet production

Following heterozygous matings, it has been shown that *Efhd2*$^{+/+}$, *Efhd2*$^{+/-}$ and *Efhd2*$^{-/-}$ mice are born according to the expected Mendelian ratio and are morphologically indistinguishable indicating that EFhd2 is dispensable for embryonic development.[156]

Genotyping of *Efhd2*$^{+/+}$, *Efhd2*$^{+/-}$ and *Efhd2*$^{-/-}$ mice was performed by PCR as previously described (Figure 3.19 A).[156] In a first experiment, the expression of EFhd2 in platelet lysates of *Efhd2*$^{+/+}$ mice and the absence of EFhd2 in platelet lysates of *Efhd2*$^{-/-}$ mice was confirmed by Western blotting with GPIIIa serving as loading control (Figure 3.19 B).

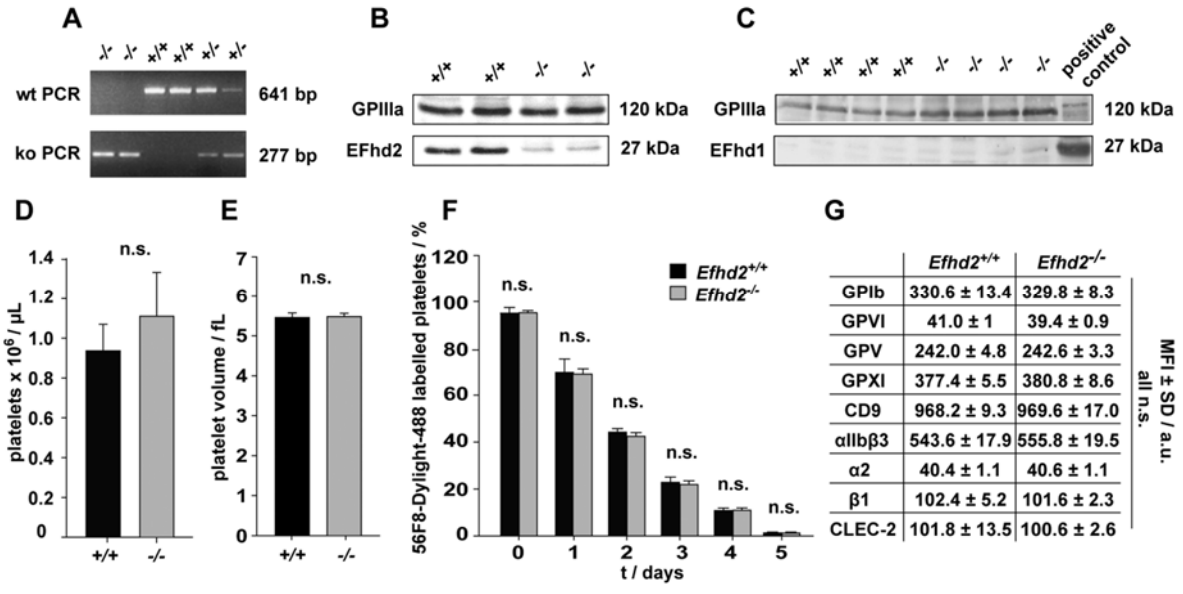

	Efhd2$^{+/+}$	*Efhd2*$^{-/-}$
GPIb	330.6 ± 13.4	329.8 ± 8.3
GPVI	41.0 ± 1	39.4 ± 0.9
GPV	242.0 ± 4.8	242.6 ± 3.3
GPXI	377.4 ± 5.5	380.8 ± 8.6
CD9	968.2 ± 9.3	969.6 ± 17.0
αIIbβ3	543.6 ± 17.9	555.8 ± 19.5
α2	40.4 ± 1.1	40.6 ± 1.1
β1	102.4 ± 5.2	101.6 ± 2.3
CLEC-2	101.8 ± 13.5	100.6 ± 2.6

Figure 3.19: EFhd2-deficient platelets display normal size and volume, GP-expression levels and normal life span. (A) Genotyping of *Efhd2*$^{+/+}$, *Efhd2*$^{+/-}$ and *Efhd2*$^{-/-}$ mice by PCR. (B) Western blot analysis confirmed EFhd2 expression in platelets and absence of EFhd2 in the analysed *Efhd2*$^{-/-}$ mice. GPIIIa served as loading control. (C) Absence of EFhd1 in platelet lysates of *Efhd2*$^{+/+}$ and *Efhd2*$^{-/-}$ mice. GPIIIa served as loading control and the pro-B cell line 38B9 lysate served as positive control (D) Platelet count, (E) platelet volume and (F) platelet life span in *Efhd2*$^{+/+}$ and *Efhd2*$^{-/-}$ mice are comparable. (G) Mean fluorescence intensity (MFI) ± SD of GP-expression levels of *Efhd2*$^{-/-}$ platelets and *Efhd2*$^{+/+}$ platelets are comparable. n.s. = not significant, SD = standard deviation.

EFhd1, a homologue of EFhd2, was not expressed in wild-type platelets. It was also not expressed or up-regulated in compensation for the loss of EFhd2 in platelets of EFhd2-deficient mice as shown by Western blot. GPIIIa served as loading control and the pro-B cell line 38B9 lysate served as positive control (Figure 3.19 C). In subsequent experiments, platelet production and glycoprotein expression levels of *Efhd2*$^{-/-}$ platelets compared to controls were investigated by flow cytometry and a haematologic analyser. *Efhd2*$^{-/-}$ mice displayed normal platelet counts (Figure 3.19 D), platelet volume (Figure 3.19 E) and platelet life span (Figure 3.19 F). Furthermore, EFhd2-deficiency did not have any effect on the expression of major platelet glycoproteins as shown by flow cytometry (Figure 3.19 G).

3.4.2 EFhd2-deficient mice display normal haematologic parameters

To rule out that EFhd2-deficiency influences the production of other blood cells, blood of *Efhd2*$^{+/+}$ and *Efhd2*$^{-/-}$ mice was collected and subsequently analysed in a Sysmex cell counter to assess basic blood parameters. This analysis revealed unaltered white and red blood cell counts as well as unchanged haemoglobin content of red blood cells and haematocrit in *Efhd2*$^{-/-}$ mice compared to controls (Table 3.1).

Table 3.1: *Efhd2*$^{-/-}$ mice display normal haematologic parameters. White blood cell count (WBC), red blood cells (RBC), haemoglobin (HGB) and haematocrit (HCT) were determined with an haematologic analyser (Sysmex)(n = 5 versus 5, two independent experiments, n.s. = not significant).

Genotype EFhd2	WBC x 10^3	RBC x 10^6	HGB / g /dL	HCT / %
+/+	10.78 ± 3.78	8.39 ± 0.87	14.28 ± 0.80	44.24 ± 3.51
-/-	12.95 ± 3.16	8.29 ± 1.40	13.58 ± 2.20	42.98 ± 7.10
p value	n.s.	n.s.	n.s.	n.s

3.4.3 EFhd2-deficient platelets show unaltered activation and aggregation

In order to study the effect of EFhd2-deficiency in platelets, platelets were activated with major agonists and the active form of αIIbβ3 and the exposure of P-selectin was analysed by flow cytometry. Interestingly, all experiments performed indicated that the platelet activation upon stimulation with ITAM and GPCR-agonists of *Efhd2*$^{+/+}$ and *Efhd2*$^{-/-}$ platelets was comparable (Figure 3.20 A and B).

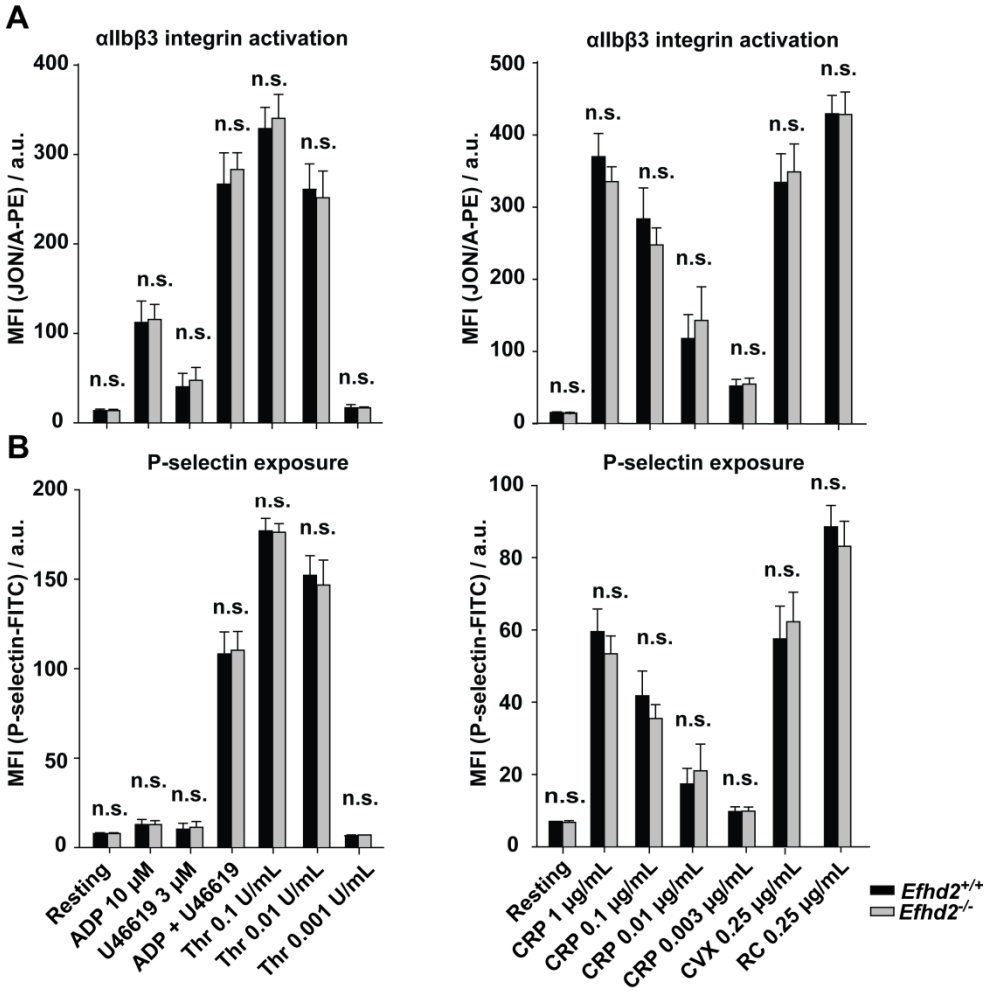

Figure 3.20: Activation of αIIbβ3 integrins and α-granule release of *Efhd2*$^{-/-}$ platelets upon stimulation with different agonists. Platelet activation was measured using flow cytometry by binding of JON/A-PE to active αIIbβ3 integrin (A) and binding of anti-P-selectin-FITC (B) to P-selectin exposed at the platelet surface. *EFhd2*$^{-/-}$ platelets show comparable levels of platelet activation for GPCR (left panel) and (hem)ITAM-signalling (right panel). The values represent the mean fluorescence intensity (MFI) ± SD for five mice per group in three independent experiments. Abbreviations: Thr = thrombin, CVX = convulxin, RC = rhodocytin, CRP = collagen related peptide, n.s. = not significant.

In order to test the ability of EFhd2-deficient platelets to aggregate, platelet aggregation experiments were performed in a Born aggregometer. In this aggregometer platelet activation is recorded by changes in light transmission. Whereas initial platelet shape change is detectable as a reduced light transmission compared to the resting platelet suspension, platelet aggregation leads to an increased transmission of light. In this assay, also the release of second wave mediators is an important factor as the concentration of platelets in the used suspension is relatively high. The release of granule content upon initial platelet stimulation, therefore, reinforces platelet aggregation.[157] Corresponding to the results obtained by flow cytometry, no defect in platelet aggregation or platelet shape change in EFhd2-deficient mice was detected upon stimulation with different agonists (Figure 3.21).

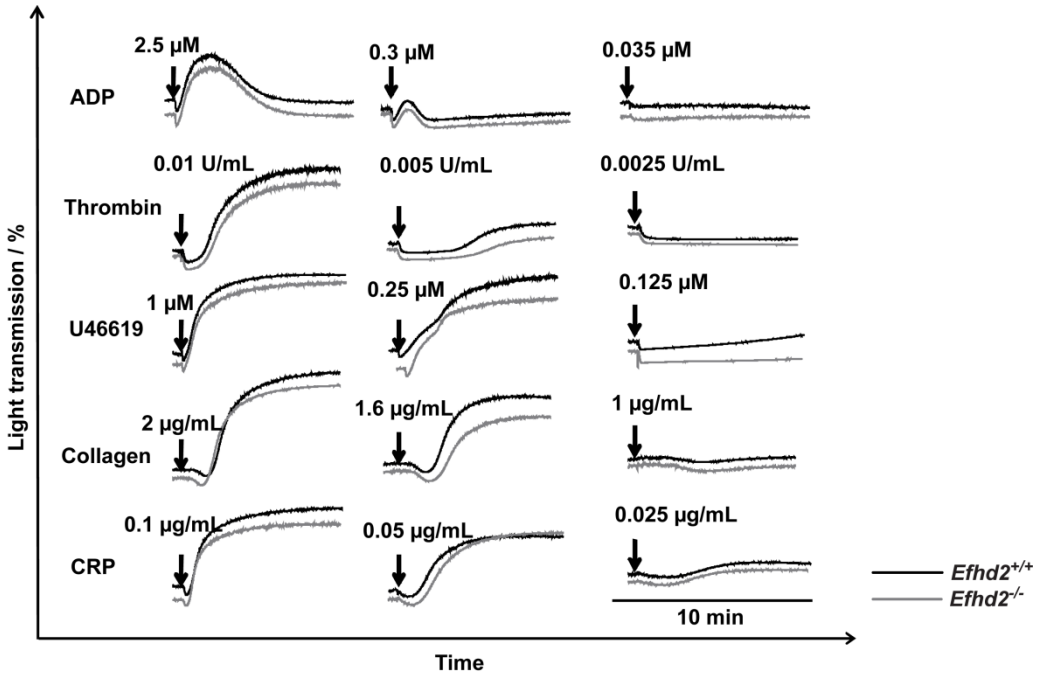

Figure 3.21: Unaltered aggregation of *Efhd2*$^{-/-}$ platelets. Platelets were stimulated with the indicated agonists and the ability of platelets to aggregate was recorded in a Born aggregometer. *Efhd2*$^{-/-}$ platelets (grey line) and *Efhd2*$^{+/+}$ platelets (black line) show comparable aggregation traces.

3.4.4 Clot retraction and spreading of *Efhd2*$^{-/-}$ platelets is unaltered

Clot retraction is a process that relies on integrin outside-in signalling and the mobilization of intracellular Ca^{2+}. As EFhd2 is a Ca^{2+}-binding protein that may interfere with the Ca^{2+}-mobilization, clot retraction was performed for *Efhd2*$^{+/+}$ and *Efhd2*$^{-/-}$ platelets. In the beginning of the clotting process, platelets tightly adhere to fibrin strands and start to extend pseudopodia that via αIIbβ3 integrins adhere along the fibres. In the final phase, these pseudopodia are pulled back toward the central mass. This effect has been postulated to pull wound edges into closer proximity thereby facilitating wound healing.[46] In the clot retraction assay, *Efhd2*$^{-/-}$ and *Efhd2*$^{+/+}$ platelets formed a clot with similar kinetics. The observation time for clot retraction was 4 h. After 30 min the first clot formation became visible and was completed after 3 h. The excess fluid measured after termination of the experiment was 93% and 96% in control and *Efhd2*$^{-/-}$ platelets, respectively (n.s.). The kinetics of clot formation as well as the volume of the excess fluid after 4 h showed that clot retraction in *Efhd2*$^{-/-}$ platelets was comparable to that of *Efhd2*$^{+/+}$ platelets (Figure 3.22 A).

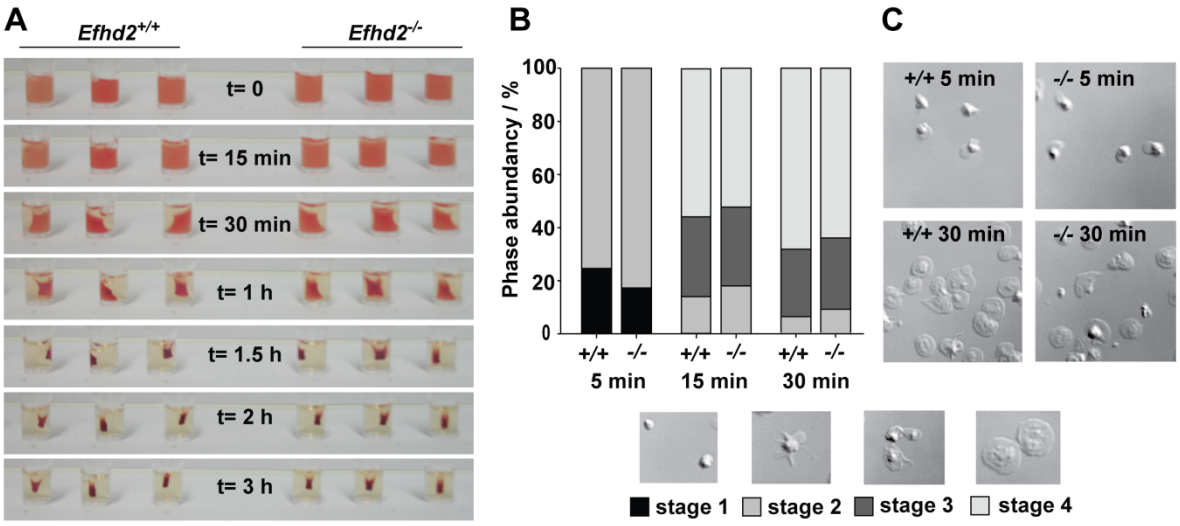

Figure 3.22: Unaltered clot retraction and spreading characteristics of *Efhd2*$^{-/-}$ platelets compared to *Efhd2*$^{+/+}$ platelets. (A) Clot retraction of *Efhd2*$^{-/-}$ and *Efhd2*$^{+/+}$ platelets at the indicated time points. *Efhd2*$^{-/-}$ and *Efhd2*$^{+/+}$ platelets retract with similar speed upon stimulation with 0.01 U/mL thrombin. (B) Platelets were allowed to spread on fibrinogen-coated surfaces in the presence of 0.01 U/mL thrombin. Statistic evaluation of the percentage of spread platelets after the indicated time intervals 5, 15, and 30 min and characteristics of the different stages of platelet spreading: stage 1 - roundish; stage 2 - filopodia only; stage 3 - filopodia and lamellipodia; stage 4 - fully spread (lower panel). (C) Representative images of the platelet spreading assay at the indicated time points.

Similar to clot retraction, platelet spreading is important to seal the wound site and is mainly mediated through the binding of fibrinogen to platelet αIIbβ3 integrin.[158] Spreading also requires outside-in signalling of platelets and the mobilization of Ca^{2+}. To test whether EFhd2 plays a role in platelet spreading, *Efhd2*$^{+/+}$ and *Efhd2*$^{-/-}$ platelets were spread on fibrinogen-coated surfaces in the presence of thrombin (0.01 U/mL). In line with the clot retraction results, no defect in *Efhd2*$^{-/-}$ platelets was observed compared to control. *Efhd2*$^{-/-}$ platelets were able to form filopodia and lamellipodia similarly to *Efhd2*$^{+/+}$ platelets and after 30 min approximately 65% of either platelet group was fully spread (Figure 3.22 B and C).

3.4.5 *Efhd2*$^{-/-}$ platelets show a slightly increased PS exposure but normal Ca^{2+} influx upon stimulation

During platelet activation the increase in cytosolic Ca^{2+} is a very important step in the onset of coagulation as it induces the exposure of PSs on the platelet surface. Exposed PSs provide a negatively charged surface at the site of injury thus greatly enhancing the generation of active coagulation factors. To measure PS-exposure, activated platelets were incubated with Annexin-A5, a protein that at physiologic Ca^{2+} concentration binds aminophospholipids with high affinity and specifity.[159] The highest pro-coagulant activity of platelets is reached upon

simultaneous stimulation with collagen and thrombin and is much less for treatment with single agonists only.[159,160] To test whether PS exposure is altered in *Efhd2*$^{-/-}$ platelets, washed platelets were stimulated with agonists and the percentage of Annexin-A5-DyLight488 labelled platelets was analysed by flow cytometry. In this assay, a small but significant increase in the pro-coagulant activity of *Efhd2*$^{-/-}$ platelets versus *Efhd2*$^{+/+}$ upon stimulation with CRP (7.4 ± 2.4 % versus 4.1 ± 1.5%, p = 0.02) was observed. Stimulation with other agonists was comparable to control (Figure 3.23 A).

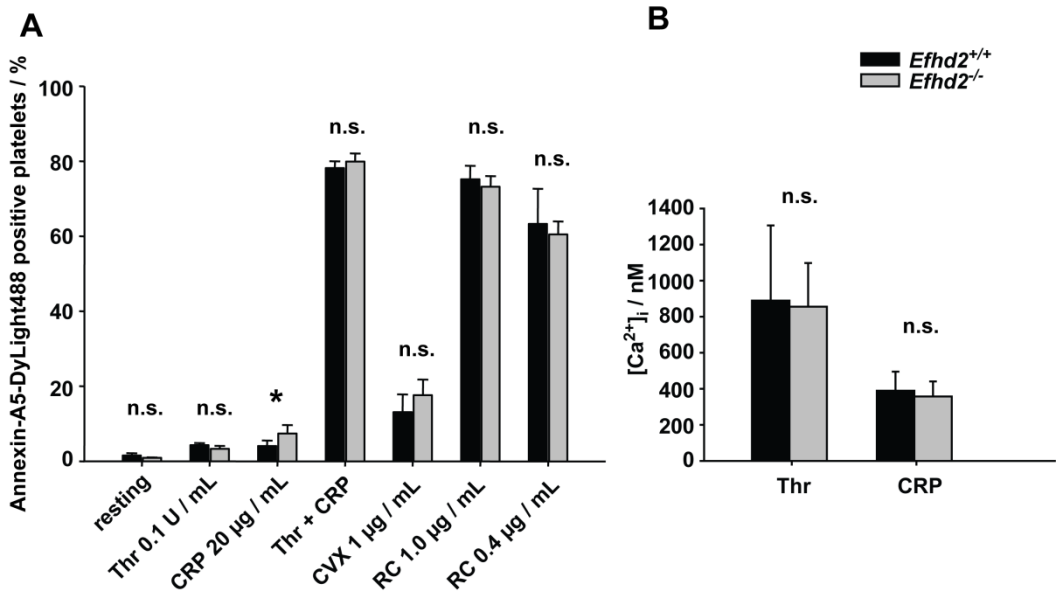

Figure 3.23: Slightly altered pro-coagulant activity in EFhd2-deficient platelets but normal Ca^{2+} influx upon stimulation. (A) Upon stimulation with the indicated agonists, platelets expose negatively charged PSs which enable the association of Ca^{2+} to the platelet surface. Ca^{2+} at the platelet surface can be detected flow cytometrically by incubation with Annexin-A5-DyLight488. The values represent the mean fluorescence intensity (MFI) ± SD for five mice per group in three independent experiments. (B) Measurement of Ca^{2+} influx in *Efhd2*$^{+/+}$ and *Efhd2*$^{-/-}$ platelets upon stimulation with thrombin and CRP. Abbreviations: Thr = thrombin, CRP = collagen related peptide, CVX = convulxin, RC = rhodocytin, n.s. = not significant, *p <0.05.

The increase of the intracellular calcium concentration ($[Ca^{2+}]_i$) is important to obtain proper platelet aggregation after stimulation with agonists. EFhd2 contains two EF-hand domains which bind to Ca^{2+}.[127] To investigate whether the increase of $[Ca^{2+}]_i$ is altered in EFhd2-deficient platelets, changes in $[Ca^{2+}]_i$ upon stimulation were measured fluorimetrically. The changes observed in $[Ca^{2+}]_i$ upon stimulation with either CRP or thrombin in *Efhd2*$^{+/+}$ and *Efhd2*$^{-/-}$ platelets was comparable. For *Efhd2*$^{+/+}$ platelets, the Ca^{2+} influx was 389 ± 106 nM and was 357 ± 83 nM for *Efhd2*$^{-/-}$ platelets upon stimulation with CRP. For agonist treatment with thrombin, Ca^{2+} influx was 889 ± 416 nM and 855 ± 242 nM for *Efhd2*$^{+/+}$ and *Efhd2*$^{-/-}$ platelets, respectively (Figure 3.23 B).

3.4.6 Thrombus formation under flow is unaltered in *Efhd2*$^{-/-}$ platelets

To test the ability of EFhd2-deficient platelets to form thrombi under shear conditions, anti-coagulated whole blood was perfused over a collagen-coated surface. The flow chamber assay was performed at intermediate (1000 s^{-1}) and high (1700 s^{-1}) shear rates which correspond to the shear forces in intermediate and small vessels. At a shear rate of 1000 s^{-1} the surface coverage of *Efhd2*$^{+/+}$ and *Efhd2*$^{-/-}$ platelets was comparable (44.8 ± 14.4% and 39.9 ± 9.8%, respectively, Figure 3.24 A, left). Similarly, at a shear rate of 1700 s^{-1} the surface coverage of *Efhd2*$^{+/+}$ and *Efhd2*$^{-/-}$ platelets was unaltered (34.2 ± 10.2% and 33.7 ± 5.6%, respectively, Figure 3.24 B, left). The relative thrombus volume was comparable for *Efhd2*$^{+/+}$ and *Efhd2*$^{-/-}$ platelets at both shear rates (Figure 3.24 A and B, right).

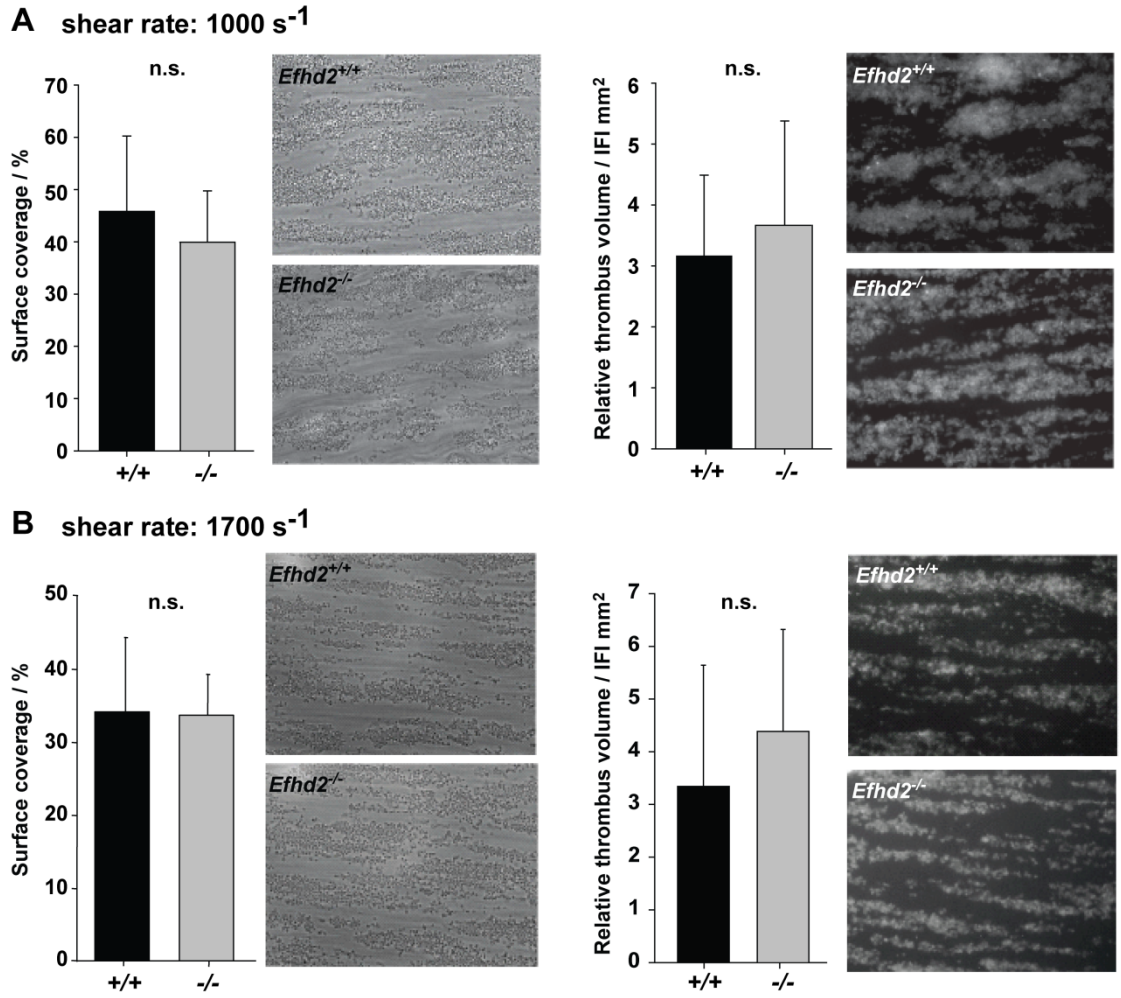

Figure 3.24: Thrombus formation under flow conditions of EFhd2-deficient platelets is comparable to control. To test the ability to form thrombi under different shear rates, anti-coagulated blood was perfused over collagen-coated surfaces. (A) Statistic evaluation and representative images of the surface coverage (left) and the relative thrombus formation (right panel) at a shear rate of 1000 s^{-1}. (B) Statistic evaluation and representative images of the surface coverage (left panel) and the relative thrombus formation (right panel) at a shear rate of 1700 s^{-1}. Fluorescence images were obtained by labelling platelets with an anti-GPIX-DyLight488 derivative.

3.4.7 Thrombosis and haemostasis are unaltered in EFhd2-deficient mice

To test the function of EFhd2-deficient platelets in thrombosis and haemostasis, three different *in vivo* models were applied: the tail bleeding time assay, the mechanical injury of the abdominal aorta and the $FeCl_3$-induced injury of mesenteric arterioles.

In the tail bleeding time assay, EFhd2-deficient mice displayed a mean time to haemostatic plug formation which was comparable to control (Figure 3.25 A). Time to haemostatic plug formation in *Efhd2*$^{+/+}$ mice was 527 ± 229 s and 542 ± 189 s in *Efhd2*$^{-/-}$ mice.

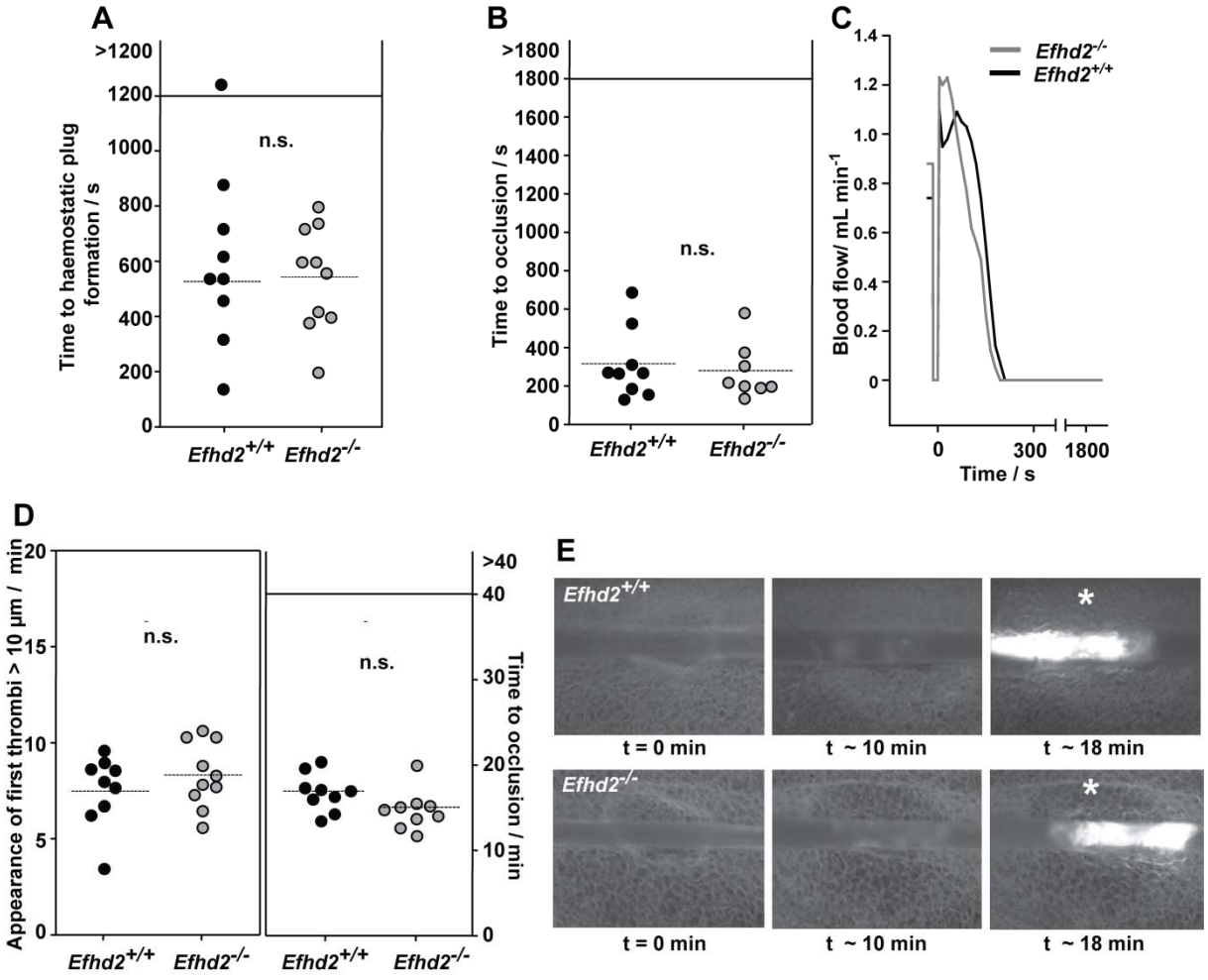

Figure 3.25: Unaltered thrombotic and haemostatic function in EFhd2-deficient mice. (A) EFhd2-deficient mice subjected to the tail bleeding time assay displayed comparable times to occlusive plug formation as *Efhd2*$^{+/+}$ mice. (B) Occlusive thrombus formation in the aorta injury model (each dot represents one aorta) and (C) representative blood flow measurements. (D) The $FeCl_3$-induced injury model of mesenteric arterioles in *Efhd2*$^{+/+}$ and *Efhd2*$^{-/-}$ mice, each dot represents one mesenteric arteriole. (E) Representative images of the $FeCl_3$-induced injury model of mesenteric arterioles in *Efhd2*$^{+/+}$ and *Efhd2*$^{-/-}$ mice, asterisk indicates stable occlusion of the vessel. The horizontal dotted line indicates the mean value to vessel occlusion. (n.s. = not significant).

The *in vivo* model of the mechanical injury of the abdominal aorta is a largely ITAM-signalling-driven mouse model.[102] In this model, blood flow was measured with an ultrasonic flow probe for 30 min and the injury was induced by a firm compression with a forceps. Compared to the $FeCl_3$-induced injury of mesenteric arterioles, the time to occlusive thrombus formation is in this model relatively fast and takes place within few minutes. Time to occlusion for *Efhd2*$^{+/+}$ and *Efhd2*$^{-/-}$ mice was comparable (315 ± 182 s and 279 ± 144 s, respectively (Figure 3.25 B)). Representative curves of the blood flow measurements are shown in Figure 3.25 C.

To analyse the ability of *Efhd2*$^{-/-}$ platelets to form thrombi *in vivo* in a second widely used model, these mice were also subjected to the $FeCl_3$-induced injury model of mesenteric arterioles. In this model, two specific time points are recorded: the time to appearance of first thrombi and the time to full vessel occlusion. The mean time to the appearance of first thrombi >10 µm for *Efhd2*$^{+/+}$ and for *Efhd2*$^{-/-}$ mice was comparable and was 7.58 ± 1.87 min and 8.36 ± 1.70 min, respectively. Similarly, the time to vessel occlusion was unaltered for *Efhd2*$^{+/+}$ and *Efhd2*$^{-/-}$ mice (16.89 ± 2.23 min and 15.51 ± 2.75 min, respectively) (Figure 3.25 D). Representative images of occlusive thrombus formation in *Efhd2*$^{+/+}$ and *Efhd2*$^{-/-}$ mice are shown in Figure 3.25 E.

Taken together, the results obtained in these *in vivo* models are in agreement with the results obtained in *in vitro* platelet assays. EFhd2-deficient mice did not display major alterations in platelet function compared to control.

4 Discussion

The occurrence of thrombotic events in myocardial or cerebral vessels is a major cause of death in the developed world.[161] As arterial thrombi largely consist of activated and aggregated platelets, platelets can be considered as a major player in these thrombotic diseases. On the other hand, platelet activation and aggregation at a site of injury is essential for the life-saving process of haemostatic plug formation. This close relation between pathological thrombus and physiological plug formation is clearly illustrated by the increased risk of bleeding during anti-thrombotic treatment. A detailed understanding of platelet function is, therefore, indispensable for the effective and safe therapy of thrombotic diseases.

A major focus of this dissertation was on the impact of platelet counts on haemostatic and thrombotic function *in vivo*. Thrombocytopenia of different severity was induced in mice by injection of low amounts of platelet-depleting antibodies. Whereas it is known that haemostatic function in patients during thrombocytopenia is only mildly impaired, which was also confirmed in the bleeding time experiments performed in mice (Figure 3.4), there is almost no data available on the effect of reduced platelet counts on thrombotic or thrombo-inflammatory processes. In this study, critical thrombotic platelet count thresholds were identified for different arterial thrombosis models (Figure 3.7 to Figure 3.10). Additionally, tMCAO experiments were performed with thrombocytopenic mice and revealed a platelet count threshold at which mice were protected from stroke but did not show any intracranial bleeding (Figure 3.11). Taken together, the average platelet count greatly exceeds the number of platelets necessary for haemostatic and thrombotic function and a mild thrombocytopenia does not affect haemostasis or thrombosis in mice.

In a different approach, a complete loss of all platelets from the circulation was induced by the injection of high amounts of platelet-depleting antibody. During recovery from thrombocytopenia, the kinetics of platelet count recovery, blood parameters and newly generated platelets were characterised. Interestingly, a major defect in platelet ITAM-signalling on day five after injection of high amounts of platelet-depleting antibody was observed *in vitro* and *in vivo*, pointing to a possible defect in platelet activation at a very early stage of platelet generation.

To further investigate the regulation of ITAM-signalling *in vivo*, three different mouse strains with genetic alterations of the ITAM-signalling pathway were analysed. *Grb2*$^{-/-}$ mice show compromised platelet activation *in vitro* which was also translated into delayed arterial thrombus formation after ASA treatment. In line with this, the increased platelet activation of SLAP/SLAP2-deficient mice and *CLP36*$^{\Delta LIM}$ bone marrow chimeric mice translated into enhanced thrombus formation *in vivo*. In a last set of experiments, EFhd2-deficient mice, lacking a putative ITAM-modulating adapter protein, were analysed *in vivo* and *in vitro*.

4.1 Robust haemostatic and thrombotic function in thrombocytopenic mice

In this study, haemostasis and thrombosis were analysed in thrombocytopenic mice using different *in vivo* models. These experiments showed that a 70-80% reduction of the platelet count in mice did not impair occlusive thrombus formation in large vessels and even lower platelet counts were effective to maintain haemostasis and thrombotic occlusion of small arterioles. These data provided the first direct experimental evidence that only severe platelet count reductions have significant effects on haemostasis, thrombosis or thrombo-inflammatory pathologies.

Consistently, in several studies on human patients it has been found that thrombocytopenia with functional platelets generally induces no or only minor bleeding symptoms with only rare cases of life threatening haemorrhages.[68,162,163] This complies with the observations in mice made in this study, demonstrating that isolated thrombocytopenia only mildly affects normal haemostasis as assessed in a tail bleeding assay. Although there is no clear correlation between bleeding time and bleeding risk,[164] one may speculate on the grounds of these results that also in humans the occurrence of bleeding episodes during thrombocytopenia might to a great extent be determined by other factors than the degree of thrombocytopenia. This has impressively been demonstrated in mice where only the combination of severe thrombocytopenia and inflammation resulted in spontaneous haemorrhage in different organs.[81] In-depth clinical studies will be required to identify the factors that may trigger haemorrhagic complications in thrombocytopenic patients.

While numerous studies on human patients[68,162,163] have assessed the causal relationship between thrombocytopenia and increased bleeding, only very limited and partially

contradictory information is available on the effect of isolated thrombocytopenia on the risk of acute thrombotic disease in humans. Sarpatwari et al.[48] described an increased risk for arterial and venous thromboembolism in humans suffering from ITP. Others have reported that the risk for arterial thrombosis was decreased in male ITP patients but increased two-fold in female ITP patients compared to non-thrombocytopenic controls.[165] Similarly, various case reports of thrombotic events such as ischaemic stroke[166] or myocardial infarction during ITP[167] have indicated that thrombocytopenia caused by auto-antibodies does not generally protect humans from thrombotic events but in some cases may even increase the thrombotic risk. One possible explanation might be that auto-antibodies directed against platelet surface proteins may affect the function and/or the activation state of the cells and thereby increase their reactivity. This assumption is supported by observations in mice showing that the antigenic specificity of anti-platelet receptor antibodies determines to a great extent possible functional alterations in the cells and also whether or not they are cleared from the circulation.[54,138,168]

The anti-GPIbα antibodies used here are known to rapidly deplete circulating platelets independently of their Fc portion and thus immune effector mechanisms[54] thereby inducing only minimal side effects. Consistently, it was found that the population of circulating platelets after anti-GPIbα antibody treatment was functionally intact (Figure 3.3). The appearance of a small population of newly generated platelets (Figure 3.2), which can be considered as a specific response to the induced thrombocytopenia,[88] did not lead to a significantly different activation response of the overall platelet population. However, a detailed analysis of this small population of newly generated platelets revealed an increased expression of prominent platelet surface receptors. An unaltered reactivity of the overall platelet population, therefore, does not definitively rule out subtle differences in the reactivity of the newly generated platelets compared to the older platelets. Furthermore, this increased expression of prominent platelet surface receptors in newly generated platelets during thrombocytopnia may be relevant for the pro-thrombotic properties of young stressed platelets.[83,87,89] In this study, this small population of newly generated platelets corresponded to only 12% of the whole population, thus it can be considered as very unlikely that such differences, if existent, account for the unexpectedly robust haemostatic and thrombotic activity in the thrombocytopenic animals. This model system, therefore, allows studies on the effect of a largely isolated thrombocytopenia on

haemostasis and thrombosis. Using this model system, no signs of spontaneous bleeding in severely thrombocytopenic mice were observed, confirming that thrombocytopenia alone is not sufficient to induce spontaneous haemorrhage in mice.[81] Furthermore, it was found that even severe reductions of the PC (~97.5%) had no major effect on haemostasis or occlusive thrombus formation in small arterioles (Figure 3.4 and Figure 3.9). In contrast, occlusive thrombus formation in larger arteries required higher PCs (carotid artery: ~20% and abdominal aorta: ~30% of control (Figure 3.8 and Figure 3.7)) demonstrating that considerable differences in the sensitivity for PC reductions exist between these thrombosis models. This may, at least partially, be explained by the different diameters of the injured vessels indicating that the formation of a large vessel-occluding thrombus may require a higher PC than a thrombus that occludes a smaller vessel. Considering that in smaller vessels higher shear rates prevail, it may also be speculated that the mechanisms promoting platelet recruitment and activation as well as thrombus stabilisation are more stringent under such conditions and, therefore, less dependent on the actual number of platelets per blood volume than under low or intermediate shear conditions. In agreement with this assumption, occlusive thrombus formation in the aorta of thrombocytopenic mice was not only delayed due to slower recruitment of platelets from the circulation, but also compromised by the embolisation of large thrombus fragments (Figure 3.7). This indicates impaired thrombus stability which might be a consequence of inefficient local accumulation of released or locally produced agonists, such as ADP, TxA_2 or thrombin.

Additionally, also other factors, such as the blood pressure in the injured vessel or the nature and severity of the injury (Figure 3.8, Figure 3.18 B and C), are likely to influence the sensitivity of the different models to a reduction of the PC. Contrarily, the mechanism of platelet count reduction or mouse strain-specific effects were excluded as a cause for the robust haemostatic and thrombotic function observed (Figure 3.5 and Figure 3.6). It is challenging to completely dissect how these and other possible factors determine the “threshold PC” required for vessel occlusion in a certain vascular bed and the situation in diseased humans is likely to be even more complex. Irrespective of these important but yet unanswered questions, the data presented here, shows that vessel-occluding platelet-rich thrombi can form with virtually unaltered kinetics at remarkably low PCs in mice, indicating that thrombocytopenia might not provide protection from thrombotic events in humans.

Genetic mouse models are increasingly used to study platelet function *in vitro* and *in vivo.*[93] Some of these mouse strains display altered platelet function in association with reduced PCs.[169,170] Based on this data, it can be speculated that bleeding abnormalities or impaired experimental thrombosis in such mice is to a great extent related to the functional platelet defect rather than a reduced PC. This might have important implications for the interpretation of the data obtained in these mouse models. Based on this assumption, it might be speculated that the bleeding phenotypes seen in humans suffering from inherited platelet disorders such as the grey platelet syndrome, Wiskott-Aldrich syndrome or Bernard-Soulier syndrome[63,65,67] are primarily caused by functional platelet defects but not by the reduced PC.

Ischaemic stroke is a leading cause of death or severe disability worldwide [161] and platelets are essential components of vessel occluding emboli in the brain. Considering the results of the thrombosis models, it can be assumed that also the formation of large embolising thrombi would not be strongly affected by moderate to even pronounced PC reductions. However, further studies in animals or in patients will be required to test this directly. A major challenge in stroke treatment is, however, that spontaneous or therapeutic recanalization of a previously occluded cerebral artery is often followed by a reperfusion injury of the affected brain territory leading to the development of large infarcts.[105] The exact mechanisms through which platelets contribute to this pathology have not been established but integrin αIIbβ3-dependent thrombus formation was shown not to be essential.[106] Rather, platelets appear to orchestrate a thrombo-inflammatory cascade involving T cells and the contact activation system, finally leading to a dysregulation of the blood-brain-barrier and neurological damage.[148,171] Experimental evidence suggests that the GPIb-vWF-GPVI signalling axis in platelets is of central importance, but the molecular interplay of the contributing pathogenic factors is still poorly understood.[106] Further support that the GPIb-vWF interaction may be essential in the outcome of stroke has been shown by a recent study on guinea pigs which were treated with ALX-0081, a vWF-blocking nanobody.[172] In the present study, it was found that infarct growth following tMCAO was virtually unaffected by PC reductions up to 90%, whereas a further reduction was highly protective (Figure 3.11). This indicates that also thrombo-inflammatory pathologies, similar to occlusive thrombus formation, may not be significantly affected even by pronounced platelet count reductions. On the other hand, it was found that a platelet count of less than

110 platelets/nL blood during tMCAO did not lead to intracranial bleeding, which represents a major challenge in ischaemic stroke. This demonstrates that even at low platelet counts platelets are able to mediate vascular integrity. Thus, the efficiency to prevent intracranial bleeding in mice in a model of ischaemic stroke rather depends on other specific platelet functions than the platelet count. Indeed, studies in mice have shown that the inhibition of platelet aggregation with αIIbβ3-blocking $F(ab)_2$ fragments in the tMCAO model increased the events of intracerebral bleeding complications.[106] Congruently, emergency administration of abciximab to patients with acute ischaemic stroke in a clinical multi-centre phase III trial has increased the incidence of symptomatic or fatal intracranial haemorrhage.[173] The same outcome has been observed with tirofiban-treated patients undergoing stroke therapy[174] making the opportunity of innovative and alternative treatments even more attractive.[172] Besides αIIbβ3-mediated vascular integrity in ischaemic stroke, a recent study has revealed that platelet ITAM-signalling is critical to maintain vascular integrity during inflammation whereas GPCR-signalling is not.[175] In contrast to a possible role of αIIbβ3 and ITAM-signalling to maintain vascular integrity in different diseases, mice lacking Munc14-3-mediated platelet granule secretion have not been susceptible to intracranial bleeding in the tMCAO model of ischaemic stroke.[176] Taken together, these studies contribute to the understanding of the relation between platelet count, platelet function and the maintenance of vascular integrity.

Noteworthy in the context of the presented tMCAO experiments in thrombocytopenic mice is a study by Goerge et al.[81] In that study, mice were subjected to the tMCAO model of ischaemic stroke and rendered strongly thrombocytopenic (platelet count >25 platelets/nL blood) 3 h after the operation procedure. In this very different setting, mice were not protected from stroke. However, the strongly reduced platelet count 3 hours after tMCAO induces massive intracranial haemorrhage at the site of the infarcted area. From this experiment as well as from results obtained in a murine model of dermatitis and a model of reverse passive Arthus reaction (rpA), the authors concluded that the bleeding risk during thrombocytopenia is linked to inflammation. Interestingly, in the model of the rpA-induced inflammation, haemorrhage is significantly reduced after platelet transfusions to 5%-8% of the normal platelet count. At platelet transfusions to 10%-15% of the normal platelet count, the degree of bleeding is comparable to non-depleted mice. The observations made in the rpA cannot be directly compared with our results due to the differences in experimental

procedures. However, it is important to note that mice depleted to >110 platelets/nL blood (~11% of normal platelet count) which were subjected to tMCAO, showed infarcted areas comparable to controls but no signs of bleeding. A platelet count threshold of 10% may, therefore, be sufficient to maintain vascular integrity also in other inflammatory mouse models. However, further experiments are necessary to elucidate the critical platelet count level preventing haemorrhages during inflammation.

At lower platelet count values (<110 platelets/nL blood), mice were protected from stroke but platelets were still able to maintain vascular integrity. This indicates that, at least in the murine tMCAO model of ischaemic stroke, a reduced platelet count may be beneficial in the outcome of stroke. Even though the relevance of the platelet count as a pharmaceutical target remains unproven, the results provide basic insights into platelet count-dependent risks in ischaemic stroke.

Thrombocytopenic mice showed a robust haemostatic and thrombotic function in small arterioles (PC threshold ~2.5%). In larger vessels, the platelet count threshold required to experimentally achieve occlusive arterial thrombus formation increased (PC threshold carotid artery: ~30% and abdominal aorta: ~40%). In humans, the critical platelet count to maintain the haemostatic function is >10 platelets/nL blood (approximately 4% of normal PC).[68,177] For surgical intervention in large vessels a platelet count of >100 platelets/nL blood (approximately 40% of normal) and for neurosurgical procedures a platelet count of 50-100 platelets/nL blood is required (approximately 20-40% of normal).[92] Thus, in both species similar relative platelet counts are necessary to maintain platelet haemostatic function. Additionally, in humans and in mice higher platelet counts are required to occlude vessels after larger injuries. This finding encourages the use of mice for a better understanding of platelet counts in human physiology.[178]

Taken together, haemostasis, thrombosis and ischaemic brain infarction are largely unaffected over a wide range of PC reduction in mice. Furthermore, the *in vivo* findings in mice comply with several recent studies and can be correlated to observations in humans, reinforcing the validity of murine models as a tool in the analysis of thrombosis and haemostasis. Although data obtained in experimental mouse models cannot be directly extrapolated to the situation in humans, it may be speculated that low platelet counts alone would not significantly reduce the risk of thrombotic events such as myocardial infarction or stroke in humans. This may have important implications for the risk assessment in

cardiovascular patients but also for the development of novel therapeutic strategies to prevent or treat acute ischaemic events.

4.2 Platelet defect in ITAM-signalling after high-dose anti-GPIbα-mediated thrombocytopenia

NMRI male mice were treated with a high dose of anti-GPIbα antibody which caused a profound thrombocytopenia for several days and the platelet count only recovered to approximately 50% of normal on day five. These newly generated platelets displayed an increased size and a major defect in ITAM-signalling.

The data obtained after low-dose treatment with anti-GPIbα (and thus a low reduction of the platelet count) showed that MKs are able to increase the number of platelets by fast release of new platelets within hours (Figure 3.2). By injecting mice with 100 µg depletion antibody, all platelets were cleared from the circulation and the recovery from thrombocytopenia took days. On day five after injection still small amounts of anti-GPIbα on the surface of platelets were detectable by flow cytometry (data not shown). However, the platelet count had recovered to about 50-60% of normal. This several days lasting absence of platelets from the circulation led to a massive increase in spleen size and a partly enhanced megakaryopoiesis (Figure 3.14). Platelets generated after high-dose antibody treatment and assessed on day five were considerably enlarged (Figure 3.12 B) but showed normal expression of platelet surface receptors (Figure 3.13). This was in contrast to the consistently increased expression of platelet surface receptors in platelets which were generated during low-dose anti-GPIbα-induced thrombocytopenia (Figure 3.2). The discrepancy between newly generated platelets during low- and high-dose antibody-mediated thrombocytopenia may, therefore, indicate that treatment with 100 µg antibody leads to an exhaustive production of platelets from MKs. Under these conditions, MKs may not be able to respond to thrombocytopenia by generating platelets with an increased number of prominent platelets surface proteins.

This also indicates that new platelets generated during moderate or severe thrombocytopenia are different. To distinguish between these platelets, newly generated platelets after high-dose anti-GPIbα injection were termed early platelets as it may be speculated that these platelets are at a very early stage of maturation when released into

the blood stream. Besides unaltered glycoprotein expression levels, these early platelets showed also comparable amounts of prominent intracellular signalling molecules such as PLCγ2, Syk, and LAT in a Western blot analysis compared to control (Figure 4.1, in collaboration with Dr. Shuchi Gupta).

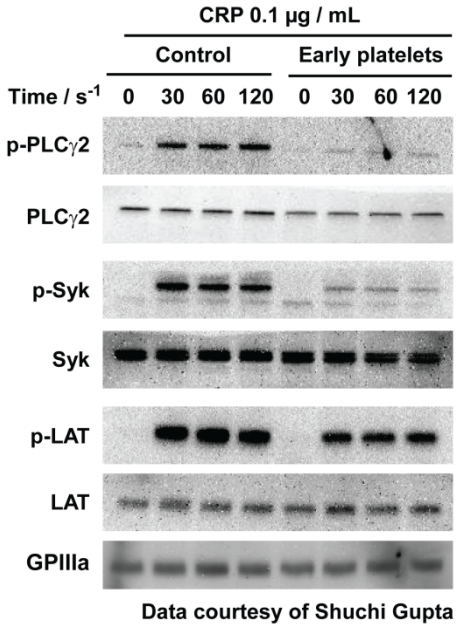

Figure 4.1: Western blot analysis of platelet lysates (2 x 10^6 platelets/µL) of PBS-injected (control) and high-dose anti-GPIbα-injected mice (early platelets). Platelet lysates of early and control platelets were analysed by Western blot with the indicated phospho-specific antibodies after stimulation with 0.1 µg/mL CRP at the respective time intervals. Staining of the respective non-phosphorylated proteins and GPIIIa served as loading controls (in collaboration with Dr. Shuchi Gupta).

However, incubation with phospho-specific antibodies against PLCγ2, Syk, and LAT revealed a reduced tyrosine phosphorylation of these proteins in early platelets upon stimulation with CRP (Figure 4.1). This indicates that ITAM-signalling is compromised in these early platelets. To correctly estimate protein expression levels and to exclude effects of the difference in platelet size, platelet lysates for Western blot analysis were adjusted to 2 x 10^6 platelets/µL.

A reduced ITAM-signalling in these platelets was also confirmed by flow cytometry upon stimulation with CRP and CVX (Figure 3.15). In contrast, early platelets stimulated with GPCR-agonists (thrombin, ADP and U46619) and assessed by flow cytometry produced normal activation responses (Figure 3.15).

To confirm the results obtained with the anti-GPIbα antibody, further experiments were performed with mice rendered thrombocytopenic by treatment with 100 µg of anti-αIIbβ3 antibody and PAF inhibitor. Similarly, a major defect in platelet ITAM-signalling and regular

platelet glycoprotein expression levels were observed in these mice on day five after treatment (Figure 3.15). Hence, the observations on early platelets after severe thrombocytopenia are presumably valid and not caused by side effects of certain antibodies.

In summary, the mechanism of how platelets are released from MKs through the vessel wall which contains platelet activating collagen remains unknown.[14] The experiments conducted with early platelets may indicate that ITAM- but not GPCR-signalling is compromised at an early stage of platelet formation. Additionally, high-dose GPIbα-treated mice showed a reduced thrombus formation *in vivo* (Figure 3.16). However, the used model system showed two shortcomings. Even on day five after injection, small amounts of anti-GPIbα antibody were detected on the platelet surface which may lead to unintended side effects on platelets. Additionally, the low platelet count caused severe subcutaneous bleeding events in these high-dose anti-GPIbα-injected mice (Figure 3.12) leading to significant reductions of the haematocrit. Hence, further experiments are necessary to elucidate the effect of high doses of antibodies in mice. Additionally, the observed defect in ITAM-signalling in early platelets may have to be confirmed using alternative assays.

4.3 Arterial thrombosis models in genetically modified mice showing altered ITAM-signalling *in vitro*

GPVI has been established as the major collagen receptor in platelets and extensively studied as a potential target for anti-thrombotic treatment, especially due to the observation that absence of GPVI on the platelet surface only mildly affects haemostasis in humans.[31] Indeed, studies in GPVI-deficient (antibody-mediated or genetically modified) mice have shown that these mice exhibit no major bleeding symptoms and are protected in arterial thrombosis models.[146] In contrast, other groups have reported no[179,180] or only a minor role for GPVI in *in vivo* thrombosis models.[100,181] The possibility to down regulate GPVI from the platelet surface through injection of anti-GPVI antibodies, (JAQ1-3) has further emphasised GPVI as a promising anti-thrombotic target.[182]

GPVI-ITAM-signalling involves different intracellular proteins which regulate GPVI signal transduction. To further investigate the regulatory mechanisms of GPVI-ITAM-signalling *in vivo*, three different genetically modified mouse strains, showing alterations in ITAM-signalling *in vitro*, were analysed. *Grb2*$^{-/-}$ mice display profoundly compromised platelet

activation upon stimulation with GPVI-ITAM-signalling inducing agonists. In contrast, *Clp36*$^{\Delta LIM}$ bone marrow chimeric mice and SLAP/SLAP2-deficient mice exhibit an ITAM-dependent hyper-reactivity of the platelets.

4.3.1 *Grb2*$^{-/-}$ mice show reduced occlusive thrombus formation after ASA treatment *in vivo*

Grb2 is an important adapter protein and its germline inactivation leads to early embryonic lethality.[117] Hence, a platelet-specific knock out mouse was used for *in vivo* analysis of Grb2 function in platelets. Several *in vitro* experiments on *Grb2*$^{-/-}$ platelets have shown a profound impairment in ITAM-signalling due to a defective stabilization of the LAT signalosome despite normal GPVI expression profiles.[121] This mouse strain, therefore, presented a promising tool to investigate ITAM-dependent thrombus formation *in vivo*. Interestingly, under the initial experimental settings applied in the *in vivo* models, no defect in arterial thrombus formation was detected (Figure 3.17 A). Considering the protection of GPVI-deficient mice in the thrombosis models and the low response of Grb2-deficient platelets upon stimulation with ITAM-signalling inducing agonists *in vitro*, this result was rather surprising. Taking into account that GPVI expression is intact in these mice and that GPVI-signalling is reduced but not abolished, the results may indicate that the GPVI-receptor still plays a relevant role in thrombus formation. A possible protein in platelets that may transduce GPVI-signalling to a small extent to the LAT signalosome, thereby rescuing Grb2 function *in vivo,* is the Grb2 family member and functional homolog Grb2-related adapter protein 2 (Gads).[108,183,184] To investigate this in more detail, Grb2-Gads double-deficient mice may be useful but still have to be generated. A different approach to analyse the contribution of the LAT signalosome upon stimulation of GPVI has been the analysis of LAT-deficient mice. Similar to Grb2-deficient platelets, LAT-deficient platelets have been reported to show compromised activation after stimulation with ITAM-signalling agonists.[185] However, also in this mouse strain no difference was detected for the time to occlusion after mechanical injury of the abdominal aorta (data not shown) although a compromised arterial thrombus formation in a laser injury model has been described.[186] In both mouse strains, several other factors contribute to thrombus formation *in vivo* and their function partly overlaps with GPVI-signalling. For example, Mangin et al. have shown that *in vivo* thrombin generation may compensate for GPVI/FcRγ-deficiency in different arterial thrombosis

models.[181] In a different study, stimulation of the TxA_2 receptor has been reported to be sufficient to restore compromised GPVI-signalling in primary haemostasis.[153] In agreement with this, ASA treatment of mice with a GPVI-defect leads to a severe bleeding defect, whereas haemostasis in ASA-treated control mice has only a minor effect.[153] To test this directly, *Grb2*$^{-/-}$ mice were injected with ASA to further impair thrombus formation *in vivo*. Using these experimental settings, a delay in thrombus formation was detected *in vivo* (Figure 3.17 B).

In summary, Grb2 is an important protein for several processes such as early embryonic development and T and B cell development.[117-119] Additionally, the functional relevance of Grb2 in GPVI and CLEC-2-mediated platelet signalling due to the stabilization of the LAT signalosome has been demonstrated.[121] *In vivo* analysis showed that arterial thrombus formation in *Grb2*$^{-/-}$ mice was only impaired after ASA treatment. This result supports the hypothesis that *in vivo* a defect in ITAM-signalling can be compensated by GPCR-signalling.[153,181]

4.3.2 *Clp36*$^{\Delta LIM}$ bone marrow chimeric mice and SLAP/SLAP2-deficient mice show enhanced thrombus formation *in vivo*

In contrast to Grb2, *Clp36*$^{\Delta LIM}$ and SLAP/SLAP2-deficient platelets display pro-thrombotic properties. Hence, both mouse strains provide a valuable tool to investigate adapter molecules which negatively regulate GPVI-signalling. Besides platelets, CLP36 is also expressed in the endothelium and SLAP/SLAP2 is also expressed in T cells. To rule out ambiguities due to the expression of the proteins in other tissues, platelets from SLAP/SLAP2-double deficient mice were transfused into wild-type mice and bone marrow chimeric mice for the *Clp36*$^{\Delta LIM}$ mouse strain were generated.

Clp36$^{\Delta LIM}$ platelets were shown to be pro-thrombotic in several *in vitro* assays.[115] To further investigate this, these mice were analysed in several *in vivo* models. In a first set of experiments, these mice were subjected to the tMCAO model of ischaemic stroke. Surprisingly, it was found that *Clp36*$^{\Delta LIM}$ mice were protected from ischaemic stroke.[187] CLP36 is expressed in different cell types and tissues including endothelial cells. To circumvent platelet-unspecific contributions to thrombus formation *in vivo*, the expression of CLP36 lacking the LIM domain was restricted to the haematopoietic system by generating bone marrow chimeras. These *Clp36*$^{\Delta LIM}$ bone marrow chimeric mice were subjected to the

mechanical injury of the abdominal aorta model and pro-thrombotic thrombus formation was detected (Figure 3.18).

Endothelial cells are important for haemostasis and thrombosis.[188] CLP36 binds to α-actinin-1 and associates with stress fibers in endothelial cells.[112] Stress fibers consist of actin filaments and are the major contractile structures in cells.[189] The contribution of stress fiber formation in endothelial cells to arterial thrombus formation is not fully understood. However, the protection of *Clp36$^{\Delta LIM}$* mice in the tMCAO model[187] versus the enhanced *in vivo* thrombus formation in *Clp36$^{\Delta LIM}$* bone marrow chimeric mice indicates that CLP36 in endothelial cells may be important for vascular endothelial wall integrity.

In T and B cells, SLAP proteins are involved in the negative regulation of T cell receptor and B cell receptor signalling complexes as well as ubiquitination and trafficking of components thereof.[122] In human platelets, SLAP2 negatively regulate GPVI-mediated platelet signalling indicating that SLAP family members may be involved in GPVI-signalling in murine platelets.[123] Indeed, platelets of SLAP/SLAP2-deficient mice show an enhanced activity *in vitro* (Cherpokova et al, personal communication) and this phenotype clearly translated into an enhanced thrombus formation *in vivo*. This result was also confirmed in platelet-depleted wild-type mice transfused with wild-type or *Slap/Slap2$^{-/-}$* platelets thus ruling out any platelet-unspecific contributions. These results indicate that an increased activity of SLAP/SLAP2 in platelets may reduce platelet activation. Thus the development of drugs promoting SLAP/SLAP2 activity in platelets may be a promising tool for the treatment of acute ischemic disease states such as myocardial infarction or stroke. Whether this protection from arterial thrombosis of SLAP/SLAP2-deficient mice is also valid in SLAP or SLAP2 single protein-deficient mice[123] remains to be elucidated.

Taken together, an alteration in platelet function *in vitro* is very often translated into a specific change in thrombus formation *in vivo*. However, *in vivo* many factors may compensate for the loss of an important protein. Hence, the data obtained *in vivo* describes a far more complex and multilayered system compared to the analysis of isolated platelets *in vitro*. Given that most proteins are expressed in several tissues, the interpretation of data obtained from genetically modified mice *in vivo* is further complicated and makes it difficult to unambiguously and specifically attribute the change of e.g. *in vivo* thrombus formation to the functional alteration in platelets. However, the generation of bone marrow chimeric or platelet-specific knockout mice or the transfusion of platelets in depleted mice are valuable

tools to minimise platelet-unspecific contributions to *in vivo* thrombus formation. Additionally, an appropriate adaption of the *in vivo* models used may be necessary as a specific platelet defect can be concealed by the many factors contributing to arterial thrombus formation.[153,154] In this study, treatment with ASA or the modulation of the severity of the injuries applied, e.g. by the application of a reduced concentration of $FeCl_3$, proved to be valuable tools to modulate *in vivo* thrombus formation. This process of model optimisation requires experience with different mouse models, experience with different genetic backgrounds and a continuous practical training.

4.4 EFhd2 is dispensable for platelet function *in vivo* and *in vitro*

Similar to Grb2, CLP36 and SLAP/SLAP2, EFhd2 has been proposed to modulate ITAM-signalling due to its association with Syk.[127] Furthermore, EFhd2 is involved in Ca^{2+} signalling in B cells.[129] In this dissertation the function of EFhd2 in platelets was investigated for the first time.

EFhd2-deficient mice developed normally, displayed normal platelet life span, platelet count and platelets size. Glycoprotein expression levels were comparable to wild-type, showing that EFhd2 is dispensable for platelet production (Figure 3.19). In further *in vitro* experiments, EFhd2-deficient platelets showed normal activation upon stimulation with ITAM or GPCR agonists using flow cytometry (Figure 3.20) or aggregometry (Figure 3.21). Similarly, Ca^{2+} influx upon stimulation was not impaired in EFhd2-deficient platelets as well as other Ca^{2+}-dependent processes such as platelet spreading and clot retraction (Figure 3.23 B and Figure 3.22). Only upon stimulation with CRP a very small but significant increase in PS exposure was detectable (Figure 3.23 A). This indicates that EFhd2 may, to a very minor extent, influence platelet activation upon stimulation with CRP.

In addition to the *in vitro* assays, several *in vivo* assays analysing haemostatic and thrombotic function in these mice were conducted. In these assays no difference was observed, demonstrating that EFhd2 is dispensable for *in vivo* thrombus or haemostatic plug formation (Figure 3.24). Western blot analysis ruled out the possibility that the absence of EFhd2 in platelets can be compensated by an up-regulation of its homolog EFhd1.

Taken together, EFhd2 is of minor relevance for platelet activation and is dispensable for *in vivo* thrombus formation. Given that EFhd2 is up-regulated during sepsis[135,136] and has been

associated with neurodegenerative processes,[134] it may be speculated that EFhd2 is relevant for proper platelet functions in longer time intervals than those observed for the acute thrombotic or haemostatic responses of platelets. Possibly, EFhd2 carries out a different function in platelets but different assays maybe necessary to elucidate those.

4.5 Concluding remarks and perspective

In this dissertation different aspects of platelet function in thrombocytopenic and genetically modified mice were investigated. The major findings are:

Impact of thrombocytopenia on in vivo *thrombus formation in mice:*

- Low-dose antibody-mediated reduction of the platelet count was established as a new model to study thrombocytopenia in mice.
- Thrombocytopenic mice show a robust haemostatic and thrombotic function at unexpectedly low platelet counts.
- Platelet count thresholds to maintain experimental arterial thrombus formation increase with the diameter of the injured vessel.
- Relative platelet count thresholds determined in mice correlate well to those observed in humans.

Haemostatic or thrombotic function of platelets in mice is only affected at surprisingly low platelet counts. The therapeutic reduction of platelet counts may, therefore, not be a promising strategy to prevent the occurrence of thrombotic disease states. On the other hand, the impact of elevated platelet counts on thrombosis and haemostasis counts is not yet completely understood. Genetic, drug- or antibody-mediated approaches to elevate the platelet count in mice exist. The analysis of thrombocytotic mice in *in vivo* thrombosis or haemostasis models may provide insight into the correlation of an increased platelet count and the occurrence of thrombotic diseases or bleeding. This may also show if modulating the platelet count is therapeutically viable at all.

Early platelets:

- High-dose antibody-mediated thrombocytopenia leads to an increased number of MKs in bone marrow.

- High-dose antibody-mediated thrombocytopenia leads to the production of early platelets which display a defect in ITAM-signalling. This defect in a very early stage of platelet formation may prevent proplatelet activation during migration through collagen-rich bone marrow vessel walls.

Low and high-dose antibody-mediated thrombocytopenia leads to the generation of new platelets. However, their function is still poorly understood. A detailed analysis of these platelets may be a promising approach to investigate platelet function at a very early stage of platelet formation which is otherwise (experimentally) hardly accessible.

In vivo *thrombus formation in genetically modified mice which display altered GPVI-signalling* in vitro*:*

- Altered GPVI-signalling in platelets *in vitro* often correlates with a specific defect in thrombosis *in vivo*.
- Platelet-specific knockout of Grb2 leads to reduced occlusive thrombus formation after ASA treatment in mice.
- Mice deficient for SLAP and SLAP2 show enhanced thrombus formation *in vivo*.
- Platelets lacking the LIM domain of CLP36 show an enhanced arterial thrombus formation *in vivo*.
- EFhd2 is dispensable for platelet thrombotic and haemostatic function.

GPVI is important for platelet activation and is considered as a promising target to prevent thrombotic disease states. The experiments in this study confirmed the modulating role of Grb2, CLP36 and SLAP/SLAP2 in GPVI-signalling *in vivo* and, therefore, validate their potential as a therapeutic target to develop anti-thrombotic drugs. For example, inhibition of Grb2 may decrease the risk for thrombotic events. Contrarily, CLP36 and SLAP/SLAP2 have to be activated to fulfil their anti-thrombotic functions.

5 References

1. Tsakiris DA, Scudder L, Hodivala-Dilke K, Hynes RO, Coller BS. Hemostasis in the mouse (Mus musculus): a review. *Thrombosis and haemostasis*. 1999;81(2):177-188.
2. Schmitt A, Guichard J, Masse JM, Debili N, Cramer EM. Of mice and men: comparison of the ultrastructure of megakaryocytes and platelets. *Exp Hematol*. 2001;29(11):1295-1302.
3. Kisucka J, Butterfield CE, Duda DG, et al. Platelets and platelet adhesion support angiogenesis while preventing excessive hemorrhage. *Proc Natl Acad Sci U S A*. 2006;103(4):855-860.
4. Echtler K, Stark K, Lorenz M, et al. Platelets contribute to postnatal occlusion of the ductus arteriosus. *Nat Med*. 2010;16(1):75-82.
5. Carramolino L, Fuentes J, Garcia-Andres C, Azcoitia V, Riethmacher D, Torres M. Platelets play an essential role in separating the blood and lymphatic vasculatures during embryonic angiogenesis. *Circ Res*. 2010;106(7):1197-1201.
6. Elzey BD, Sprague DL, Ratliff TL. The emerging role of platelets in adaptive immunity. *Cell Immunol*. 2005;238(1):1-9.
7. Wagner DD, Burger PC. Platelets in inflammation and thrombosis. *Arterioscler Thromb Vasc Biol*. 2003;23(12):2131-2137.
8. Clark SR, Ma AC, Tavener SA, et al. Platelet TLR4 activates neutrophil extracellular traps to ensnare bacteria in septic blood. *Nat Med*. 2007;13(4):463-469.
9. Nurden AT. Platelets, inflammation and tissue regeneration. *Thromb Haemost*. 2011;105 Suppl 1:S13-33.
10. Buergy D, Wenz F, Groden C, Brockmann MA. Tumor-platelet interaction in solid tumors. *Int J Cancer*. 2012;130(12):2747-2760.
11. Massberg S, Brand K, Gruner S, et al. A critical role of platelet adhesion in the initiation of atherosclerotic lesion formation. *J Exp Med*. 2002;196(7):887-896.
12. Italiano JE, Jr. Unraveling mechanisms that control platelet production. *Semin Thromb Hemost*. 2013;39(1):15-24.
13. Machlus KR, Italiano JE, Jr. The incredible journey: From megakaryocyte development to platelet formation. *J Cell Biol*. 2013;201(6):785-796.
14. Junt T, Schulze H, Chen Z, et al. Dynamic visualization of thrombopoiesis within bone marrow. *Science*. 2007;317(5845):1767-1770.
15. Zhang L, Orban M, Lorenz M, et al. A novel role of sphingosine 1-phosphate receptor S1pr1 in mouse thrombopoiesis. *J Exp Med*. 2012;209(12):2165-2181.
16. Schwertz H, Weyrich AS. Platelet precursors display bipolar behavior. *J Cell Biol*. 2010;191(4):699-700.
17. Varga-Szabo D, Pleines I, Nieswandt B. Cell adhesion mechanisms in platelets. *Arterioscler Thromb Vasc Biol*. 2008;28(3):403-412.
18. Versteeg HH, Heemskerk JW, Levi M, Reitsma PH. New fundamentals in hemostasis. *Physiol Rev*. 2013;93(1):327-358.

19. Michelson AD. Platelets. San Diego: Academic Press; 2002.

20. Papaioannou TG, Stefanadis C. Vascular wall shear stress: basic principles and methods. *Hellenic J Cardiol*. 2005;46(1):9-15.

21. Bluestein D, Niu L, Schoephoerster RT, Dewanjee MK. Fluid mechanics of arterial stenosis: relationship to the development of mural thrombus. *Ann Biomed Eng*. 1997;25(2):344-356.

22. Siegel JM, Markou CP, Ku DN, Hanson SR. A scaling law for wall shear rate through an arterial stenosis. *J Biomech Eng*. 1994;116(4):446-451.

23. Mailhac A, Badimon JJ, Fallon JT, et al. Effect of an eccentric severe stenosis on fibrin(ogen) deposition on severely damaged vessel wall in arterial thrombosis. Relative contribution of fibrin(ogen) and platelets. *Circulation*. 1994;90(2):988-996.

24. Nesbitt WS, Westein E, Tovar-Lopez FJ, et al. A shear gradient-dependent platelet aggregation mechanism drives thrombus formation. *Nat Med*. 2009;15(6):665-673.

25. Yago T, Lou J, Wu T, et al. Platelet glycoprotein Ibalpha forms catch bonds with human WT vWF but not with type 2B von Willebrand disease vWF. *J Clin Invest*. 2008;118(9):3195-3207.

26. Ruggeri ZM, Orje JN, Habermann R, Federici AB, Reininger AJ. Activation-independent platelet adhesion and aggregation under elevated shear stress. *Blood*. 2006;108(6):1903-1910.

27. Savage B, Almus-Jacobs F, Ruggeri ZM. Specific synergy of multiple substrate-receptor interactions in platelet thrombus formation under flow. *Cell*. 1998;94(5):657-666.

28. Moroi M, Jung SM. Platelet glycoprotein VI: its structure and function. *Thromb Res*. 2004;114(4):221-233.

29. Clemetson JM, Polgar J, Magnenat E, Wells TN, Clemetson KJ. The platelet collagen receptor glycoprotein VI is a member of the immunoglobulin superfamily closely related to FcalphaR and the natural killer receptors. *J Biol Chem*. 1999;274(41):29019-29024.

30. Jandrot-Perrus M, Busfield S, Lagrue AH, et al. Cloning, characterization, and functional studies of human and mouse glycoprotein VI: a platelet-specific collagen receptor from the immunoglobulin superfamily. *Blood*. 2000;96(5):1798-1807.

31. Moroi M, Jung SM, Okuma M, Shinmyozu K. A patient with platelets deficient in glycoprotein VI that lack both collagen-induced aggregation and adhesion. *J Clin Invest*. 1989;84(5):1440-1445.

32. Jung SM, Moroi M, Soejima K, et al. Constitutive dimerization of glycoprotein VI (GPVI) in resting platelets is essential for binding to collagen and activation in flowing blood. *J Biol Chem*. 2012;287(35):30000-30013.

33. Watson SP. Collagen receptor signaling in platelets and megakaryocytes. *Thromb Haemost*. 1999;82(2):365-376.

34. Li Z, Delaney MK, O'Brien KA, Du X. Signaling during platelet adhesion and activation. *Arterioscler Thromb Vasc Biol*. 2010;30(12):2341-2349.

35. Watson SP, Herbert JM, Pollitt AY. GPVI and CLEC-2 in hemostasis and vascular integrity. *J Thromb Haemost*. 2010;8(7):1456-1467.

36. Spalton JC, Mori J, Pollitt AY, Hughes CE, Eble JA, Watson SP. The novel Syk inhibitor R406 reveals mechanistic differences in the initiation of GPVI and CLEC-2 signaling in platelets. *J Thromb Haemost*. 2009;7(7):1192-1199.

37. Cicmil M, Thomas JM, Leduc M, Bon C, Gibbins JM. Platelet endothelial cell adhesion molecule-1 signaling inhibits the activation of human platelets. *Blood*. 2002;99(1):137-144.

38. Mazharian A, Wang YJ, Mori J, et al. Mice lacking the ITIM-containing receptor G6b-B exhibit macrothrombocytopenia and aberrant platelet function. *Sci Signal*. 2012;5(248):ra78.

39. Wong C, Liu Y, Yip J, et al. CEACAM1 negatively regulates platelet-collagen interactions and thrombus growth in vitro and in vivo. *Blood*. 2009;113(8):1818-1828.

40. Senis YA. Protein-tyrosine phosphatases: a new frontier in platelet signal transduction. *J Thromb Haemost*. 2013;11(10):1800-1813.

41. Varga-Szabo D, Braun A, Nieswandt B. Calcium signaling in platelets. *J Thromb Haemost*. 2009;7(7):1057-1066.

42. Jin J, Quinton TM, Zhang J, Rittenhouse SE, Kunapuli SP. Adenosine diphosphate (ADP)-induced thromboxane A(2) generation in human platelets requires coordinated signaling through integrin alpha(IIb)beta(3) and ADP receptors. *Blood*. 2002;99(1):193-198.

43. Monroe DM, Hoffman M, Roberts HR. Platelets and thrombin generation. *Arterioscler Thromb Vasc Biol*. 2002;22(9):1381-1389.

44. Offermanns S. Activation of platelet function through G protein-coupled receptors. *Circ Res*. 2006;99(12):1293-1304.

45. Bevers EM, Comfurius P, van Rijn JL, Hemker HC, Zwaal RF. Generation of prothrombin-converting activity and the exposure of phosphatidylserine at the outer surface of platelets. *Eur J Biochem*. 1982;122(2):429-436.

46. Carr ME, Jr. Development of platelet contractile force as a research and clinical measure of platelet function. *Cell Biochem Biophys*. 2003;38(1):55-78.

47. Vannucchi AM, Barbui T. Thrombocytosis and thrombosis. *Hematology Am Soc Hematol Educ Program*. 2007:363-370.

48. Sarpatwari A, Bennett D, Logie JW, et al. Thromboembolic events among adult patients with primary immune thrombocytopenia in the United Kingdom General Practice Research Database. *Haematologica*. 2010;95(7):1167-1175.

49. Cines DB, Liebman H, Stasi R. Pathobiology of secondary immune thrombocytopenia. *Semin Hematol*. 2009;46(1 Suppl 2):S2-14.

50. Provan D, Stasi R, Newland AC, et al. International consensus report on the investigation and management of primary immune thrombocytopenia. *Blood*. 2010;115(2):168-186.

51. Beardsley DS, Ertem M. Platelet autoantibodies in immune thrombocytopenic purpura. *Transfus Sci*. 1998;19(3):237-244.

52. McMillan R, Tani P, Millard F, Berchtold P, Renshaw L, Woods VL, Jr. Platelet-associated and plasma anti-glycoprotein autoantibodies in chronic ITP. *Blood*. 1987;70(4):1040-1045.

53. Webster ML, Zhu G, Li Y, Ni H. Fc-independent phagocytosis: implications for intravenous IgG therapy in immune thrombocytopenia. *Cardiovasc Hematol Disord Drug Targets*. 2008;8(4):278-282.

54. Nieswandt B, Bergmeier W, Rackebrandt K, Gessner JE, Zirngibl H. Identification of critical antigen-specific mechanisms in the development of immune thrombocytopenic purpura in mice. *Blood*. 2000;96(7):2520-2527.

55. Van der Wal DE, Li J, Zhu G, et al. Anti-GPIb antibody induces platelet desialylation: A novel mechanism of Fc-independent immune thrombocytopenia, and a potential new diagnosis and therapy against refractory ITP ISTH 2013. Amsterdam: International society of thrombosis and hemostatsis; 2013.

56. Rumjantseva V, Grewal PK, Wandall HH, et al. Dual roles for hepatic lectin receptors in the clearance of chilled platelets. *Nat Med*. 2009;15(11):1273-1280.

57. George JN, Aster RH. Drug-induced thrombocytopenia: pathogenesis, evaluation, and management. *Hematology / the Education Program of the American Society of Hematology American Society of Hematology Education Program*. 2009:153-158.

58. Kenney B, Stack G. Drug-induced thrombocytopenia. *Archives of pathology & laboratory medicine*. 2009;133(2):309-314.

59. Prasad HK, Kaushal V, Mehta P. Isolated thrombocytopenia induced by thalidomide in a patient with multiple myeloma: case report and review of literature. *American journal of hematology*. 2007;82(9):855-857.

60. Andres E, Dali-Youcef N, Serraj K, Zimmer J. Recognition and management of drug-induced cytopenias: the example of idiosyncratic drug-induced thrombocytopenia. *Expert opinion on drug safety*. 2009;8(2):183-190.

61. Passos AM, Treitinger A, Spada C. An overview of the mechanisms of HIV-related thrombocytopenia. *Acta haematologica*. 2010;124(1):13-18.

62. Louie KS, Micallef JM, Pimenta JM, Forssen UM. Prevalence of thrombocytopenia among patients with chronic hepatitis C: a systematic review. *Journal of viral hepatitis*. 2011;18(1):1-7.

63. Kahr WH, Hinckley J, Li L, et al. Mutations in NBEAL2, encoding a BEACH protein, cause gray platelet syndrome. *Nat Genet*. 2011;43(8):738-740.

64. Nurden AT, Nurden P. The gray platelet syndrome: clinical spectrum of the disease. *Blood reviews*. 2007;21(1):21-36.

65. Lopez JA, Andrews RK, Afshar-Kharghan V, Berndt MC. Bernard-Soulier syndrome. *Blood*. 1998;91(12):4397-4418.

66. Massaad MJ, Ramesh N, Geha RS. Wiskott-Aldrich syndrome: a comprehensive review. *Ann N Y Acad Sci*. 2013;1285:26-43.

67. Ochs HD. Mutations of the Wiskott-Aldrich Syndrome Protein affect protein expression and dictate the clinical phenotypes. *Immunologic research*. 2009;44(1-3):84-88.

68. Harker LA, Slichter SJ. The bleeding time as a screening test for evaluation of platelet function. *N Engl J Med*. 1972;287(4):155-159.

69. Elting LS, Rubenstein EB, Martin CG, et al. Incidence, cost, and outcomes of bleeding and chemotherapy dose modification among solid tumor patients with chemotherapy-induced thrombocytopenia. *Journal of clinical oncology : official journal of the American Society of Clinical Oncology*. 2001;19(4):1137-1146.

70. Neunert C, Lim W, Crowther M, Cohen A, Solberg L, Jr., Crowther MA. The American Society of Hematology 2011 evidence-based practice guideline for immune thrombocytopenia. *Blood*. 2011;117(16):4190-4207.

71. Ambler KL, Vickars LM, Leger CS, et al. Clinical Features, Treatment, and Outcome of HIV-Associated Immune Thrombocytopenia in the HAART Era. *Advances in hematology*. 2012;2012:910954.

72. Eberl W, Dickerhoff R. Newly diagnosed immune thrombozytopenia--German guideline concerning initial diagnosis and therapy. *Klinische Padiatrie*. 2012;224(3):207-210.

73. Cortelazzo S, Finazzi G, Buelli M, Molteni A, Viero P, Barbui T. High risk of severe bleeding in aged patients with chronic idiopathic thrombocytopenic purpura. *Blood*. 1991;77(1):31-33.

74. Lakshmanan S, Cuker A. Contemporary Management of Primary Immune Thrombocytopenia (ITP) in Adults. *Journal of thrombosis and haemostasis : JTH*. 2012.

75. Iyori H, Bessho F, Ookawa H, et al. Intracranial hemorrhage in children with immune thrombocytopenic purpura. Japanese Study Group on childhood ITP. *Annals of hematology*. 2000;79(12):691-695.

76. Bettaieb A, Fromont P, Louache F, et al. Presence of cross-reactive antibody between human immunodeficiency virus (HIV) and platelet glycoproteins in HIV-related immune thrombocytopenic purpura. *Blood*. 1992;80(1):162-169.

77. Nomura S, Matsuzaki T, Ozaki Y, et al. Clinical significance of HLA-DRB1*0410 in Japanese patients with idiopathic thrombocytopenic purpura. *Blood*. 1998;91(10):3616-3622.

78. Pockros PJ, Duchini A, McMillan R, Nyberg LM, McHutchison J, Viernes E. Immune thrombocytopenic purpura in patients with chronic hepatitis C virus infection. *The American journal of gastroenterology*. 2002;97(8):2040-2045.

79. Stanworth SJ, Turner DM, Brown J, et al. Major histocompatibility complex susceptibility genes and immune thrombocytopenic purpura in Caucasian adults. *Hematology*. 2002;7(2):119-121.

80. Dominguez V, Govezensky T, Gevorkian G, Larralde C. Low platelet counts alone do not cause bleeding in an experimental immune thrombocytopenic purpura in mice. *Haematologica*. 2003;88(6):679-687.

81. Goerge T, Ho-Tin-Noe B, Carbo C, et al. Inflammation induces hemorrhage in thrombocytopenia. *Blood*. 2008;111(10):4958-4964.

82. Aledort LM, Hayward CP, Chen MG, Nichol JL, Bussel J. Prospective screening of 205 patients with ITP, including diagnosis, serological markers, and the relationship

between platelet counts, endogenous thrombopoietin, and circulating antithrombopoietin antibodies. *American journal of hematology*. 2004;76(3):205-213.

83. Blajchman MA, Senyi AF, Hirsh J, Genton E, George JN. Hemostatic function, survival, and membrane glycoprotein changes in young versus old rabbit platelets. *J Clin Invest*. 1981;68(5):1289-1294.

84. Karpatkin S, Khan Q, Freedman M. Heterogeneity of platelet function. Correlation with platelet volume. *The American journal of medicine*. 1978;64(4):542-546.

85. Hirsh J, Glynn MF, Mustard JF. The effect of platelet age on platelet adherence to collagen. *J Clin Invest*. 1968;47(3):466-473.

86. Peng J, Friese P, Heilmann E, George JN, Burstein SA, Dale GL. Aged platelets have an impaired response to thrombin as quantitated by P-selectin expression. *Blood*. 1994;83(1):161-166.

87. Tong M, Seth P, Penington DG. Proplatelets and stress platelets. *Blood*. 1987;69(2):522-528.

88. Odell TT, Murphy JR, Jackson CW. Stimulation of megakaryocytopoiesis by acute thrombocytopenia in rats. *Blood*. 1976;48(5):765-775.

89. Ginsburg AD, Aster RH. Changes associated with platelet aging. *Thromb Diath Haemorrh*. 1972;27(3):407-415.

90. Webster ML, Sayeh E, Crow M, et al. Relative efficacy of intravenous immunoglobulin G in ameliorating thrombocytopenia induced by antiplatelet GPIIbIIIa versus GPIbalpha antibodies. *Blood*. 2006;108(3):943-946.

91. Li J, van der Wal DE, Zhu L, et al. Fc-independent phagocytosis: implications for IVIG and other therapies in immune-mediated thrombocytopenia. *Cardiovasc Hematol Disord Drug Targets*. 2012;13(1):50-58.

92. Slichter SJ. Evidence-based platelet transfusion guidelines. *Hematology Am Soc Hematol Educ Program*. 2007:172-178.

93. Sachs UJ, Nieswandt B. In vivo thrombus formation in murine models. *Circulation research*. 2007;100(7):979-991.

94. Kurz KD, Main BW, Sandusky GE. Rat model of arterial thrombosis induced by ferric chloride. *Thromb Res*. 1990;60(4):269-280.

95. Farrehi PM, Ozaki CK, Carmeliet P, Fay WP. Regulation of arterial thrombolysis by plasminogen activator inhibitor-1 in mice. *Circulation*. 1998;97(10):1002-1008.

96. Barr JD, Chauhan AK, Schaeffer GV, Hansen JK, Motto DG. Red blood cells mediate the onset of thrombosis in the ferric chloride murine model. *Blood*. 2013;121(18):3733-3741.

97. Eckly A, Hechler B, Freund M, et al. Mechanisms underlying FeCl3-induced arterial thrombosis. *J Thromb Haemost*. 2011;9(4):779-789.

98. Matsuno H, Uematsu T, Nagashima S, Nakashima M. Photochemically induced thrombosis model in rat femoral artery and evaluation of effects of heparin and tissue-type plasminogen activator with use of this model. *J Pharmacol Methods*. 1991;25(4):303-317.

99. Nonne C, Lenain N, Hechler B, et al. Importance of platelet phospholipase Cgamma2 signaling in arterial thrombosis as a function of lesion severity. *Arterioscler Thromb Vasc Biol*. 2005;25(6):1293-1298.

100. Hechler B, Nonne C, Eckly A, et al. Arterial thrombosis: relevance of a model with two levels of severity assessed by histologic, ultrastructural and functional characterization. *J Thromb Haemost*. 2010;8(1):173-184.

101. Renne T, Pozgajova M, Gruner S, et al. Defective thrombus formation in mice lacking coagulation factor XII. *J Exp Med*. 2005;202(2):271-281.

102. Massberg S, Gawaz M, Gruner S, et al. A crucial role of glycoprotein VI for platelet recruitment to the injured arterial wall in vivo. *J Exp Med*. 2003;197(1):41-49.

103. Murray CJ, Lopez AD. Mortality by cause for eight regions of the world: Global Burden of Disease Study. *Lancet*. 1997;349(9061):1269-1276.

104. Feigin VL, Lawes CM, Bennett DA, Anderson CS. Stroke epidemiology: a review of population-based studies of incidence, prevalence, and case-fatality in the late 20th century. *Lancet Neurol*. 2003;2(1):43-53.

105. Nieswandt B, Kleinschnitz C, Stoll G. Ischaemic stroke: a thrombo-inflammatory disease? *J Physiol*. 2011;589(Pt 17):4115-4123.

106. Kleinschnitz C, Pozgajova M, Pham M, Bendszus M, Nieswandt B, Stoll G. Targeting platelets in acute experimental stroke: impact of glycoprotein Ib, VI, and IIb/IIIa blockade on infarct size, functional outcome, and intracranial bleeding. *Circulation*. 2007;115(17):2323-2330.

107. Ware J. Dysfunctional platelet membrane receptors: from humans to mice. *Thromb Haemost*. 2004;92(3):478-485.

108. Hughes CE, Auger JM, McGlade J, Eble JA, Pearce AC, Watson SP. Differential roles for the adapters Gads and LAT in platelet activation by GPVI and CLEC-2. *J Thromb Haemost*. 2008;6(12):2152-2159.

109. Garcia A, Senis YA, Antrobus R, et al. A global proteomics approach identifies novel phosphorylated signaling proteins in GPVI-activated platelets: involvement of G6f, a novel platelet Grb2-binding membrane adapter. *Proteomics*. 2006;6(19):5332-5343.

110. Krcmery J, Camarata T, Kulisz A, Simon HG. Nucleocytoplasmic functions of the PDZ-LIM protein family: new insights into organ development. *Bioessays*. 2010;32(2):100-108.

111. Bozulic LD, Malik MT, Powell DW, et al. Plasma membrane Ca(2+) -ATPase associates with CLP36, alpha-actinin and actin in human platelets. *Thromb Haemost*. 2007;97(4):587-597.

112. Bauer K, Kratzer M, Otte M, et al. Human CLP36, a PDZ-domain and LIM-domain protein, binds to alpha-actinin-1 and associates with actin filaments and stress fibers in activated platelets and endothelial cells. *Blood*. 2000;96(13):4236-4245.

113. Tamura N, Ohno K, Katayama T, Kanayama N, Sato K. The PDZ-LIM protein CLP36 is required for actin stress fiber formation and focal adhesion assembly in BeWo cells. *Biochem Biophys Res Commun*. 2007;364(3):589-594.

114. Miyazaki K, Ohno K, Tamura N, Sasaki T, Sato K. CLP36 and RIL recruit alpha-actinin-1 to stress fibers and differentially regulate stress fiber dynamics in F2408 fibroblasts. *Exp Cell Res*. 2012;318(14):1716-1725.

115. Gupta S, Braun A, Morowski M, et al. CLP36 is a negative regulator of glycoprotein VI signaling in platelets. *Circ Res*. 2012;111(11):1410-1420.

116. Rozakis-Adcock M, Fernley R, Wade J, Pawson T, Bowtell D. The SH2 and SH3 domains of mammalian Grb2 couple the EGF receptor to the Ras activator mSos1. *Nature*. 1993;363(6424):83-85.

117. Cheng AM, Saxton TM, Sakai R, et al. Mammalian Grb2 regulates multiple steps in embryonic development and malignant transformation. *Cell*. 1998;95(6):793-803.

118. Ackermann JA, Radtke D, Maurberger A, Winkler TH, Nitschke L. Grb2 regulates B-cell maturation, B-cell memory responses and inhibits B-cell Ca2+ signalling. *EMBO J*. 2011;30(8):1621-1633.

119. Jang IK, Zhang J, Chiang YJ, et al. Grb2 functions at the top of the T-cell antigen receptor-induced tyrosine kinase cascade to control thymic selection. *Proc Natl Acad Sci U S A*. 2010;107(23):10620-10625.

120. Asazuma N, Wilde JI, Berlanga O, et al. Interaction of linker for activation of T cells with multiple adapter proteins in platelets activated by the glycoprotein VI-selective ligand, convulxin. *J Biol Chem*. 2000;275(43):33427-33434.

121. Dutting S, Vogtle T, Morowski M, et al. Grb2 Contributes to (hem)ITAM-Mediated Signaling in Platelets. *Circ Res*. 2013.

122. Dragone LL, Shaw LA, Myers MD, Weiss A. SLAP, a regulator of immunoreceptor ubiquitination, signaling, and trafficking. *Immunol Rev*. 2009;232(1):218-228.

123. Sugihara S, Katsutani S, Deckmyn H, Fujimura K, Kimura A. Roles of Src-like adaptor protein 2 (SLAP-2) in GPVI-mediated platelet activation SLAP-2 and GPVI signaling. *Thromb Res*. 2010;126(4):e276-285.

124. Dutting S, Brachs S, Mielenz D. Fraternal twins: Swiprosin-1/EFhd2 and Swiprosin-2/EFhd1, two homologous EF-hand containing calcium binding adaptor proteins with distinct functions. *Cell Commun Signal*. 2011;9:2.

125. Grabarek Z. Structural basis for diversity of the EF-hand calcium-binding proteins. *J Mol Biol*. 2006;359(3):509-525.

126. Vuadens F, Rufer N, Kress A, Corthesy P, Schneider P, Tissot JD. Identification of swiprosin 1 in human lymphocytes. *Proteomics*. 2004;4(8):2216-2220.

127. Avramidou A, Kroczek C, Lang C, Schuh W, Jack HM, Mielenz D. The novel adaptor protein Swiprosin-1 enhances BCR signals and contributes to BCR-induced apoptosis. *Cell Death Differ*. 2007;14(11):1936-1947.

128. Kroczek C, Lang C, Brachs S, et al. Swiprosin-1/EFhd2 controls B cell receptor signaling through the assembly of the B cell receptor, Syk, and phospholipase C gamma2 in membrane rafts. *J Immunol*. 2010;184(7):3665-3676.

129. Mielenz D, Vettermann C, Hampel M, et al. Lipid rafts associate with intracellular B cell receptors and exhibit a B cell stage-specific protein composition. *J Immunol*. 2005;174(6):3508-3517.

130. Brownlow SL, Harper AG, Harper MT, Sage SO. A role for hTRPC1 and lipid raft domains in store-mediated calcium entry in human platelets. *Cell Calcium*. 2004;35(2):107-113.

131. Thylur RP, Kim YD, Kwon MS, et al. Swiprosin-1 is expressed in mast cells and up-regulated through the protein kinase C beta I/eta pathway. *J Cell Biochem*. 2009;108(3):705-715.

132. Ramesh TP, Kim YD, Kwon MS, Jun CD, Kim SW. Swiprosin-1 Regulates Cytokine Expression of Human Mast Cell Line HMC-1 through Actin Remodeling. *Immune Netw*. 2009;9(6):274-284.

133. Huh YH, Kim SH, Chung KH, et al. Swiprosin-1 modulates actin dynamics by regulating the F-actin accessibility to cofilin. *Cell Mol Life Sci*. 2013.

134. Vega IE, Traverso EE, Ferrer-Acosta Y, et al. A novel calcium-binding protein is associated with tau proteins in tauopathy. *J Neurochem*. 2008;106(1):96-106.

135. Freishtat RJ, Natale J, Benton AS, et al. Sepsis alters the megakaryocyte-platelet transcriptional axis resulting in granzyme B-mediated lymphotoxicity. *Am J Respir Crit Care Med*. 2009;179(6):467-473.

136. Yu Y, Leng T, Yun D, et al. Global analysis of the rat and human platelet proteome - the molecular blueprint for illustrating multi-functional platelets and cross-species function evolution. *Proteomics*. 2010;10(13):2444-2457.

137. Nieswandt B, Schulte V, Bergmeier W, et al. Long-term antithrombotic protection by in vivo depletion of platelet glycoprotein VI in mice. *J Exp Med*. 2001;193(4):459-469.

138. May F, Hagedorn I, Pleines I, et al. CLEC-2 is an essential platelet-activating receptor in hemostasis and thrombosis. *Blood*. 2009;114(16):3464-3472.

139. Bergmeier W, Schulte V, Brockhoff G, Bier U, Zirngibl H, Nieswandt B. Flow cytometric detection of activated mouse integrin alphaIIbbeta3 with a novel monoclonal antibody. *Cytometry*. 2002;48(2):80-86.

140. Nieswandt B, Echtenacher B, Wachs FP, et al. Acute systemic reaction and lung alterations induced by an antiplatelet integrin gpIIb/IIIa antibody in mice. *Blood*. 1999;94(2):684-693.

141. Bederson JB, Pitts LH, Tsuji M, Nishimura MC, Davis RL, Bartkowski H. Rat middle cerebral artery occlusion: evaluation of the model and development of a neurologic examination. *Stroke; a journal of cerebral circulation*. 1986;17(3):472-476.

142. Armstrong RA, Slade SV, Eperjesi F. An introduction to analysis of variance (ANOVA) with special reference to data from clinical experiments in optometry. *Ophthalmic Physiol Opt*. 2000;20(3):235-241.

143. Fisher RA. Statistical Methods for Research Workers. Edinburgh: Oliver and Boyd; 1925.

144. Bergmeier W, Rackebrandt K, Schroder W, Zirngibl H, Nieswandt B. Structural and functional characterization of the mouse von Willebrand factor receptor GPIb-IX with novel monoclonal antibodies. *Blood*. 2000;95(3):886-893.

145. Alugupalli KR, Michelson AD, Barnard MR, Leong JM. Serial determinations of platelet counts in mice by flow cytometry. *Thrombosis and haemostasis*. 2001;86(2):668-671.

146. Bender M, Hagedorn I, Nieswandt B. Genetic and antibody-induced glycoprotein VI deficiency equally protects mice from mechanically and FeCl(3) -induced thrombosis. *Journal of thrombosis and haemostasis : JTH*. 2011;9(7):1423-1426.

147. Kleinschnitz C, De Meyer SF, Schwarz T, et al. Deficiency of von Willebrand factor protects mice from ischemic stroke. *Blood*. 2009;113(15):3600-3603.

148. Nieswandt B, Kleinschnitz C, Stoll G. Ischaemic stroke: a thrombo-inflammatory disease? *The Journal of physiology*. 2011;589(Pt 17):4115-4123.

149. Nieswandt B, Varga-Szabo D, Elvers M. Integrins in platelet activation. *J Thromb Haemost*. 2009;7 Suppl 1:206-209.

150. Harrison P, Cramer EM. Platelet alpha-granules. *Blood Rev*. 1993;7(1):52-62.

151. Lanza F, Beretz A, Stierle A, Hanau D, Kubina M, Cazenave JP. Epinephrine potentiates human platelet activation but is not an aggregating agent. *Am J Physiol*. 1988;255(6 Pt 2):H1276-1288.

152. Spalding A, Vaitkevicius H, Dill S, MacKenzie S, Schmaier A, Lockette W. Mechanism of epinephrine-induced platelet aggregation. *Hypertension*. 1998;31(2):603-607.

153. Gruner S, Prostredna M, Aktas B, et al. Anti-glycoprotein VI treatment severely compromises hemostasis in mice with reduced alpha2beta1 levels or concomitant aspirin therapy. *Circulation*. 2004;110(18):2946-2951.

154. Pamuklar Z, Federico L, Liu S, et al. Autotaxin/lysopholipase D and lysophosphatidic acid regulate murine hemostasis and thrombosis. *J Biol Chem*. 2009;284(11):7385-7394.

155. Stoll G, Kleinschnitz C, Nieswandt B. Combating innate inflammation: a new paradigm for acute treatment of stroke? *Ann N Y Acad Sci*. 2010;1207:149-154.

156. Brachs S. Untersuchungen zur Funktion des murinen Proteins EFhd2/Swiprosin-1 in der B Zellentwicklung und Immunantwort in vivo. Der Naturwissenschaftlichen Fakultät der Friedrich-Alexander-Universität Erlangen-Nürnberg. Vol. Dr. rer. nat. Erlangen-Nürnberg: Friedrich-Alexander-Universität Erlangen-Nürnberg; 2012.

157. Born GV. Aggregation of blood platelets by adenosine diphosphate and its reversal. *Nature*. 1962;194:927-929.

158. Pytela R, Pierschbacher MD, Ginsberg MH, Plow EF, Ruoslahti E. Platelet membrane glycoprotein IIb/IIIa: member of a family of Arg-Gly-Asp--specific adhesion receptors. *Science*. 1986;231(4745):1559-1562.

159. Dachary-Prigent J, Freyssinet JM, Pasquet JM, Carron JC, Nurden AT. Annexin V as a probe of aminophospholipid exposure and platelet membrane vesiculation: a flow cytometry study showing a role for free sulfhydryl groups. *Blood*. 1993;81(10):2554-2565.

160. Verhallen PF, Bevers EM, Comfurius P, Zwaal RF. Correlation between calpain-mediated cytoskeletal degradation and expression of platelet procoagulant activity. A role for the platelet membrane-skeleton in the regulation of membrane lipid asymmetry? *Biochim Biophys Acta*. 1987;903(1):206-217.

161. Go AS, Mozaffarian D, Roger VL, et al. Heart disease and stroke statistics--2013 update: a report from the American Heart Association. *Circulation*. 2013;127(1):e6-e245.

162. Neunert CE, Buchanan GR, Imbach P, et al. Severe hemorrhage in children with newly diagnosed immune thrombocytopenic purpura. *Blood*. 2008;112(10):4003-4008.

163. Chong BH, Ho SJ. Autoimmune thrombocytopenia. *Journal of thrombosis and haemostasis : JTH*. 2005;3(8):1763-1772.

164. Rodgers RP, Levin J. A critical reappraisal of the bleeding time. *Seminars in thrombosis and hemostasis*. 1990;16(1):1-20.

165. Norgaard M, Severinsen MT, Lund Maegbaek M, Jensen AO, Cha S, Sorensen HT. Risk of arterial thrombosis in patients with primary chronic immune thrombocytopenia: a Danish population-based cohort study. *British journal of haematology*. 2012;159(1):109-111.

166. De La Pena A, Fareed J, Thethi I, Morales-Vidal S, Schneck MJ, Shafer D. Ischemic stroke in the setting of chronic immune thrombocytopenia in an elderly patient--a therapeutic dilemma. *Clinical and applied thrombosis/hemostasis : official journal of the International Academy of Clinical and Applied Thrombosis/Hemostasis*. 2012;18(3):324-326.

167. Gracia MC, Cebollero IC, Lezcano JS, Osuna GG, Miguel JA, Peralta LP. Invasive treatment performed for acute myocardial infarction in a patient with immune thrombocytopenic purpura. *International journal of cardiology*. 2008;127(3):e183-185.

168. Nieswandt B, Bergmeier W, Schulte V, Rackebrandt K, Gessner JE, Zirngibl H. Expression and function of the mouse collagen receptor glycoprotein VI is strictly dependent on its association with the FcRgamma chain. *The Journal of biological chemistry*. 2000;275(31):23998-24002.

169. Pleines I, Hagedorn I, Gupta S, et al. Megakaryocyte-specific RhoA deficiency causes macrothrombocytopenia and defective platelet activation in hemostasis and thrombosis. *Blood*. 2012;119(4):1054-1063.

170. Schwer HD, Lecine P, Tiwari S, Italiano JE, Jr., Hartwig JH, Shivdasani RA. A lineage-restricted and divergent beta-tubulin isoform is essential for the biogenesis, structure and function of blood platelets. *Current biology : CB*. 2001;11(8):579-586.

171. Stoll G, Kleinschnitz C, Nieswandt B. Molecular mechanisms of thrombus formation in ischemic stroke: novel insights and targets for treatment. *Blood*. 2008;112(9):3555-3562.

172. Momi S, Tantucci M, Van Roy M, Ulrichts H, Ricci G, Gresele P. Reperfusion of cerebral artery thrombosis by the GPIb-VWF blockade with the Nanobody ALX-0081 reduces brain infarct size in guinea pigs. *Blood*. 2013;121(25):5088-5097.

173. Adams HP, Jr., Effron MB, Torner J, et al. Emergency administration of abciximab for treatment of patients with acute ischemic stroke: results of an international phase III trial: Abciximab in Emergency Treatment of Stroke Trial (AbESTT-II). *Stroke*. 2008;39(1):87-99.

174. Kellert L, Hametner C, Rohde S, et al. Endovascular stroke therapy: tirofiban is associated with risk of fatal intracerebral hemorrhage and poor outcome. *Stroke*. 2013;44(5):1453-1455.

175. Boulaftali Y, Hess PR, Getz TM, et al. Platelet ITAM signaling is critical for vascular integrity in inflammation. *J Clin Invest*. 2013;123(2):908-916.

176. Stegner D, Deppermann C, Kraft P, et al. Munc13-4-mediated secretion is essential for infarct progression but not intracranial hemostasis in acute stroke. *J Thromb Haemost*. 2013;11(7):1430-1433.

177. Hanson SR, Slichter SJ. Platelet kinetics in patients with bone marrow hypoplasia: evidence for a fixed platelet requirement. *Blood*. 1985;66(5):1105-1109.

178. Mitchell WB, Bussel JB. How low can you go? *Blood*. 2013;121(24):4817-4818.

179. Dubois C, Panicot-Dubois L, Merrill-Skoloff G, Furie B, Furie BC. Glycoprotein VI-dependent and -independent pathways of thrombus formation in vivo. *Blood*. 2006;107(10):3902-3906.

180. Dubois C, Panicot-Dubois L, Gainor JF, Furie BC, Furie B. Thrombin-initiated platelet activation in vivo is vWF independent during thrombus formation in a laser injury model. *J Clin Invest*. 2007;117(4):953-960.

181. Mangin P, Yap CL, Nonne C, et al. Thrombin overcomes the thrombosis defect associated with platelet GPVI/FcRgamma deficiency. *Blood*. 2006;107(11):4346-4353.

182. Bender M, Hofmann S, Stegner D, et al. Differentially regulated GPVI ectodomain shedding by multiple platelet-expressed proteinases. *Blood*. 2010;116(17):3347-3355.

183. Ishiai M, Kurosaki M, Inabe K, Chan AC, Sugamura K, Kurosaki T. Involvement of LAT, Gads, and Grb2 in compartmentation of SLP-76 to the plasma membrane. *J Exp Med*. 2000;192(6):847-856.

184. Lewitzky M, Kardinal C, Gehring NH, et al. The C-terminal SH3 domain of the adapter protein Grb2 binds with high affinity to sequences in Gab1 and SLP-76 which lack the SH3-typical P-x-x-P core motif. *Oncogene*. 2001;20(9):1052-1062.

185. Pasquet JM, Gross B, Quek L, et al. LAT is required for tyrosine phosphorylation of phospholipase cgamma2 and platelet activation by the collagen receptor GPVI. *Mol Cell Biol*. 1999;19(12):8326-8334.

186. Kalia N, Auger JM, Atkinson B, Watson SP. Critical role of FcR gamma-chain, LAT, PLCgamma2 and thrombin in arteriolar thrombus formation upon mild, laser-induced endothelial injury in vivo. *Microcirculation*. 2008;15(4):325-335.

187. Gupta S. The role of the Canonical transient receptor potential 6 (TRPC6) channel and the C-terminal LIM domain protein of 36 kDa (CLP36) for platelet function. Vol. Dr. rer. nat. Würzburg: Julius-Maximilians-Universität Würzburg; 2012.

188. Pearson JD. Endothelial cell function and thrombosis. *Baillieres Best Pract Res Clin Haematol*. 1999;12(3):329-341.

189. Tojkander S, Gateva G, Lappalainen P. Actin stress fibers--assembly, dynamics and biological roles. *J Cell Sci*. 2012;125(Pt 8):1855-1864.

5.1 Publications

Articles

Morowski M, Vögtle T, Kraft P, Kleinschnitz C, Stoll G, Nieswandt B. Only severe thrombocytopenia results in bleeding and defective thrombus formation in mice. Blood. 2013 Jun 13;121(24):4938-47.

Dütting S, Vögtle T, **Morowski M**, Schießl S, Schäfer CM, Watson SK, Hughes CE, Ackermann JA, Radtke D, Hermanns HM, Watson S, Nitschke L, Nieswandt B. Grb2 Contributes to (hem)ITAM-Mediated Signaling in Platelets. Circ Res. 2013 Nov 21. [Epub ahead of print]

Pleines I, Dütting S, Cherpokova D, Eckly A, Meyer I, **Morowski M**, Krohne G, Schulze H, Gachet C, Debili N, Brakebusch C, Nieswandt B. Defective tubulin organization and proplatelet formation in murine megakaryocytes lacking Rac1 and Cdc42. Blood. 2013 Oct 31;122(18):3178-87.

Stegner D, Deppermann C, Kraft P, **Morowski M**, Kleinschnitz C, Stoll G, Nieswandt B. Munc13-4-mediated secretion is essential for infarct progression but not intracranial hemostasis in acute stroke. J Thromb Haemost. 2013 Jul;11(7):1430-3.

Gupta S, Braun A, **Morowski M**, Premsler T, Bender M, Nagy Z, Sickmann A, Hermanns HM, Bösl M, Nieswandt B. CLP36 is a negative regulator of glycoprotein VI signaling in platelets. Circ Res. 2012 Nov 9;111(11):1410-20.

Oral presentations

Annual Retreat of the Rudolf Virchow Center, Luisenthal, Oct. 2012	Only severe thrombocytopenia results in bleeding and defective thrombus formation in mice
EUPLAN Platelet Conference, Maastricht, The Netherlands, Sep. 2012	Only severe thrombocytopenia results in bleeding and defective thrombus formation in mice

Poster presentation

International Symposium of the Graduate School of Life Sciences, Würzburg, Oct. 2013	The protein adapter molecule EFhd2 plays only a minor role in platelet activation
International Symposium of the Graduate School of Life Sciences, Würzburg, Oct. 2012	Only severe thrombocytopenia results in bleeding and defective thrombus formation in mice

International Symposium of the Graduate School of Life Sciences, Würzburg, Oct. 2011	Cathepsin D- many functions of one aspartic protease
XXXIV Congress of the International Society on Thrombosis and Haemostasis, Amsterdam, The Netherlands, July 2013	Only severe thrombocytopenia results in bleeding and defective thrombus formation in mice
Joint Symposium of the Collaborative Research Center (SFB) 688, the Rudolf Virchow Center and the Comprehensive Heart Failure Center Würzburg, June 2012	Only severe thrombocytopenia results in bleeding and defective thrombus formation in mice

5.2 Affidavit

I hereby declare that my thesis entitled “Relevance of platelet count and ITAM-signalling pathway in murine models of haemostasis, thrombosis and thrombo-inflammation" is the result of my own work. I did not receive any help or support from commercial consultants. All sources and / or materials applied are listed and specified in the thesis. Furthermore, I verify that this thesis has not yet been submitted as part of another examination process neither in identical nor in similar form.

Würzburg, 1st April 2014 …….

Signature

Hiermit erkläre ich an Eides statt, die Dissertation „Relevanz der Thrombozytenzahl und des ITAM-Signalwegs in Mausmodellen der Hämostase, Thrombose und Thromboinflammation“ eigenhändig, d.h. insbesondere selbständig und ohne Hilfe eines professionellen Promotionsberaters, angefertigt und keine anderen als die von mir angegebenen Quellen und Hilfsmittel verwendet zu haben.

Ich erkläre außerdem, dass die Dissertation weder in gleicher noch in ähnlicher Form bereits in einem anderen Prüfungsverfahren vorgelegen hat.

Würzburg, den 1. April 2014…….

Unterschrift